FEATURES OF HIGHLY HYDROPHOBIC PLANT OIL-BASED VINYL MONOMERS IN CATIONIC AND FREE RADICAL POLYMERIZATION

A Dissertation
Submitted to the Graduate Faculty
of the
North Dakota State University
of Agriculture and Applied Science

By

Kyle Marvin Kingsley

In Partial Fulfillment of the Requirements
for the Degree of
DOCTOR OF PHILOSOPHY

Major Department:
Coatings and Polymeric Materials

February 2019

Fargo, North Dakota

North Dakota State University
Graduate School

Title

FEATURES OF HIGHLY HYDROPHOBIC PLANT OIL-BASED VINYL MONOMERS IN CATIONIC AND FREE RADICAL POLYMERIZATION

By

Kyle Kingsley

The Supervisory Committee certifies that this ***disquisition*** complies with North Dakota State University's regulations and meets the accepted standards for the degree of

DOCTOR OF PHILOSOPHY

SUPERVISORY COMMITTEE:

Dr. Andriy Voronov
Chair

Dr. Dean C. Webster

Dr. Mohiuddin Quadir

Dr. Jessica Striker

Dr. Bret J. Chisholm

Approved:

3/29/2019
Date

Dr. Dean C. Webster
Department Chair

ABSTRACT

The demand for polymeric materials, which have traditionally been produced from petroleum-based resources over the last century, continues to grow each year. However, the supply of fossil fuels is limited. This, along with price volatility, harmful effects on the environment, and stricter regulations, have led to a surge in the exploration of suitable replacements, namely renewable resources such as plant and vegetable oils. In this work, newly synthesized highly hydrophobic plant oil-based vinyl monomers were polymerized using different mechanisms and processes to obtain polymer coatings and crosslinked films.

First, novel vinyl ether monomers derived from soybean oil were copolymerized with vinyl ether counterparts derived from poly(ethylene glycol) (PEG) *via* cationic polymerization to prepare alkyd-type coatings. Soybean oil-derived polymer coatings and free films were formed by autoxidation of the unsaturation provided by the parent soybean oil moieties. Studies revealed that mechanical and viscoelastic properties, hydrophobicity, and morphology of coatings were dependent on copolymer composition and even more strongly on molecular weight and molecular weight distribution. The soybean oil-derived polymer coatings exhibited T_g values below room temperature, and it was shown that their thermomechanical properties were dependent on crosslink density.

Next, plant oil-based acrylic monomers (POBMs) from soybean, high oleic soybean, and olive oils were copolymerized with styrene, methyl (meth)acrylate, and vinyl acetate to yield latexes and prepare polymer films with tailorable thermomechanical properties. Feasibility of the emulsion process was realized with regard to parent plant oil structure (unsaturation amount), POBM content and comonomer aqueous solubility, by determining copolymerization kinetics, mode(s) of latex particle nucleation, and molecular weight of resulting latex copolymers. POBM-

emulsifier interactions, competing modes of latex particle nucleation, and effect of comonomer radical reactivity have all been investigated. Total monomer conversion and molecular weight of latex copolymers were enhanced by incorporation of an amphiphilic oligosaccharide (methyl-β-cyclodextrin) within the reaction system, which increases the availability of the POBMs and simultaneously diminishes degradative chain transfer reactions that are triggered by POBM fatty acid unsaturation fragments.

ACKNOWLEDGEMENTS

I would like to express my sincere gratitude to my advisor, Dr. Andriy Voronov, for his tremendous support and guidance throughout the duration of this research. Thank you for your continuous help and enlightenment throughout this work, without which, this dissertation would not be possible. To my committee members, Dr. Bret J. Chisholm, Dr. Dean C. Webster, Dr. Mohiuddin Quadir, and Dr. Jessica Striker, thank you for your time, effort, and guidance during my graduate career at North Dakota State University.

I would like to thank all the former members of Dr. Chisholm's group, especially Ihor, Olena, Satyabrata, Jim, Shane, Lyndsi, and Deep for sharing their expertise when I first entered the program. Additionally, a special thank you to the members of Dr. Voronov's group, Zoriana, Oksana, Vasylyna, Dr. Ananiy Kohut, and Dr. Oleh Shevchuk, for welcoming me into their group and sharing their wisdom when I struggled with my research. Without proper instrumentation, much of this research would not be possible. Thank you to Chunju and Greg for taking care of the characterization labs and sharing their knowledge on interpreting data.

None of this research would be possible without constant support and encouragement from my parents and brother, Andrew. Thank you all for pushing me and supporting me mentally, emotionally, and financially throughout this journey. Without you, this goal would not have been achieved.

Thank you to all past and present faculty, staff, and students in the Department of Coatings and Polymeric Materials who have shared their knowledge and have become great friends over the years.

Finally, I would like to thank the National Science Foundation EPSCoR program (grant IIA-1355466) for providing financial support for my research.

DEDICATION

To my parents, Randy and Rhonda Kingsley. Thank you for everything.

TABLE OF CONTENTS

LIST OF TABLES

LIST OF FIGURES

LIST OF APPENDIX FIGURES

CHAPTER 1. INTRODUCTION

1.1. Renewable resources in the chemical industry

1.1.1. Resurgence of renewable resources

Since the beginning of the 20th century, raw materials in the chemical industry have been predominately derived from petroleum resources such as natural gas and oil[1]. High demand, tremendous investment into infrastructure (i.e. oil refineries), relatively cheap prices, and facile processes have been the driving forces for the utilization of petroleum-derived chemicals and products[2]. In 2009, about 7% of the worldwide use of fossil fuels was dedicated to the manufacturing of plastics[3]. Even more alarming, the average consumption of plastics in the United States in 2010 was more than 140 kg per person[4]. Today, a finite supply of fossil fuels, fluctuating costs, and harmful impacts on the environment have prompted the search for alternative resources available to the chemical industry and the products thereof[5-6].

Aimed at reducing the world's dependence on oil, while simultaneously reducing the negative impacts on the environment, a large surge in research of renewable resources has begun. Over the past two decades, sustainability has been guided by different principles such as the "12 Principles of Green Chemistry" and the "12 Principles of Green Engineering"[7]. Scientists are not the only group of people concerned with finding sustainable alternatives to petroleum sources. In the United States, legislators have become more eco-conscious, evidenced by the Biomass R&D Act of 2000 and the Farm Security and Rural Investment Act of 2002[8]. In terms of the chemical industry, the use of renewable feedstocks is on the rise and expected to surpass fossil-based resources by the end of the 21st century (**Figure 1.1**)[2]. However, this is not the first time renewable feedstocks have been the primary source for the chemical industry. Prior to the boom of using

petroleum resources in the mid-20th century, bio-based resources were the predominate source of materials for the chemical industry[1-2, 9].

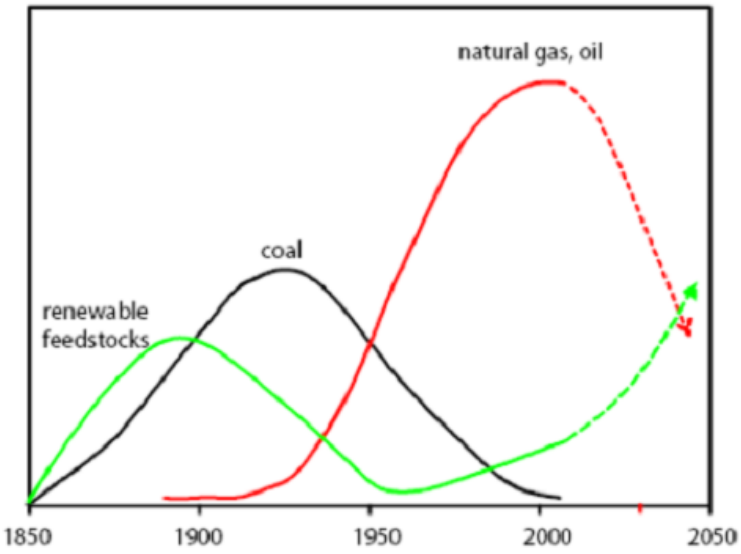

Figure 1.1. Renewable resources used to prepare raw materials in the chemical industry since 1850 (Reproduced from reference 2)

The most commonly utilized non-fuel applications of renewable resources are derived from polysaccharides, wood, sugars, proteins, and plant and vegetable oils[10-12]. Apart from obvious sustainability benefits, bio-based feedstocks are attractive alternatives to fossil fuels for a number of reasons. These materials are available worldwide, comparatively cheap to attain, introduce aspects of inherent biodegradability, and reduce dependence on volatile organic compounds[3, 13].

1.1.2. Utility of plant and vegetable oils

Of the available renewable feedstocks, plant and vegetable oils are the most widely used in the chemical and paint industries. In 2016-2017, the annual production of major plant and vegetable oils was reported to be 189 million metric tons, which increased from 177 million metric tons in 2015-2016[14]. Soybean oil contributes approximately 25% of the annual production of oils[15]. Plant oils are composed of triglycerides, or tri-esters of glycerol with long chain fatty acids[16]. Depending on the parent plant oil, the composition of the fatty acid chains will vary (**Figure 1.2**)[17].

The physical and chemical properties of the plant oils are dependent on parameters such as stereochemistry of the double bonds of the fatty acid chains and the length of the carbon chain, but the biggest impact factor is typically the amount of unsaturation present in the molecule[13, 15]. Iodine value (IV), defined as the amount of iodine in g that can react with double bonds present in 100 g of sample, is a simple way to characterize plant oils. Oils are classified into one of three categories based on their IV. Drying oils (i.e. linseed oil) have IV > 170, semi-drying oils (i.e. soybean oil) have IV between 100-170, and non-drying oils (i.e. palm oil) have IV < 100[15].

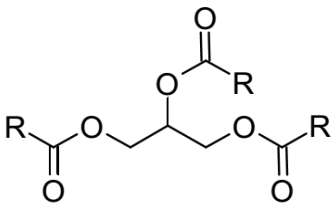

Oil Type	Fatty Acids				
	Saturated		Unsaturated		
	Stearic	Palmitic	Oleic	Linoleic	Linolenic
Olive	7.5–20	0.5–5	65–85	3.5–20	0–1.5
Sunflower	3–6	1–3	14–35	44–75	1–2
Soybean	7–11	2–6	22–34	43–56	7–10
Linseed	4–7	2–5	12–34	17–24	35–60

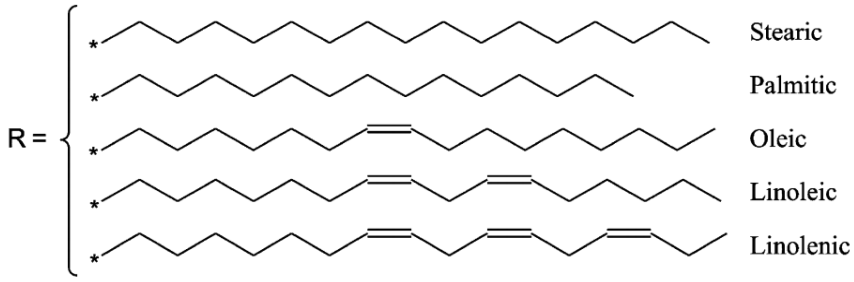

Figure 1.2. Chemical structure of plant oil triglycerides and typical compositions of commonly used plant oils in the chemical industry (Reproduced from reference 17)

Plant oil-based monomers are highly regarded in the chemical industry because of their potential for preparing a multitude of starting materials with different functionalities. Based on the desired properties of the final polymers, plant oil-based monomers with different functional groups can be utilized in various polymerization processes or in post-polymerization modification reactions to prepare polymer coatings through different crosslinking chemistries[14, 18]. Most bio-based monomers synthesized in the last few decades have been polymerized by step growth polymerization processes to prepare thermosetting polymers such as polyurethanes, polyepoxides,

and phenolic compounds. Step growth polymerization, such as polycondensation, is commonly used due to the abundance of alcohols, phenols, acids, amines, etc. present in renewable resources[14].

On the other hand, few bio-based monomers have been investigated in the preparation of polymers by free radical polymerization. The challenge of utilizing free radical polymerization is the slow development of monomers with proper functionality[14, 19]. From an industrial standpoint, chain growth polymerization is one of the most commonly used processes, and typically incorporates monomers containing carbon-carbon double bonds. Although plant oils contain double bonds (unsaturation) in the fatty acid chains, they are not suitable for direct radical polymerization because of their poor reactivity[14]. Compared to step growth polymerization processes, cationic polymerization is capable of achieving higher molecular weights in shorter reaction times.

In this chapter, the incorporation of plant oil-based monomers in two different chain growth polymerization processes, cationic and radical (with a focus on emulsion processes) polymerizations, will be discussed. The basic mechanisms of each process will be introduced before giving a brief overview of previous research that has been conducted in regard to plant-oil based monomers containing proper functionality for polymer synthesis using chain growth polymerization mechanisms and processes.

1.2. Plant oils in cationic polymerization

1.2.1. Cationic polymerization mechanism

Cationic polymerizations have been reported since before the 19th century. **Figure 1.3** describes the general mechanism of cationic polymerization. The main components found within the reaction mixture include monomer(s), cationic initiator (cationogen), Lewis acid co-initiator,

solvent, and a Lewis base additive [20]. Unlike conventional free radical polymerization, termination in cationic polymerization never occurs through bimolecular coupling of two propagating species of the same charge[21]. Side reactions, such as β-proton abstraction, chain transfer to monomer, and backbiting, occur in non-living cationic polymerization reactions due to the high reactivity of the carbocation. These side reactions are capable of causing unexpected termination of the carbocation.

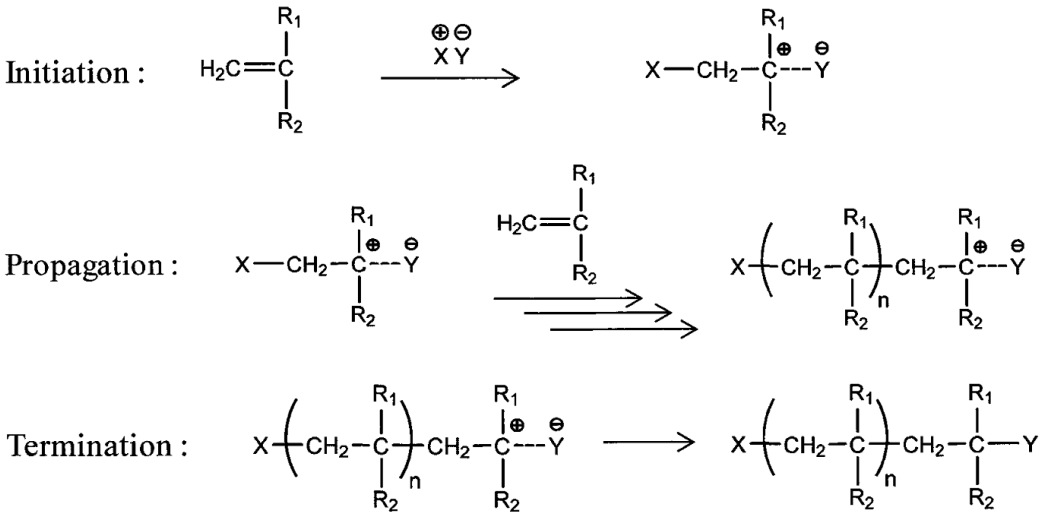

Figure 1.3. Mechanism of cationic polymerization (Reproduced from reference 21)

For cationic polymerization, monomers that can produce stable carbocations can be utilized. Examples of monomers used in cationic polymerization include vinyl ethers, styrene, and 2,3-dihydrofuran (DHF) and their derivatives. Vinyl ether monomers can generate stable carbocations due to resonance stabilization by delocalization of the positive charge as described in **Figure 1.4**. The reactivity of the resulting carbocation is reduced due to the conjugation of the π bond with the lone pair electrons of oxygen which supersedes the negative inductive effect of the oxygen atom in the vinyl ether[22].

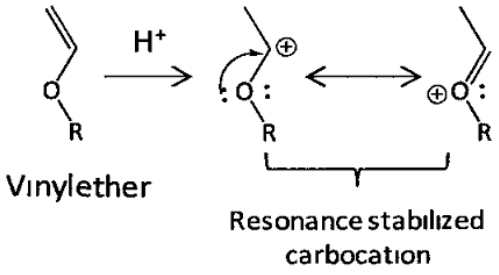

Figure 1.4. Carbocation from vinyl ether monomer exhibiting resonance stability (Reproduced from reference 22)

A number of initiators (i.e. cationogens) that react with Lewis acids to produce a cationic species can be used in cationic polymerizations[23-24]. Commonly used initiators in living reaction systems include hydrogen iodide (HI) or cationogen adducts of vinyl ether with a protonic acid[25-29]. The main consideration for initiator selection is that the counter-ion is not too nucleophilic, which limits the use of strong acids.

Cationic polymerizations are typically conducted at low temperatures due to the use of Lewis acid co-initiators. Examples of common co-initiators include metal halides[30-32] ($AlCl_3$, $ZnCl_2$, $TiCl_4$, PCl_5, $SbCl_4$, BF_3), oxyhalides[33-34] ($VOCl_3$, $SOCl_2$, CrO_2Cl, $POCl_3$), and organometallic compounds[35-36] (R_3Al, R_2AlCl, $RAlCl_2$, $R_3Al_2Cl_3$).

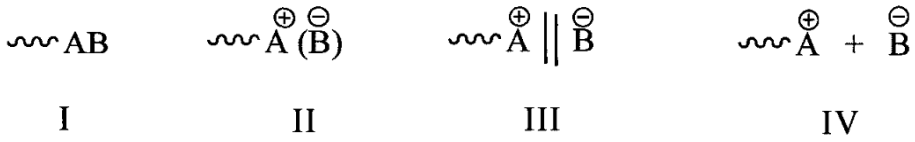

Figure 1.5. Effect of solvating power of solvent on propagating carbocations; (I) Covalent species, (II) contact ion pair, (III) solvent separated ion pair, and (IV) highly solvated ion pair (Reproduced from reference 21)

The solvent (i.e. reaction medium) can have a large impact on the reaction kinetics by altering the relative concentration of free-ion, ion pair, and gegenion[21]. During cationic polymerization, the nature of propagating carbocations can vary based on the solvating power of the solvent (**Figure 1.5**). Solvents with poor solvating power yield covalently bonded carbocations

(I) while solvents with high solvating power produce higher relative concentrations of free-ions (highly solvated) (IV). Rate and degree of polymerization are generally directly related to the solvating power of the solvent.

1.2.2. Living cationic polymerization

As mentioned above, unexpected termination of cationic propagating chains can occur in non-living cationic reactions due to side reactions such as β-proton abstraction, chain transfer to the monomer, or backbiting. A Lewis base, typically an ester or ether compound, is added to the reaction mixture and creates an equilibrium between dormant and active chain ends, with dormant chain ends predominating[37]. The Lewis base reduces both the concentration and reactivity of the active chain ends, allowing uniform and simultaneous propagation of all carbocations generated by the initiator[38]. This type of control over the polymerization is termed "living" polymerization, which was first introduced (for anionic polymerization mechanisms) by Szwarc[39].

1.2.3. Cationic polymerization of plant oil-based vinyl ether monomers

Until recently, very little has been reported on plant oil-based polymers synthesized *via* cationic polymerization. As discussed previously, monomers must contain proper functionality in order to participate in cationic polymerization reactions, but many renewable resources- including plant oils- do not possess adequate functionality in their raw forms to participate in such reactions. In the 1950's, researchers from the United States Department of Agriculture (USDA) prepared vinyl ether monomers from soybean and linseed oils[40-42]. Reaction of the plant oils with alcohols produced fatty alcohol derivatives of the parent plant oils. Next, vinyl ether monomers were synthesized by vinylating the fatty alcohol monomers with acetylene. Different Lewis acid co-initiators were investigated for the cationic polymerization of the vinyl ether monomers. Analysis of the resulting poly(vinyl ether)s demonstrated that the cationic polymerization was non-living in

nature, as some of the unsaturation from the parent plant oil was consumed during the polymerization which suggested the presence of side reactions, such as chain transfer. Applications as protective coatings were investigated by comparing the coating properties of linseed oil-based vinyl ether homopolymer and copolymers of linseed vinyl ether with styrene[43]. Styrene, chosen to improve compatibility with commercial resins, was reacted with a pre-formed linseed oil-based poly(vinyl ether). The styrenated vinyl ether copolymers exhibited improved properties, such as gloss, hardness, and adhesion, compared to films prepared from the linseed-based homopolymer.

For the last decade, researchers at North Dakota State University have investigated plant oil-based vinyl ether monomers (**Figure 1.6**) in cationic polymerization for applications as thermoset coatings. Vinyl ether monomers from plant oils with different amounts of unsaturation in the fatty acid chains were prepared by base-catalyzed transesterification of plant oil triglyceride with 2-vinyloxy ethanol[37, 44]. Depending on the parent plant oil, the composition of the fatty acid chains will vary, as described previously in **Figure 1.2**.

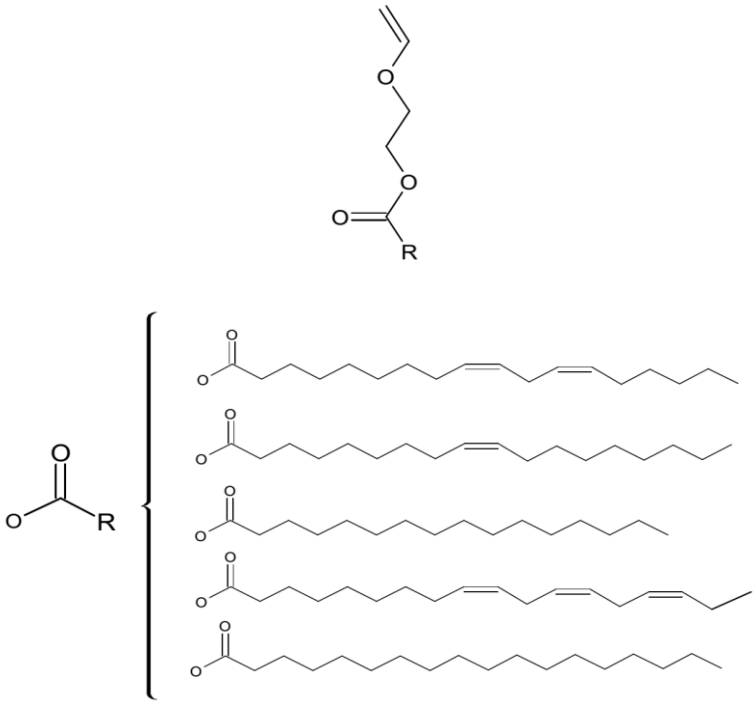

Figure 1.6. Chemical structure of plant oil-based vinyl ether monomers

Unlike the vinyl ether monomers previously studied by researchers at the USDA, these vinyl ether monomers possess an ester group, which can potentially be used as a Lewis base to form a living cationic polymerization. With enhanced control of the polymerization mechanism, feasibility of preparing linear polymer chains with pendent fatty acids containing unsaturation for post-polymerization crosslinking or derivatization was realized, as described in **Figure 1.7**.

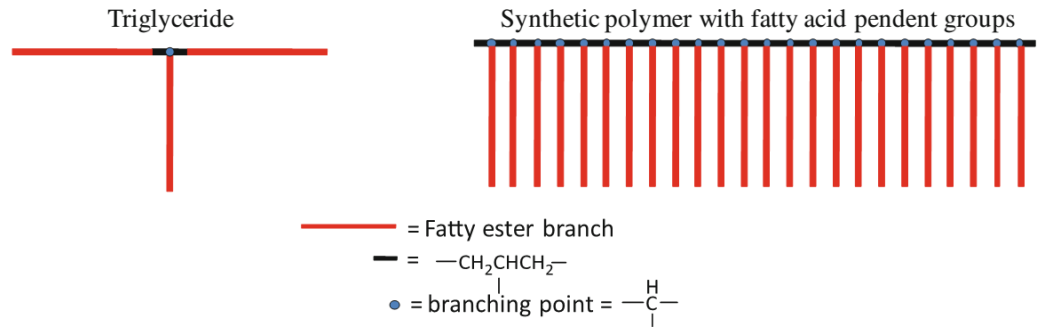

Figure 1.7. Differences in molecular architecture between a plant oil triglyceride and a synthetic polymer containing fatty acid pendent groups. Not drawn to scale. (Reproduced from reference 44)

Using living cationic polymerization, the unsaturation within the fatty acid chains is preserved to prepare crosslinked polymer networks *via* autoxidation or can be further derivatized. This was demonstrated by Alam et. al.[44-45] who prepared polymers with epoxy- and acrylate-functionality. Soybean-based vinyl ether monomers (2-VOES) were copolymerized with vinyl ether monomers from poly(ethylene glycol) *via* cationic polymerization and investigated as safer alternatives in surfactant applications[46]. Investigations to prepare alkyd-type coatings from 2-VOES *via* cationic polymerization were also conducted. Copolymerization with menthol vinyl ether[47] or cyclohexyl vinyl ether[45] increased T_g and improved thermomechanical properties of the crosslinked coatings. A comprehensive review on soybean-based vinyl ether monomers in cationic polymerization was prepared by Kalita et. al.[48]. Similar studies on living cationic polymerization of different plant oils, such as palm oil (2-VOEP)[49], linseed oil (2-VOEL), and camelina oil (2-VOEC)[50] have been reported, along with renewable resources like cardanol and eugenol.

1.3. Plant oils in emulsion polymerization

Emulsion polymerization, a type of free radical polymerization process, has been another area of intense investigation for the preparation of polymers from renewable feedstocks. Waterborne processes are inherently more environmentally friendly compared to solventborne reaction systems, which contribute to the amount of volatile organic compounds (VOCs)[14]. Furthermore, the use of water as the continuous phase offers benefits of reduced viscosity of the reaction mixture, is non-flammable, and improves the heat transfer within the reaction which allows for greater control of the reaction temperature. These features make emulsion polymerization an attractive option for polymer processing at an industrial scale.

1.3.1. Emulsion polymerization mechanism

The basic components of an emulsion reaction mixture include monomer(s), surfactant, a water-soluble initiator, and water[51]. Within the system, an emulsion of monomer droplets is formed throughout the continuous phase (water). At the beginning of the polymerization, approximately 95% of the monomer is found in large reservoirs (monomer droplets). The monomer droplets are stabilized by oil-in-water surfactant (emulsifier) at the beginning of the polymerization. A small portion of monomer may be found in the micelles or dispersed in the aqueous phase prior to polymerization. When the concentration of surfactant exceeds the critical micelle concentration (CMC), free surfactant molecules dispersed throughout the continuous phase aggregate together to form a solution of colloidal clusters, known as micelles[21]. Polymerization is started upon the introduction of a water-soluble initiator, typically persulfates. A characteristic emulsion polymerization is generally described by three distinct intervals, as shown in **Figure 1.8**.

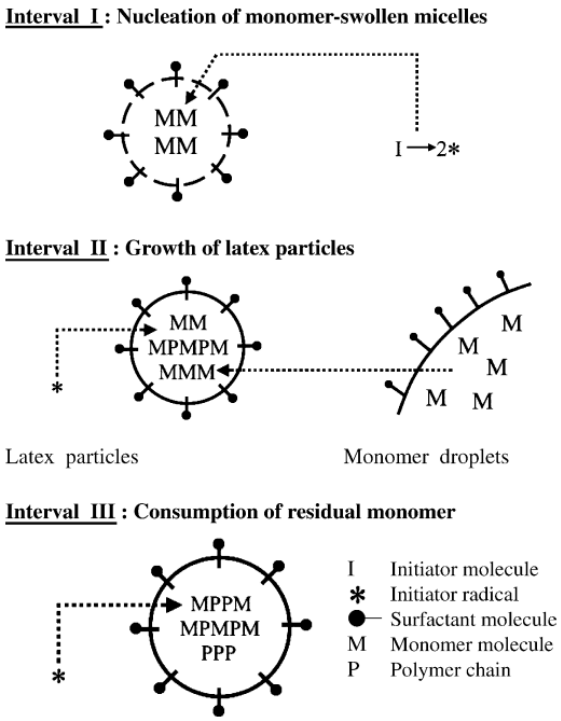

Figure 1.8. A schematic representation of the three intervals of emulsion polymerization of hydrophobic monomers by the micelle nucleation model (Reproduced from reference 51)

The first interval (stage) of the emulsion process is particle nucleation. Radicals are formed from the water-soluble initiators in the continuous phase before entering the monomer-swollen micelles. In typical emulsion processes, the concentration of surfactant is well above that of the CMC, therefore creating a large number of micelles from available surfactant. Because of this, polymerization occurs primarily in the monomer-swollen micelles rather than the large monomer droplets due to the much larger overall surface area of the micelles compared to the monomer droplets[52]. This mode of nucleation is referred to as *micellar (heterogeneous) nucleation* and is commonly employed for hydrophobic monomers such as styrene[53]. According to Smith and Ewart[54], the number of nucleated polymer particles per unit volume of water (N_p) is proportional to the concentrations of surfactant ([S]) and initiator ([I]) to the 0.6 and 0.4 powers, respectively.

Oil-soluble monomer(s) must have at least a finite level of aqueous solubility in order to diffuse from the monomer reservoirs (droplets) through the reaction medium into the growing

polymer particles. But for more hydrophilic monomers (i.e. vinyl acetate or methyl acrylate), polymerization may occur in the aqueous bulk (*homogeneous nucleation)*[55]. Originally soluble in water, these small oligomers precipitate out of solution once a critical chain length is reached. Available surfactant then adsorbs onto the surface of these polymer nuclei, forming a polymer particle. The growing polymer particles are stabilized by available surfactant from the aqueous medium or disbanded micelles that do not participate in polymerization. Particle nucleation occurs rapidly and the end of stage one (typically between 10-20% monomer conversion, **Figure 1.9**) is designated by the exhaustion of micelles[51]. The number of polymer particles per unit volume remains relatively unchanged throughout the remainder of the polymerization.

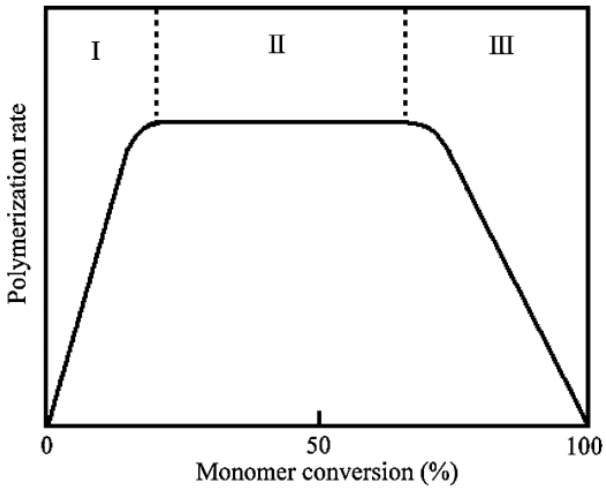

Figure 1.9. Rate of polymerization as a function of monomer conversion (Reproduced from reference 51)

The second interval of emulsion polymerization is the growth of the polymer particles. Within the polymer nuclei, free radicals propagate with monomer molecules that have diffused from the monomer droplet reservoirs. Zero-one kinetics (Smith-Ewart case 2) states that within a polymer particle there is either no free radical (idle) or a single free radical (active)[51]. Assuming no new particles are formed (nucleated), a pseudo steady-state rate of polymerization is achieved

which is proportional to the concentration of monomer in the polymer particles and N_p (**Figure 1.9**). The end of interval two occurs upon the consumption of all monomer droplet reservoirs.

The final stage of the emulsion polymerization, interval three, observes a decrease in the rate of polymerization as the concentration of monomer within the polymer particles decreases. All remaining monomer is located in the polymer particles and consumed by the propagation reaction with free radicals[21, 51].

1.3.2. Emulsion polymerization of plant oil-based monomers

Due to the stability of the internal double bonds of fatty acid monomers, direct radical polymerization of plant oil-based monomers with unsaturated fatty acid chains is difficult[56]. Different processes have been utilized to incorporate plant oils into emulsion polymerization. Functionalization of internal double bonds is described in **Figure 1.10**. Bunker and Wool[57-58] prepared an acrylated oleic acid methyl ester (AMO) by first epoxidizing the unsaturation of the fatty acid chain. Emulsion homopolymerization of the monomer was performed to prepare bio-based latexes for pressure sensitive adhesive applications. From this method, no unsaturation from oleic acid remained for post-polymerization autoxidative reactions. Furthermore, the conversion and molecular weight of the homopolymer were low due to the hydrophobicity of the monomer. Improvements to the emulsion polymerization of AMO were attempted by Jensen et al.[59] who reported on the copolymerization of AMO and styrene. As the amount of AMO increased to 30 wt.%, induction times increased and final conversion and molecular weight increased. The same difficulties were encountered when the research group attempted copolymerization of acrylated soybean oil with methyl methacrylate[60].

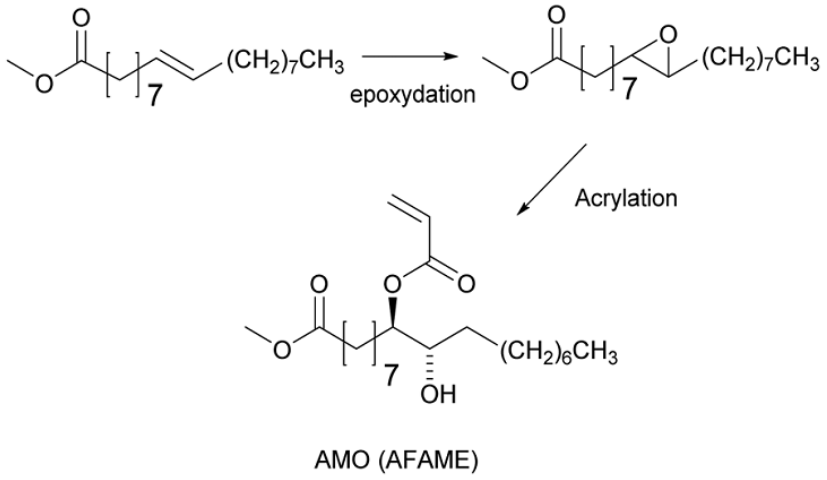

Figure 1.10. Synthesis of acrylated methyl oleate (AMO) for emulsion polymerization through internal double bonds of fatty acid monomers (Reproduced from reference 14)

Another method to prepare fatty acid monomers for chain growth polymerization is by end-capped functional groups, described in **Figure 1.11**. The Thames research group from the University of Southern Mississippi has reported on the emulsion copolymerization of functionalized vegetable oil macromonomers (VOMMs) that contain at least one unsaturated double bond in the pendent fatty acid chains that can be utilized for post-polymerization crosslinking[61-70]. (Meth)acrylate functional fatty acid monomers were prepared from plant oils such as soybean and linseed oils. The VOMMs were polymerized *via* emulsion polymerization to prepare latex homopolymers and copolymers with conventional acrylic monomers, such as butyl acrylate and methyl methacrylate. Researchers in the Thames group observed increased induction times and lower rates of (co)polymerization, conversion, and molecular weights as the content and unsaturation of VOMMs increased. Diffusion limitations and degradative chain transfer to the fatty acid double bonds make the incorporation of highly hydrophobic VOMMs in polymer latexes by emulsion polymerization difficult. Attempts to overcome these challenges were reported by Quintero et al.[62] after incorporating ethoxylate groups to improve the hydrophilicity of the VOMMs.

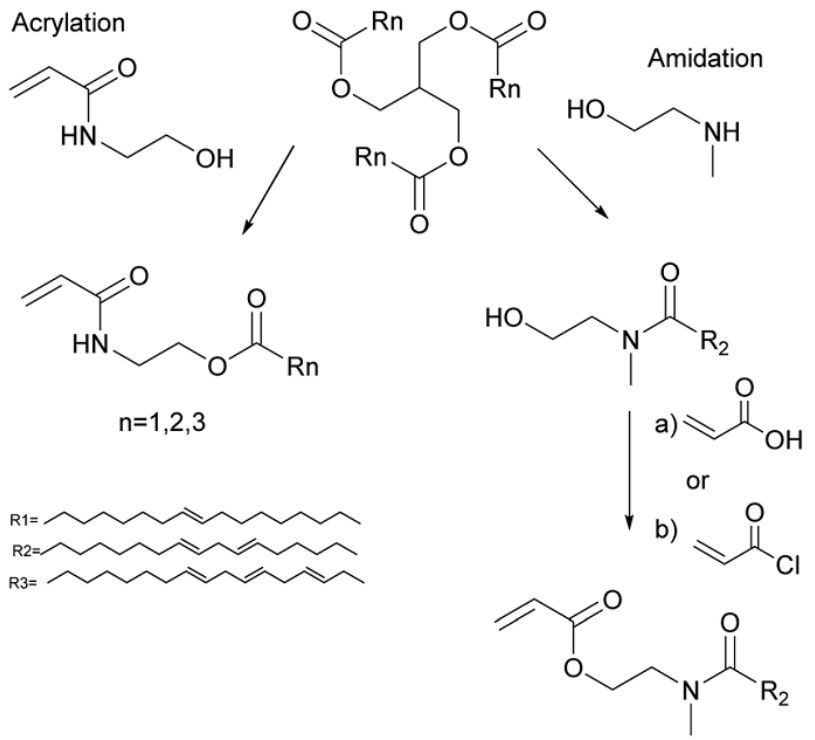

Figure 1.11. Different synthetic routes to prepare end-cap functionalized plant oil-based monomers (Reproduced from reference 14)

Recent reviews[14, 56] discuss the state of the art associated with incorporating plant oil-based monomers in different free radical polymerization processes. Within the reviews are sections dedicated to recent reports on the advances and challenges associated with the emulsion polymerization of plant oil-based monomers.

1.3.3. Synthesis of acryl amide-functional plant oil-based monomers

In this study, acryl amide-functional plant oil-based monomers were copolymerized with significantly more soluble in water comonomers, styrene, methyl (meth)acrylate, and vinyl acetate. Proper functionalization of the parent plant oils was required in order to prepare bio-based latexes for coating applications. The synthesis of acrylic plant oil-based monomers has been described in our group's previous research[71].

Monomers with different fatty acid chain compositions were prepared from different parent plant oils, such as linseed, soybean, sunflower, and olive oils. All monomers contain an N-acryloyl fragment that allows them to be utilized in chain radical polymerization. From ^{1}H NMR (**Figure 1.12**), noticeable differences in chemical structure were observed for different monomers from linseed and olive oils. The signal associated with the vinyl protons (H) within the fatty acid chain is more pronounced for the more highly unsaturated linseed-based monomer (LSM) compared to olive-based monomer (OVM), which is less unsaturated.

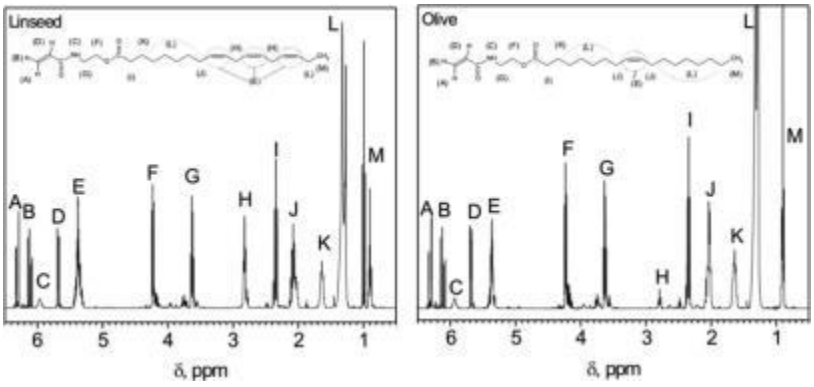

Figure 1.12. ^{1}H NMR spectra of linseed (LSM) and olive (OVM) oil-based monomers (Reproduced from reference 71)

1.4. Summary and outlook

Evidenced by the volume of previous works described in this chapter, exploration of renewable feedstocks, specifically plant oils, as starting materials in the chemical industry continues to surge forward. Proper functionalization of plant oils has allowed for incorporation of renewable vinyl monomers capable of providing improved properties such as modulus, hardness, and solvent resistance of thermoset coatings. By changing the parent plant oil starting material, changes in the composition (amount of unsaturation) within the fatty acid chains can be varied. Varying amounts of unsaturation, combined with copolymerization with other acrylic monomers and different crosslinking chemistries, the properties of thermoset coatings can be tailored to suit desired applications. Furthermore, the polymerization processes described in this chapter offer the

benefits of lower energy consumption throughout polymerization (i.e. cationic vs traditional melt polycondensation of alkyds) and reduced dependence on volatile organic compounds (i.e. waterborne polymerization systems and ability for plant oil-based monomers to act as internal plasticizers). The pioneering work described above, in conjunction with the work described in this dissertation, could help promote the widespread incorporation of bio-based resources in the polymer and coatings industries.

Moving forward, the biggest impedance of utilizing renewable feedstocks in the chemical industry remains in the cost-performance analysis. A tremendous infrastructure (i.e. oil refineries, processing plants, etc.) has been established for the production of chemicals and products derived from fossil fuels. These processes have been optimized over time, making them relatively easy and cheap to maintain. In order to transition to renewables as the predominate source for starting materials, processing conditions (i.e. bio-refineries) must be established and be cost competitive with currently used practices. Furthermore, bio-based products must offer enhanced performance or cheaper costs of production compared to their petroleum-based counterparts in order to be considered for applications.

1.5. Research objectives

This research has four main objectives:

(1) Synthesize novel vinyl monomers and (co)polymers thereof derived from plant oils.

(2) Study the structure-property relationships of crosslinked soybean oil-based poly(vinyl ether) coatings and films to determine their potential as suitable replacements for conventional alkyd coatings.

(3) Prepare copolymer latexes from novel plant oil-based acrylic monomers and determine the impacts on reaction mechanism in emulsion as a function of monomer feed composition and parent plant oil chemical structure.

(4) Explore methods to improve final conversion and molecular weight of highly hydrophobic plant oil-based polymer latexes synthesized in emulsion.

1.6. Organization of this dissertation

This dissertation contains seven independent chapters. Chapter 1 (this chapter) begins with an overview on the importance of renewable feedstocks in the chemical industry with an emphasis on plant oils and their derivatives. Next, previous works that have investigated the incorporation of plant oils in cationic and free radical polymerizations are discussed. After mentioning some challenges that lie ahead for expanding the use of renewable materials in the chemical industry, the objectives of this research are summarized. Chapter 2 investigates the synthesis of poly(vinyl ether) copolymers from novel vinyl ether monomers derived from soybean oil and poly(ethylene glycol) (PEG) *via* cationic polymerization. Parameters such as monomer feed composition and chain length of the PEG vinyl ether components were used to determine the impact on changes of coating properties such as crosslink density, tack-free time, hardness, solvent resistance, surface wettability, and flexibility. Furthermore, exploration into applications for blood contact devices is conducted using biocompatibility assays.

The remainder of this dissertation discusses the incorporation of vinyl monomers derived from different plant oils in emulsion polymerization processes. These chapters have already been submitted or published in peer reviewed journals. Chapter 3 investigates the incorporation of highly hydrophobic plant oil-based monomers (POBMs) in emulsion copolymerization with styrene. This work was used as a proof-of-concept for POBMs in emulsion due to the well-studied

behavior of styrene in emulsion polymerization. Changes in the emulsion mechanism, including parameters such as reaction kinetics, particle nucleation mechanism(s), and molecular weight were studied as a function of POBM content and amount, as well as concentration of emulsifier. Chapter 4 reports on the formation of mixed micelles caused by interactions between emulsifier (sodium dodecyl sulfate, SDS) and POBMs, which are very similar in chemical structure. This work is used to explain deviations in emulsion polymerization mechanisms of POBM-based latexes compared to classical Smith-Ewart theory described in Chapter 3. Chapter 5 reports on the effect of comonomer aqueous solubility on the emulsion mechanism, including parameters such as reaction kinetics and molecular weight in the presence of POBMs. Additionally, changes in nucleation mechanism (homogeneous *vs* micellar (heterogeneous)) as a function of comonomer aqueous solubility and POBM content and amount were evaluated using a water insoluble dye and semi-batch emulsion polymerization. Deviations of reaction orders with respect to emulsifier and initiator concentrations further confirmed the balance between the competing modes of particle nucleation with respect to monomer feed composition. Chapter 5 compliments Chapters 3 and 4 in terms of emulsion polymerization mechanism for highly hydrophobic POBMs with counterparts of various aqueous solubility.

Chapter 6 attempts to overcome issues associated with POBMs in emulsion polymerization, such as lower conversion and molecular weight, which occur due to the highly hydrophobic nature of the POBMs and degradative chain transfer to the unsaturation provided by the fatty acid chains of the parent plant oil, quantitatively described in our previous work. Amphiphilic methyl-beta-cyclodextrin (M-β-CD) is successfully utilized in POBM-based emulsion copolymerization reactions to improve the aqueous solubility (i.e. diffusion of hydrophobic POBM through the aqueous medium from monomer droplets to growing

polymer/monomer particles), and, thus, availability of POBM at polymerization loci while simultaneously diminishing chain transfer reactions (i.e. producing higher molecular weight latex polymers). Chapter 7 summarizes the overall conclusions of this study and offers insight for future directions of this work.

1.7. References

1. Güner, F. S.; Yağcı, Y.; Erciyes, A. T., Polymers from triglyceride oils. *Progress in Polymer Science* **2006,** *31* (7), 633-670.
2. Lichtenthaler, F. W.; Peters, S., Carbohydrates as green raw materials for the chemical industry. *Comptes Rendus Chimie* **2004,** *7* (2), 65-90.
3. Lu, Y.; Larock, R. C., Novel Polymeric Materials from Vegetable Oils and Vinyl Monomers: Preparation, Properties, and Applications. *ChemSusChem* **2009,** *2* (2), 136-147.
4. Yao, K.; Tang, C., Controlled polymerization of next-generation renewable monomers and beyond. *Macromolecules* **2013,** *46* (5), 1689-1712.
5. Sharma, V.; Kundu, P., Addition polymers from natural oils—a review. *Progress in Polymer Science* **2006,** *31* (11), 983-1008.
6. Bayer, I. S., Superhydrophobic and Superoleophobic Biobased Materials. *Advances in Contact Angle, Wettability and Adhesion* **2015,** *2*, 259-283.
7. Tabone, M. D.; Cregg, J. J.; Beckman, E. J.; Landis, A. E., Sustainability Metrics: Life Cycle Assessment and Green Design in Polymers. *Environmental Science & Technology* **2010,** *44* (21), 8264-8269.

8. Werpy, T.; Petersen, G.; Aden, A.; Bozell, J.; Holladay, J.; White, J.; Manheim, A.; Eliot, D.; Lasure, L.; Jones, S. *Top value added chemicals from biomass. Volume 1-Results of screening for potential candidates from sugars and synthesis gas*; DTIC Document: 2004.

9. Islam, M. R.; Beg, M. D. H.; Jamari, S. S., Development of vegetable-oil-based polymers. *Journal of applied polymer science* **2014,** *131* (18).

10. Gandini, A.; Coelho, D.; Gomes, M.; Reis, B.; Silvestre, A., Materials from renewable resources based on furan monomers and furan chemistry: work in progress. *Journal of Materials Chemistry* **2009,** *19* (45), 8656-8664.

11. Raquez, J.-M.; Deléglise, M.; Lacrampe, M.-F.; Krawczak, P., Thermosetting (bio) materials derived from renewable resources: a critical review. *Progress in Polymer Science* **2010,** *35* (4), 487-509.

12. Haveren, D. J. v., Emerging Technologies for biobased aromatics. **2014**.

13. Biermann, U.; Bornscheuer, U.; Meier, M. A.; Metzger, J. O.; Schäfer, H. J., Oils and fats as renewable raw materials in chemistry. *Angewandte Chemie International Edition* **2011,** *50* (17), 3854-3871.

14. Molina-Gutiérrez, S.; Ladmiral, V.; Bongiovanni, R.; Caillol, S.; Lacroix-Desmazes, P., Radical polymerization of biobased monomers in aqueous dispersed media. *Green Chemistry* **2019,** *21* (1), 36-53.

15. Meier, M. A.; Metzger, J. O.; Schubert, U. S., Plant oil renewable resources as green alternatives in polymer science. *Chemical Society Reviews* **2007,** *36* (11), 1788-1802.

16. de Espinosa, L. M.; Meier, M. A., Plant oils: The perfect renewable resource for polymer science?! *European Polymer Journal* **2011,** *47* (5), 837-852.

17. Demchuk, Z.; Shevchuk, O.; Tarnavchyk, I.; Kirianchuk, V.; Lorenson, M.; Kohut, A.; Voronov, S.; Voronov, A., Free-Radical Copolymerization Behavior of Plant-Oil-Based Vinyl Monomers and Their Feasibility in Latex Synthesis. *ACS Omega* **2016,** *1* (6), 1374-1382.

18. Galià, M.; de Espinosa, L. M.; Ronda, J. C.; Lligadas, G.; Cádiz, V., Vegetable oil-based thermosetting polymers. *European journal of lipid science and technology* **2010,** *112* (1), 87-96.

19. Wang, Z.; Yuan, L.; Tang, C., Sustainable elastomers from renewable biomass. *Accounts of chemical research* **2017,** *50* (7), 1762-1773.

20. Williams, G., 48. Kinetics of the catalysed polymerisation of styrene. Part I. Experimental methods and some general features of stannic chloride catalysis. *Journal of the Chemical Society (Resumed)* **1938**, 246-253.

21. Odian, G., *Principles of polymerization*. 2004; p 198-349.

22. Alam, S. Synthesis and characterization of novel polyvinylether polymers produced using carbocationic polymerization. North Dakota State University, 2012.

23. Gandini, A.; Cheradame, H., Cationic Polymerisation Initiation Processes with Alkenyl Monomers. *Cationic Polymerisation Initiation Processes with Alkenyl Monomers:, Advances in Polymer Science, Volume 34/35. ISBN 978-3-540-10049-2. Springer-Verlag, 1980* **1980**.

24. Olah, G. A., Stable carbocations. CXVIII. General concept and structure of carbocations based on differentiation of trivalent (classical) carbenium ions from three-center bound penta-of tetracoordinated (nonclassical) carbonium ions. Role of carbocations in electrophilic reactions. *Journal of the American Chemical Society* **1972,** *94* (3), 808-820.

25. Sagane, T.; Lenz, R. W., Molecular weight effects on the liquid-crystalline properties of poly (vinyl ether) s with pendant cyanobiphenyl mesogenic groups. *Macromolecules* **1989,** *22* (9), 3763-3767.

26. Namikoshi, T.; Hashimoto, T.; Kodaira, T., Living cationic polymerization of vinyl ethers with a urethane group. *Journal of Polymer Science Part A: Polymer Chemistry* **2004,** *42* (12), 2960-2972.

27. Namikoshi, T.; Hashimoto, T.; Kodaira, T., Living cationic polymerization of vinyl ethers with a tricyclodecane or tricyclodecene unit: Synthesis of new poly (vinyl ether) s with high glass-transition temperature. *Journal of Polymer Science Part A: Polymer Chemistry* **2004,** *42* (14), 3649-3653.

28. Namikoshi, T.; Hashimoto, T.; Urushisaki, M., Living cationic polymerization of vinyl ether with a cyclic acetal group. *Journal of Polymer Science Part A: Polymer Chemistry* **2007,** *45* (21), 4855-4866.

29. Matsumoto, K.; Kubota, M.; Matsuoka, H.; Yamaoka, H., Water-soluble fluorine-containing amphiphilic block copolymer: Synthesis and aggregation behavior in aqueous solution. *Macromolecules* **1999,** *32* (21), 7122-7127.

30. Kennedy, J.; Feinberg, S., Cationic polymerization with boron halides. VI. Polymerization of styrene with BF3, BCl3, and BBr3. *Journal of Polymer Science: Polymer Chemistry Edition* **1978,** *16* (9), 2191-2197.

31. Kennedy, J.; Huang, S.; Feinberg, S., Cationic polymerization with boron halides. IV. Elucidation and control of initiation and termination by the help of model experiments. *Journal of Polymer Science: Polymer Chemistry Edition* **1977,** *15* (12), 2869-2892.

32. Kennedy, J.; Huang, S.; Feinberg, S., Cationic polymerization with boron halides. III. BCl3 coinitiator for olefin polymerization. *Journal of Polymer Science: Polymer Chemistry Edition* **1977,** *15* (12), 2801-2819.

33. Biswas, M.; Kabir, G. A., Some aspects of the polymerization of n-butyl vinyl ether by chromyl chloride. *Journal of Polymer Science: Polymer Chemistry Edition* **1979,** *17* (3), 673-681.

34. Biswas, M.; Kabir, G. A., Polymerization of iso-butyl vinyl ether by oxychlorides of group V and VI elements. *European Polymer Journal* **1978,** *14* (10), 861-865.

35. Reibel, L.; Kennedy, J. P.; Chung, D. Y., Cationic polymerizations by aromatic initiating systems. II. Correlation between cationic model and polymerization reactions with the p-CH3C6H4CH2Cl/Et3Al system. *Journal of Polymer Science: Polymer Chemistry Edition* **1979,** *17* (9), 2757-2768.

36. Maina, M. D.; Cesca, S.; Giusti, P.; Ferraris, G.; Magagnini, P. L., Studies on polymerizations initiated by syncatalytic systems based on aluminium organic compounds, 6. Comparison with isobutene polymerizations initiated by ethylaluminium dichloride or aluminium trichloride. *Die Makromolekulare Chemie: Macromolecular Chemistry and Physics* **1977,** *178* (8), 2223-2234.

37. Chernykh, A.; Alam, S.; Jayasooriya, A.; Bahr, J.; Chisholm, B. J., Living carbocationic polymerization of a vinyl ether monomer derived from soybean oil, 2-(vinyloxy) ethyl soyate. *Green Chemistry* **2013,** *15* (7), 1834-1838.

38. Puskas, J.; Kaszas, G., Living carbocationic polymerization of resonance-stabilized monomers. *Progress in polymer science* **2000,** *25* (3), 403-452.

39. SZWARC, M., 'Living'polymers. *Nature* **1956,** *178* (4543), 1168.

40. Teeter, H.; Dufek, E.; Coleman, C.; Glass, C.; Melvin, E.; Cowan, J., Reactions of unsaturated fatty alcohols. I. Preparation and properties of some vinyl ethers. *Journal of the American Oil Chemists Society* **1956,** *33* (9), 399-404.

41. Gast, L.; Schneider, W. J.; Teeter, H., Reactions of unsaturated fatty alcohols. III. Viscosity and molecular weight studies on some vinyl ether polymers. *Journal of the American Oil Chemists Society* **1957,** *34* (6), 307-310.

42. Schneider, W. J.; Gast, L.; Melvin, E.; Glass, C.; Teeter, H., Reactions of unsaturated fatty alcohols. II. Polymerization of vinyl ethers and film properties of polymers. *Journal of the American Oil Chemists' Society* **1957,** *34* (5), 244-247.

43. Schneider, W. J.; Gast, L.; Schwab, A.; Teeter, H., Reactions of unsaturated fatty alcohols. XIV. Preparation and properties of styrenated fatty vinyl ether polymers. *Journal of the American Oil Chemists Society* **1962,** *39* (5), 241-244.

44. Alam, S.; Chisholm, B. J., Coatings derived from novel, soybean oil-based polymers produced using carbocationic polymerization. *J Coat Technol Res* **2011,** *8* (6), 671-683.

45. Alam, S.; Kalita, H.; Jayasooriya, A.; Samanta, S.; Bahr, J.; Chernykh, A.; Weisz, M.; Chisholm, B. J., 2-(Vinyloxy) ethyl soyate as a versatile platform chemical for coatings: An overview. *European Journal of Lipid Science and Technology* **2014,** *116* (1), 2-15.

46. Alam, S.; Kalita, H.; Kudina, O.; Popadyuk, A.; Chisholm, B. J.; Voronov, A., Soy-based surface active copolymers as a safer replacement for low molecular weight surfactants. *ACS Sustainable Chemistry & Engineering* **2012,** *1* (1), 19-22.

47. Kalita, H.; Selvakumar, S.; Jayasooriyamu, A.; Fernando, S.; Samanta, S.; Bahr, J.; Alam, S.; Sibi, M.; Vold, J.; Ulven, C., Bio-based poly (vinyl ether) s and their application as alkyd-type surface coatings. *Green Chemistry* **2014,** *16* (4), 1974-1986.

48. Kalita, H.; Alam, S.; Kalita, D.; Chernykh, A.; Tarnavchyk, I.; Bahr, J.; Samanta, S.; Jayasooriyama, A.; Fernando, S.; Selvakumar, S.; Popadyuk, A.; Wickramaratne, D. S.; Sibi, M.; Voronov, A.; Bezbaruah, A.; Chisholm, B. J., Synthesis and Characterization of Novel Soybean Oil-Based Polymers and Their Application in Coatings Cured by Autoxidation. In *Soy-Based Chemicals and Materials*, American Chemical Society: **2014**; Vol. 1178, pp 371-390.

49. Kalita, H.; Jayasooriyamu, A.; Fernando, S.; Chisholm, B. J., Novel high molecular weight polymers based on palm oil. *J. Oil Palm Res.* **2015,** *27* (March), 39-56.

50. Kalita, D. J. Polymers and Coatings Derived from Novel Bio-Based Vinyl Ether Monomers. Ph.D., North Dakota State University, Ann Arbor, **2018**.

51. Chern, C., Emulsion polymerization mechanisms and kinetics. *Progress in polymer science* **2006,** *31* (5), 443-486.

52. Chern, C.-S.; Lin, C.-H., Particle nucleation loci in emulsion polymerization of methyl methacrylate. *Polymer* **2000,** *41* (12), 4473-4481.

53. Chem, C.-S.; Lin, C.-H., Using a water-insoluble dye to probe the particle nucleation loci in styrene emulsion polymerization. *Polymer* **1999,** *40* (1), 139-147.

54. Smith, W. V.; Ewart, R. H., Kinetics of emulsion polymerization. *The journal of chemical physics* **1948,** *16* (6), 592-599.

55. Suzuki, A.; Yano, M.; Saiga, T.; Kikuchi, K.; Okaya, T., Study on the initial stage of emulsion polymerization of vinyl monomers using poly(vinyl alcohol) as a protective colloid - comparison between vinyl acetate (VAc) and methyl methacrylate (MMA). *Prog. Colloid Polym. Sci.* **2004,** *124*, 27-30.

56. Lomège, J.; Lapinte, V.; Negrell, C.; Robin, J.-J.; Caillol, S., Fatty acid-based radically polymerizable monomers: from novel poly (meth) acrylates to cutting-edge properties. *Biomacromolecules* **2018**.

57. Bunker, S. P.; Wool, R. P., Synthesis and characterization of monomers and polymers for adhesives from methyl oleate. *Journal of Polymer Science Part A: Polymer Chemistry* **2002,** *40* (4), 451-458.

58. Scala, J. L.; Wool, R. P., The effect of fatty acid composition on the acrylation kinetics of epoxidized triacylglycerols. *Journal of the American Oil Chemists' Society* **2002,** *79* (1), 59-63.

59. Jensen, A. T.; Sayer, C.; Araújo, P. H.; Machado, F., Emulsion copolymerization of styrene and acrylated methyl oleate. *European Journal of Lipid Science and Technology* **2014,** *116* (1), 37-43.

60. Ferreira, G. R.; Braquehais, J. R.; da Silva, W. N.; Machado, F., Synthesis of soybean oil-based polymer lattices via emulsion polymerization process. *Industrial Crops and Products* **2015,** *65*, 14-20.

61. Quintero, C.; Mendon, S. K.; Smith, O. W.; Thames, S. F., Vegetable oil macromonomers as copolymerizable hydrophobes in miniemulsion polymerization. *Polym. Prepr. (Am. Chem. Soc., Div. Polym. Chem.)* **2004,** *45* (1), 1110-1111.

62. Quintero, C.; Delatte, D.; Diamond, K.; Mendon, S. K.; Rawlins, J. W.; Thames, S. F., Modification of vegetable oil derived macromonomers for optimal incorporation into waterborne coating systems. *Proc. Int. Waterborne, High-Solids, Powder Coat. Symp.* **2005,** *32nd*, 348-361.

63. Quintero, C.; Mendon, S. K.; Smith, O. W.; Thames, S. F., Miniemulsion polymerization of vegetable oil macromonomers. *Progress in Organic Coatings* **2006,** *57* (3), 195-201.

64. Booth, G.; Delatte, D. E.; Thames, S. F., Incorporation of drying oils into emulsion polymers for use in low-VOC architectural coatings. *Industrial Crops and Products* **2007,** *25* (3), 257-265.

65. Thames, S. F.; Rawlins, J. W., Utilizing nature's technology for environmentally responsible coatings. *Proc. Int. Waterborne, High-Solids, Powder Coat. Symp.* **2009,** *36th*, 5-26.

66. Black, M.; Messman, J.; Rawlins, J., Chain transfer of vegetable oil macromonomers in acrylic solution copolymerization. *Journal of Applied Polymer Science* **2011,** *120* (3), 1390-1396.

67. Kaya, E.; Mendon, S. K.; Rawlins, J. W.; Thames, S. F., Emulsion polymerization of a vegetable oil macromonomer based on soybean oil and evaluation of the coating performance. *Proc. Int. Waterborne, High-Solids, Powder Coat. Symp.* **2011,** *38th*, 194-204.

68. Kaya, E.; Mendon, S. K.; Delatte, D.; Rawlins, J. W.; Thames, S. F. In *Emulsion Copolymerization of Vegetable Oil Macromonomers Possessing both Acrylic and Allylic Functionalities*, Macromolecular Symposia, Wiley Online Library: **2013**; pp 95-106.

69. Delatte, D.; Kaya, E.; Kolibal, L. G.; Mendon, S. K.; Rawlins, J. W.; Thames, S. F., Synthesis and characterization of a soybean oil-based macromonomer. *Journal of Applied Polymer Science* **2014,** *131* (10).

70. Dutta, S.; Blackwell, C.; Gariano, N.; Rawlins, J. W.; Thames, S. F., development of acrylic latex containing acrylated soybean oil macromonomer. *Proc. Int. Waterborne, High-Solids, Powder Coat. Symp.* **2005,** *32nd*, 329-345.

71. Demchuk, Z.; Shevchuk, O.; Tarnavchyk, I.; Kirianchuk, V.; Kohut, A.; Voronov, S.; Voronov, A., Free Radical Polymerization Behavior of the Vinyl Monomers from Plant Oil Triglycerides. *ACS Sustainable Chemistry & Engineering* **2016**.

CHAPTER 2. NOVEL POLY(VINYL ETHER)S BASED ON SOYBEAN OIL AND THEIR APPLICATION AS ALKYD-TYPE COATINGS

2.1. Abstract

Novel poly(vinyl ether) copolymers derived from soybean oil and poly(ethylene glycol) were prepared by cationic polymerization and investigated for application as alkyd-type surface coatings. Unlike conventional alkyd resins, which are synthesized using high temperature melt condensation, the poly(vinyl ether)s from cationic polymerization require mild reaction conditions and allow for greater control of (co)polymer molecular weight and molecular weight distribution. Utilizing the unsaturation in the pendent fatty acid chains from the parent soybean oil, crosslinked networks were formed via autoxidation. Incorporation of methyl vinyl ether comonomers derived from poly(ethylene glycol) prolonged tack-free times, reduced the glass transition temperature, and impacted coating properties such as hardness, solvent resistance, flexibility, and surface wettability. Biocompatibility assays were conducted to assess the feasibility of these systems as applications for blood contact devices. Although the protein adsorption was low, the coatings exhibited high hemolytic activity, suggesting they were not suitable for such applications.

2.2. Introduction

Prior to the 20th century, the use of renewable resources as the basis for raw materials in the chemical industry was more prominent than coal and other fossil fuels. As seen in **Figure 2.1**, the use of fossil gas and oil quickly became the go to source for raw materials throughout the second half of the century due to their high demand and tremendous infrastructure that was established to meet this demand, capable of producing chemicals at low prices[1]. Today, due to the limited supply of petroleum sources, increasing costs, and harmful impacts on the environment, a resurgence in the use of renewable resources has begun[1-2]. It is predicted that by the end of the 21st

century, the majority of raw materials for the chemical industry will once again be provided by renewable feedstocks.

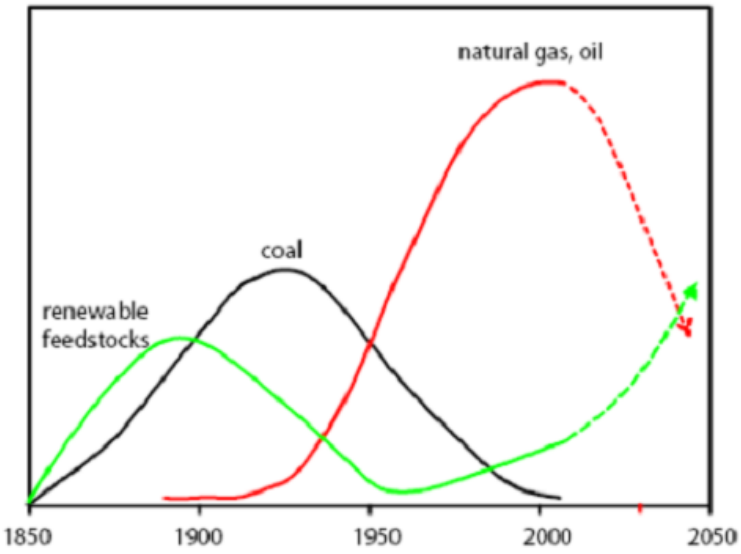

Figure 2.1. Renewable resources used to prepare raw materials in the chemical industry since 1850 (Reproduced from reference 1)

Polysaccharides, sugars, wood, and plant oils are some of the most commonly utilized non-fuel applications of renewable raw materials[3]. The most widely used raw materials in the chemical and polymer industries are plant oils. These materials offer advantages such as sustainability, reduced environmental impacts, inherent biodegradability, easy availability, and low cost[4-5].

Plant oils are composed of triglycerides, or tri-esters of glycerol with long chain fatty acids. Depending on the parent plant oil, the composition of the fatty acid chains will vary (**Table 2.1**)[6]. The physical and chemical properties of the plant oils are largely dependent on parameters such as stereochemistry of the double bonds of the fatty acid chains, length of the carbon chain, and amount of unsaturation[2-4]. The amount of unsaturation of the different oils are commonly classified into three categories based on their iodine value (IV), which is defined as the amount of iodine in g that can react with double bonds present in 100 g of sample. Drying oils (i.e. linseed oil) have IV >

170, semi-drying oils (i.e. soybean oil) have IV between 100-170, and non-drying oils (i.e. palm oil) have IV < 100[3].

Table 2.1. Fatty acid chain composition of common plant oils used in industry (x = number of chain carbon atoms; y = number of double bonds) (Data from reference 6)

	Saturated		Unsaturated		
	16:0	**18:0**	**18:1**	**18:2**	**18:3**
Olive	0.5-5	7.5-20	65-85	3.5-20	0-1.5
Sunflower	1-3	3-6	14-35	44-75	1-2
Soybean	2-6	7-11	22-34	43-56	7-10
Linseed	2-5	4-7	12-34	17-24	35-60

Plant oils possessing relatively high levels of unsaturation (i.e. drying and semi-drying oils) are capable of producing crosslinked films when exposed to air. These insoluble networks are produced through a process known as autoxidation, a free radical chain process that creates a number of crosslinking reactions primarily by free-radical coupling reactions[7-8]. Even in the presence of drier packages, coatings derived from plant oils require too long a time to complete curing/crosslinking *via* autoxidation. Furthermore, the long aliphatic chains of the plant oil triglycerides are highly flexible and produce coatings that are too soft for many applications[8].

To improve the utility of plant oil-based coatings, a new resin technology was developed. Alkyd resins, comprised of a polyol, a polyvalent acid or anhydride, and fatty acid derivatives, are typically manufactured using melt condensation polymerization at temperatures above 200 °C. Alkyds were first reported by Berzelius in 1847, who synthesized a brittle polymer from glycerin and tartaric acid. In 1901 Watson and Smith used phthalic acid instead of tartaric acid but were unable to improve the flexibility of the polymer. In 1914 an alkyd resin exhibiting good film properties was achieved by Kienle when he incorporated fatty acids into the synthesis[8]. Today, alkyds are most commonly prepared with glycerol as the polyol and phthalic anhydride as the

diacid component. The most common fatty acids for alkyd syntheses are derived from tall oil, soybean oil, or linseed oil[2-3, 8]. By using phthalic anhydride, alkyds possess higher glass transition temperatures (T_g) which reduces the time required to become dry-to-touch compared to traditional oil-based coatings[8].

Melt condensation polymerization is not the only method to produce plant oil-based coatings. Another method commonly utilized is the cationic polymerization of plant oil-based vinyl ethers. In the 1950's researchers at the United States Department of Agriculture (USDA) synthesized vinyl ether monomers by preparing fatty alcohols from plant oils, such as soybean and linseed oils, and then vinylated them using acetylene[9]. The poly(vinyl ether)s that were produced were low molecular weight (1,000-6,000 g mol^{-1}). When characterizing the poly(vinyl ether) products, it was determined that some of the unsaturation for the fatty acid chains was consumed during the polymerization through side reactions, which resulted in large molecular weight distributions[10-11]. Better control of polymer molecular weight, molecular weight distribution, and final polymer architecture can be achieved by living cationic polymerization. When the cationic polymerization system uses a Lewis acid co-initiator and a cationogen in a nonpolar solvent, a Lewis base (typically an ester or ether compound) can be introduced to produce a living system[12-14]. For Lewis base-assisted living cationic polymerizations, dormant and active chain ends exist in equilibrium, with active chain ends being fewer than dormant chains[13]. This equilibrium exists due to the fact that the Lewis base: 1) complexes with the Lewis acid coinitiator and forms a monomeric Lewis acid species as well as adjusts the acidity; 2) stabilizes active chains through direct interaction; and 3) stabilizes the counteranion generated upon initiation[15-17].

For the past decade, Lewis base-free living cationic polymerization has been investigated by members of the Chisholm group at North Dakota State University. Vinyl ether monomers were

synthesized through a base-catalyzed transesterification of a plant oil with 2-vinyloxy ethanol (2VOE), as seen in **Figure 2.2**[18]. Different plant oils were investigated, including soybean oil (2-VOES)[8, 13, 19-22], palm oil (2-VOEP)[23], linseed oil (2-VOEL), and camelina oil (2-VOEC)[24]. Homopolymers (**Figure 2.3**) were prepared using a cationic polymerization process, using 1-isobutoxy-ethyl acetate (IBEA) as the initiator (i.e. cationogen), ethylaluminum sesquichloride ($Et_3Al_2Cl_3$) as the coinitiator, and toluene as a solvent[19].

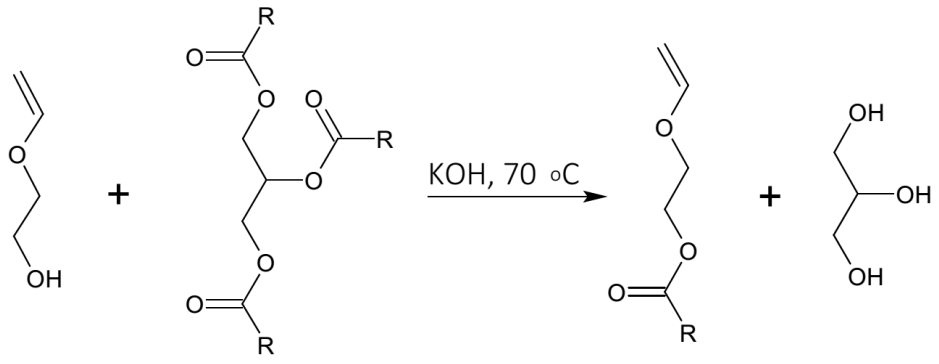

R= alkyl and alkenyl groups from plant oil fatty acids

Figure 2.2. Synthesis of 2-VOES monomer via base-catalyzed transesterification of soybean oil with 2-vinyloxy ethanol

Control of molecular weight, molecular weight distribution, and polymer architecture were achieved by polymerizing exclusively through the vinyl ether functionality, leaving the unsaturation from the fatty acid pendent chains available for post polymerization autoxidation or other derivatizations[23]. This control during polymerization was achieved due to the strong stabilizing effect of the oxygen atom next to the vinyl group which reduced the activation energy of a given carbocation upon the addition of a vinyl ether monomer[21]. By tailoring the reactivity of the carbocationic species, propagation was limited to proceed strictly through the vinyl groups. The use of these monomers in cationic polymerization systems also demonstrated the ability to produce a living polymerization system[13, 21].

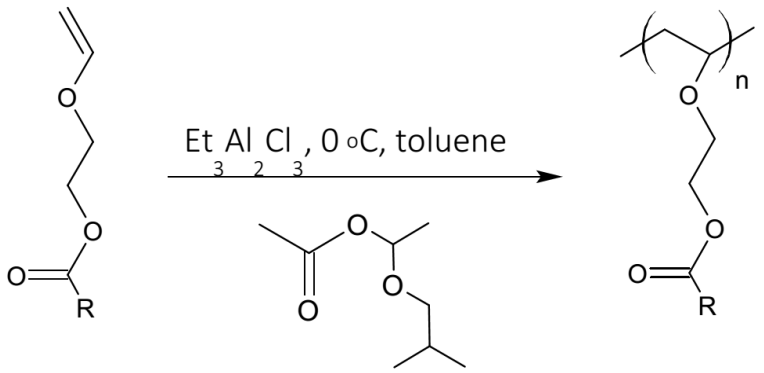

Figure 2.3. Cationic polymerization of poly(2-VOES)

From a configurational aspect, the long aliphatic fatty acid chains of the plant oil-based vinyl ether monomers reduce interactions between polymer chains, and therefore, the homopolymers possess sub-ambient T_g's. Cationic copolymerization of these plant oil-based monomers with cyclohexyl vinyl ether (CHVE)[21] and other vinyl ether monomers derived from menthol[8] and poly(ethylene glycol) (PEG)[20] has been reported to increase the overall T_g of these alkyd-type coatings. Derivatizations of the unsaturation from the fatty acid chains can also be used to modify the properties of the coatings. Through oxidation of the double bonds, epoxide functional groups can be produced and used to form thermoset networks via cationic polymerization. Derivatizations on the epoxy-functional plant oils can be achieved by reacting the epoxide functionality with acrylic acid to yield acrylate-functional plant oils. Furthermore, the epoxy-functional derivative can also be used to prepare polyols by reacting the epoxide groups with alcohols such as methanol[13, 19, 21].

Cationic polymerization of poly(vinyl ether)s offer many benefits compared to traditional alkyd resins[8, 25-30]. Unlike melt condensation polymerizations, which require temperatures greater than 200 °C for alkyd synthesis, cationic polymerizations require mild reaction conditions which result in substantial energy savings during the manufacturing process. Secondly, the cationic addition polymerization process developed for the synthesis of poly(vinyl ether)s eliminates the

potential for gelation, which is possible during alkyd resin preparation. Next, due to the living characteristics of the cationic polymerization, the poly(vinyl ether)s are expected to yield polymers with better control on final polymer molecular weight and weight distribution. Finally, poly(vinyl ether)s are expected to be free of low molecular weight species due to the efficiency of the cationic polymerization, unlike alkyd resins from melt condensation reactions that may contain unreacted monomer or low molecular weight dimers or trimers- depending on conversion- which can impact the performance of the cured coating.

In this work, the ability to tailor coating properties of alkyd-type coatings was studied. Poly(vinyl ether) copolymers from 2-VOES and PEG methyl vinyl ethers of varying ethylene glycol repeat units (PEG*n*, n=3, 5, or 24) were prepared by cationic polymerization. Parameters including drying time measurements, viscoelastic properties, surface wettability, solvent resistance, hardness, and flexibility were investigated. Furthermore, exploration into applications for blood contact devices was conducted using biocompatibility assays.

2.3. Experimental

2.3.1. Materials

The chemicals and their sources used for this study are described in **Table 2.2**. All chemicals were used as received unless specified otherwise.

Table 2.2. A description of the materials used in this study

Chemical	Designation	Vendor
Soybean oil	SBO	Crisco
Potassium hydroxide, ≥ 97%	KOH	Sigma-Aldrich
Sodium hydride, 95%	NaH	Sigma-Aldrich
Magnesium sulfate	$MgSO_4$	Sigma-Aldrich
Sodium hydroxide, ≥ 97%	NaOH	Sigma-Aldrich
Ethylaluminum sesquichloride, 97%	$Et_3Al_2Cl_3$	Sigma-Aldrich
p-toluenesulfonyl chloride, 99%	pTSCl	Sigma-Aldrich
Ethylene Glycol Vinyl Ether	2VOE	TCI America
Tri(ethylene glycol) monomethyl ether, 99%	TEGMME	Sigma-Aldrich
Methanol, 98%	Methanol	BDH Chemicals
Toluene	Toluene	BDH Chemicals
n-Hexane	n-Hexane	Sigma-Aldrich
Tetrahydrofuran, 99%	THF	J.T. Baker
Methylene chloride	CH_2Cl_2	BDH Chemicals
Cobalt 2-ethylhexanoate, 12% Co	Cobalt octoate	OMG Americas
Zirconium 2-ethylhexanoate, 18% Zr	Zirconium octoate	OMG Americas
Zinc carboxylate in mineral spirits, 8% Zn	Nuxtra® Zinc	OMG Americas

2.3.2. Synthesis and cationic homopolymerization of 2-(vinyloxy)ethyl soyate (2-VOES)

As illustrated in **Figure 2.2**, 2-VOES was synthesized *via* base-catalyzed transesterification of soybean oil (SBO) with an excess of 2-vinyloxy ethanol (2VOE). A two-neck, 100 mL round bottom flask equipped with a magnetic stirrer was charged with 20 g of SBO, 20 g of 2VOE, and 0.56 g of anhydrous KOH. The mixture was allowed to stir at 70 °C for three h under a nitrogen blanket. Following the reaction, the mixture was cooled to room temperature and diluted with 120 mL of n-hexane. The hexane layer was washed once with 30 mL of acidic, deionized (DI) water (pH 4.0), followed by multiple washes with pure DI water until the wash water was neutral. The hexane layer was dried overnight with $MgSO_4$. Using rotary evaporation, the product was collected by removal of n-hexane and dried under vacuum (50-60 mm of Hg) overnight.

Cationic polymerization of 2-VOES monomer was utilized to prepare the homopolymer, poly(2-VOES), as seen in **Figure 2.3**. Before the polymerization, 2-VOES was dried with $MgSO_4$. A three-neck round bottom flask was dried at 200 °C for 2 h before using. The cationogen, 1-isobutoxy-ethyl acetate (IBEA), was synthesized using the procedure described by Aoshima and Higashimura[12]. The Lewis acid co-initiator was $Et_3Al_2Cl_3$. The synthesis of poly(2-VOES) was conducted inside a dry nitrogen-filled glove box equipped with a heptane bath for conducting polymerizations at sub-ambient conditions. First, 20 g of 2-VOES and 0.007 g of IBEA (i.e. cationogen) were dissolved in 120 mL of dry toluene and chilled to 0 °C. Polymerization was initiated upon the rapid addition of 2.40 mL of co-initiator, $Et_3Al_2Cl_3$ solution (25 wt.% in toluene). The reaction proceeded for 18 h before being terminated upon the addition of 120 mL of chilled methanol which caused the polymer to precipitate. The isolated polymer was washed multiple times with methanol. The viscous liquid polymer was purified further by centrifuging at 4500 rpm at room temperature for 10 minutes and dried under vacuum (5-7 mm of Hg) overnight.

2.3.3. Synthesis of poly(ethylene glycol) methyl vinyl ether (PEGn) comonomers

In order to investigate the ability to tailor coating properties, such as crosslink density (XLD), tack-free times, hardness, solvent resistance, and surface wettability, of 2-VOES-based coatings, copolymers of 2-VOES and vinyl ether monomers derived from poly(ethylene glycol) (PEG) were prepared by cationic polymerization. PEG methyl vinyl ether (PEG*n*) comonomers with increasing ethylene glycol repeat units were synthesized, such that n = 3 (PEG3), 5 (PEG5), and 24 (PEG24), and used as a criterion to study changes in the previously mentioned coating properties of 2-VOES-based coatings. Pentaethylene glycol methyl vinyl ether (PEGMVE or PEG5) was synthesized using a two-step process. First, 98.5 g (0.6 mol) of triethylene glycol monomethyl ether, 24 g of sodium hydroxide, 100 mL of tetrahydrofuran (THF), and 30 mL of DI

water were added in a 500-mL, two-neck round bottom flask and produced a homogeneous solution with stirring. The mixture was cooled to 0 ℃ and then 114.3 g (0.6 mol) of p-toluenesulfonyl chloride in 50 mL of THF was added to the reaction mixture drop-wise using an addition funnel. The reaction was conducted for 2 h at 0 ℃ and 5 h at room temperature. The reaction mixture was then poured into 100 mL of ice water and the product extracted with methylene chloride (50 mL × 3). The organic layer was washed with DI water and subsequently dried with anhydrous magnesium sulfate. The tosylated product was recovered after the solvent evaporation by rotary evaporator and dried under vacuum overnight. Yield: 162.2 g (85%). 1H NMR (400 MHz, CDCl3, TMS): δ (ppm) 7.76 (d, 8Hz, 2H); 7.31 (d, 8Hz, 2H); 4.13 (t, 6Hz, 2H); 3.65 (t, 6Hz, 2H); 3.59 -3.56 (m, 6H); 3.51 -3.48 (m, 2H); 3.34 (s, 3H); 2.42 (s, 3H).

Next, 26.4 g (0.2 mol) of diethylene glycol monovinyl ether in 100 mL of THF was added dropwise to a suspension of NaH (60% dispersion in mineral oil) (10.0 g, 0.246 mol) in 450 mL of THF at 0 °C. The mixture was stirred for 2 h at 0 °C, and then a solution of tosyl compound (63.67 g, 0.06 mol) in 200 mL of THF was added dropwise. The solution was allowed to warm at room temperature and then heated at 60 °C overnight. The solid precipitation was filtered off and all volatile materials were removed by rotary evaporation. The light-yellow oil was dissolved into water (100 mL), and the upper layer (mineral oil) and lower layer (insoluble in water) separated. The aqueous layer was extracted with dichloromethane (3×100 mL). The remaining organic layer was dried with $MgSO_4$, and the solvent was removed by rotary evaporation. Yield: 41.2 g (77%). 1H NMR (400 MHz, CDCl3, TMS): δ (ppm) 6.5 (dd, 14Hz&7Hz, 1H); 4.15 (dd, 14Hz & 2Hz, 1H); 3.95 (dd, 8Hz & 2Hz, 1H); 3.81 (t, 4Hz, 2H); 3.70 (t, 4Hz, 2H); 3.66 – 3.59 (m, 14H); 3.52 (t, 4Hz, 2H); 3.35 (s, 3H).

2.3.4. Cationic copolymerization of 2-VOES and PEGn

Using the same cationic polymerization process to prepare poly(2-VOES), three different series of vinyl ether copolymers comprised of 2-VOES with PEG3, PEG5, or PEG24 were prepared (**Table 2.3**, **Figure 2.4**). Within each series, three copolymers with different monomer compositions were prepared such that the fraction of PEG*n* monomer varied from 15 wt.% to 25 wt.% to 50 wt.%. In total, nine different vinyl ether copolymers were synthesized. All polymerizations were conducted in a glove box equipped with a cold well. The synthesis of poly(2-VOES-*ran*-PEG5) (75/25) (w/w) is described as follows: 5.56 g of 2-VOES, 15 g of PEG5, and 0.007 g of IBEA initiator were dissolved in 120 mL of toluene and the reaction mixture was cooled to 0 °C. Polymerization was initiated upon the rapid addition of 2.40 mL of coinitiator, $Et_3Al_2Cl_3$ solution (25 wt.% in toluene). After 18 h, polymerization was terminated upon the addition of 120 mL of chilled methanol, causing the polymer to precipitate out of solution.

Purification of the copolymer was done by transferring the reaction mixture to a 1 L separatory funnel with 250 mL of methylene chloride. The mixture was washed with DI water (100 mL x 3) and the copolymer was collected by rotary evaporation of methylene chloride. Unreacted 2-VOES was removed by column chromatography. Silica gel was utilized as the stationary phase and hexane as the mobile phase. After unreacted monomer was eluted from the column, the purified copolymer was flushed from the column with methylene chloride. Finally, the copolymer was isolated by vacuum stripping the volatiles.

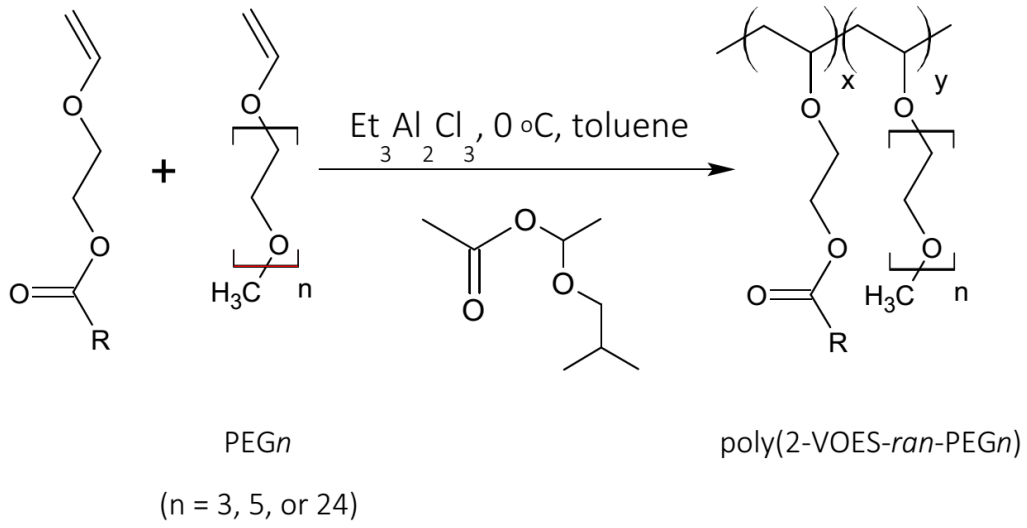

Figure 2.4. Cationic copolymerization of poly(2-VOES-ran-PEGn)

2.3.5. Preparation of poly(vinyl ether) coatings and free films

Poly(2-VOES) and the nine poly(2-VOES-*ran*-PEG*n*) copolymers described in the previous section were used to prepare crosslinked coatings by curing *via* autoxidation**.** The autoxidation drier package was composed of a mixture of Co, Zr, and Zn organometallic compounds. The preparation of each reaction mixture was as follows: 10 g of neat polymer, 8 mg of cobalt octoate, 40 mg of zirconium octoate, and 450 mg of Nuxtra® Zinc were blended using a FlakTek mixer operating at 3500 rpm for 60 seconds. Free films and coated steel panels were prepared from each reaction mixture containing the drier package. The steel panels (product number SP-105337) were purchased from Q-LAB. Coatings were prepared by casting the reaction mixtures onto the panels using a drawdown bar with a wet film thickness (WFT) of 8 mils. Free film specimens were prepared by casting each reaction mixture over Teflon®-laminated glass panels. After the coatings were properly cured, free film samples were collected by peeling the film from the Teflon® substrate. All samples were allowed to cure/crosslink for four weeks before testing. The drying times of each formulation were evaluated by casting the neat reaction mixtures onto BOROSIL® glass panels using a drawdown bar with a 1 mil WFT.

2.3.6. Methods and instrumentation

2.3.6.1. Nuclear magnetic resonance (NMR) spectroscopy

Successful synthesis and final composition of the different poly(vinyl ether)s were confirmed by proton NMR using an AVANCE III HDTM 400 MHz high-performance digital NMR spectrometer (Bruker; Billerica, MA). $CDCl_3$ was used as the lock solvent. Data acquisition was completed using 32 scans.

2.3.6.2. Dynamic mechanical analysis (DMA)

Viscoelastic properties of select free film specimens from poly(2-VOES) and 2-VOES-based copolymers were examined using a Q800 Dynamic Mechanical Analyzer (TA Instruments Inc.) over a temperature range of -90 °C to 150 °C. DMA multi-frequency strain was used as the testing mode. The heating rate, frequency, and strain amplitude for all samples was 2 °C/min, 1 Hz, and 0.1 %, respectively.

2.3.6.3. Drying time measurements

Drying time measurements of the neat polymer mixtures with the drier package were recorded according to ASTM D1640/D1640-M-14 (Method A). According to this method, a freshly cast coating was deemed “set-to-touch” when no coating material was transferred after lightly pressing a fingertip to the surface of the coating. “Dust free” times were determined by the cotton fiber test method. Finally, the coating was considered “tack-free” once a Zapon tack tester was immediately released from the surface of the coating after removing a load of 300 g from the cantilever.

2.3.6.4. Gel permeation chromatography (GPC)

Molecular weight and molecular weight distribution of all 10 poly(vinyl ether)s (poly(2-VOES) and nine copolymers derived from 2-VOES and PEG*n*) were obtained by GPC using a

Symyx Rapid-GPC equipped with an evaporative light scattering detector (PL-ELS 1000) and 2Xpl gel mixed B column (10 μm particle size). Samples were prepared in THF at a concentration of 2 mg/mL. Polystyrene was used as the calibration standard.

2.3.6.5. Water contact angle measurements

Changes in water contact angle as a function of time were observed on coatings from poly(2-VOES) and 2-VOES-based copolymers containing 15 wt.% PEG3, PEG5, and PEG24 using a contact angle/surface tension analyzer (FTA 125). A drop of DI water (5-8 μL) was dispensed on the coating surface and the contact angle was recorded once per minute for 5 minutes.

2.3.6.6. Atomic force microscopy (AFM)

Surface morphology of coatings from poly(2-VOES) and 2-VOES-based copolymers containing 25 wt.% PEG3, PEG5, and PEG24 were evaluated by AFM using a Veeco Dimension 3100 Atomic Force Microscope. Parameters such as component phase separation and surface roughness were investigated.

2.3.6.7. Coating characterization

Chemical resistance on steel coated panels with 2-VOES-based poly(vinyl ether)s was performed with a modified version of ASTM D5402, in which methyl ethyl ketone (MEK) double rubs were carried out using a 2-lb ball peen hammer. Cheese cloth was fastened to the hammer using a wire, and the hammer was dipped in MEK solvent every 25 rubs. Hardness was determined by König pendulum hardness test as described by ASTM D4366-16. ASTM D3363-05 was used to evaluate the pencil hardness of the coatings. Reverse impact resistance of the steel coated panels was conducted according to ASTM D2794-93. Flexibility of the coatings was evaluated by the conical mandrel bend test as described by ASTM D522.

2.3.6.8. Biocompatibility studies

The potential to use these 2-VOES-based coatings for applications such as blood contact devices was investigated by two separate biocompatibility studies. Bovine serum albumin (BSA) adsorption onto selected coatings was measured using a modified immunosorbent assay[31]. Three replicates of each coating composition were exposed to 0.15 mL of BSA solution prepared in phosphate buffered saline (PBS) (3.0 mg mL^{-1}) and statically incubated for 1 h at 37 °C. The protein solution was removed, and each well was rinsed thrice with PBS before the addition of 0.50 mL of TBS-T20, which was incubated for 30 minutes at 37 °C. Following the incubation time, the wells were rinsed thrice with TBS-T20. Then, 0.5 mL of goat anti-fibrinogen (HRP)-conjugated polyclonal detection antibody (1:50,000 dilution in TBS-T20) was added to each well before being incubated for 1 h at 37 °C. 0.5 mL of TMB di-HCl substrate solution was added and allowed to incubate for 30 minutes at 37 °C. The incubation was stopped upon the addition of 2 M H_2SO_4 to each well and plates were shaken on an orbital shaker for 15 minutes at room temperature. To quantify the amount of adsorbed BSA on each surface, 0.15 mL of each resulting solution was transferred to a 96-well plate, and absorbance was measured at 450 nm using a spectrophotometer (Tecan Safire^2). An unmodified silicone-coated slide served as a hydrophobic control with well-known high protein adsorption.

Red blood cell (RBC) hemolysis studies were carried out on select 2-VOES-based coatings using a variation of methods based on ASTM F756-87[32-33]. Several steps of this protocol were conducted using the Tecan EVO liquid handling system. Fresh whole blood from healthy albino rabbits (1:10 in sodium citrate) were purchased from Pel-Freez Biologicals (Rogers, AR). The whole blood was shipped overnight from Pel-Freez Biologicals and used immediately upon receipt the following day. The whole blood-sodium citrate suspension was diluted 1:10 in saline (0.9%

NaCl). 1.0 mL of this RBC suspension was added to each well of the copolymer coated plates and incubated for 4 h at 37 °C under static conditions. The RBC suspensions were transferred from each well of the 2-VOES-based coated plates into 1.5 mL tubes and centrifuged at 750 x g for 5 minutes. 0.20 mL of each sample were transferred to a 96-well plate and the absorbance was measured at 576 nm using a multi-well plate spectrophotometer to measure the release of free hemoglobin. RBCs suspended in DI water and saline (incubated in uncoated wells of tissue culture polystyrene plates) were utilized as a positive and negative control, respectively, to facilitate hemolysis comparisons among the experimental coatings.

2.4. Results and discussion

2.4.1. Synthesis and homopolymerization of 2-VOES monomer

2-VOES monomer was successfully synthesized *via* base-catalyzed transesterification of soybean oil and 2VOE. The process is similar to the production of soy biodiesel, but 2VOE was used in place of methanol[19, 21]. ^{1}H NMR of 2-VOES can be seen in **Figure 2.5a**. Successful synthesis of 2-VOES monomer was confirmed by chemical shift and integrated peak area data.

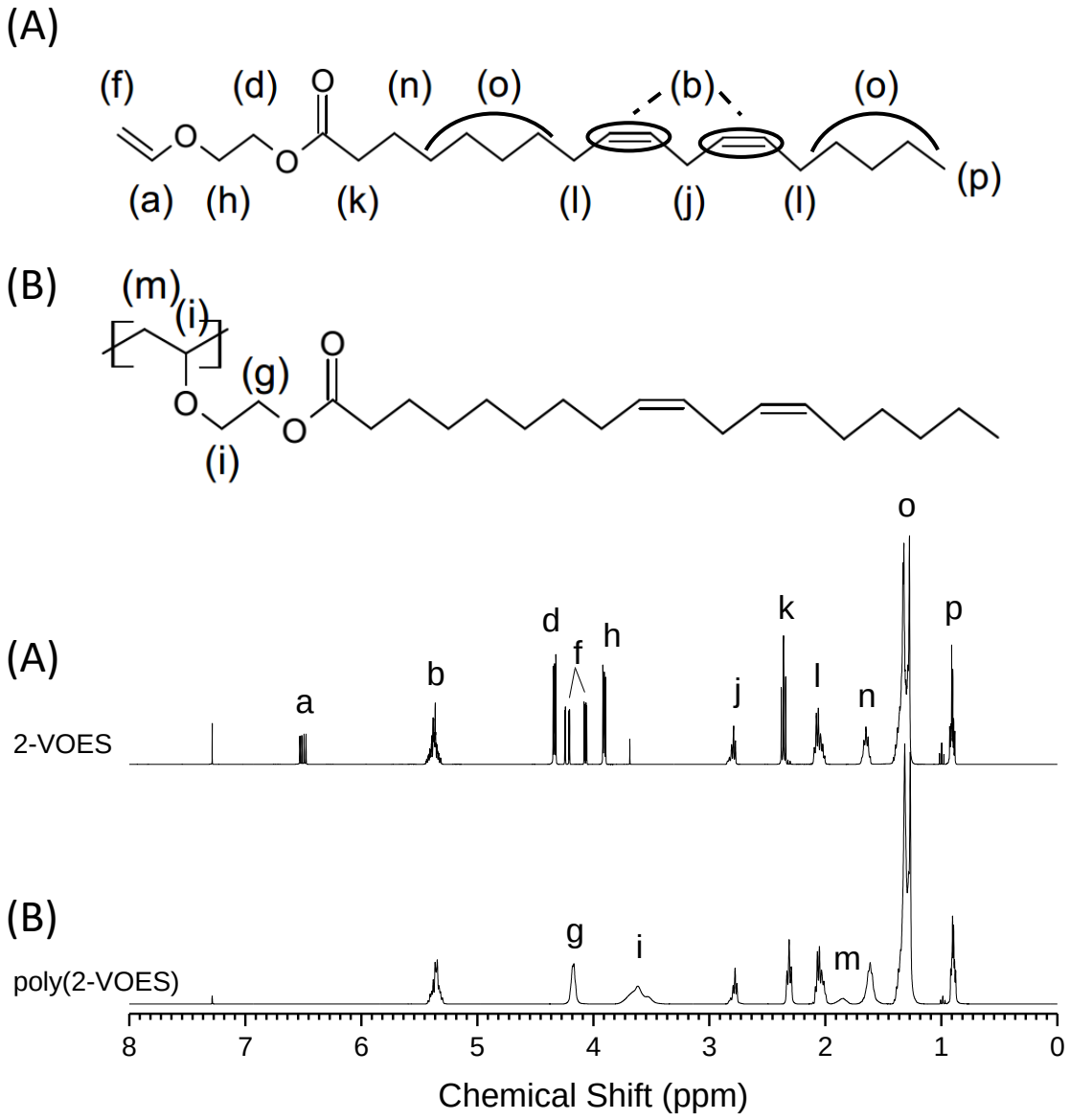

Figure 2.5. ^{1}H NMR structure and spectra of 2-VOES monomer (**A**) and poly(2-VOES) (**B**)

Cationic polymerization of 2-VOES was used to synthesize the homopolymer, poly(2-VOES). IBEA was used as the cationogen, $Et_3Al_2Cl_3$ as the co-initiator, and toluene as the solvent. As discussed previously, the oxygen atom next to the vinyl group is expected to control the activation energy of the carbocation upon the addition of a vinyl ether monomer. This strong stabilizing effect then directs the propagation reaction to proceed exclusively through the vinyl ether functionality and preserves the unsaturation of the fatty acid chains for post polymerization

autoxidation. Successful synthesis of the light-yellow homopolymer was confirmed by ^{1}H NMR and compared to 2-VOES monomer as seen in **Figure 2.5b**. From the spectra, it was determined that polymerization proceeded exclusively through the vinyl ether functionality. This was confirmed by the disappearance of the vinyl ether proton ("a") in the poly(2-VOES) spectrum. Further analysis into the preservation of the unsaturation provided by the parent soybean oil was investigated when integrating the signals correlating to the bis-allylic ("j"), allylic ("l"), and vinyl ("b") protons of the fatty acid portion of the polymers. The signal representing the end chain methyl protons ("p") was used for normalization purposes. By comparing the normalized peak integration values for the homopolymer to the corresponding signals obtained from 2-VOES monomer, it was determined that approximately 15% of the unsaturation from the fatty acid chains was consumed during the polymerization. This portion of consumed unsaturation represents termination of propagating chains and could offer an explanation to the larger polydispersity indexes (PDI) that were calculated for the poly(vinyl ether)s synthesized in this study.

2.4.2. Synthesis of copolymers from 2-VOES and PEGn

Poly(vinyl ether) copolymers from different weight percentages of 2-VOES and PEG methyl vinyl ether (PEG*n*) comonomers of varying chain length were prepared by cationic polymerization as seen in **Figure 2.4**. Three different PEG*n* comonomers with increasing length of ethylene glycol repeat units were investigated for this study; n = 3 (PEG3), 5 (PEG5), and 24 (PEG24). In order to determine the impact on 2-VOES-based coating properties, such as XLD, tack-free times, hardness, and solvent resistance, the weight ratio of the different PEG*n* comonomers with 2-VOES was varied such that copolymers were expected to contain 15, 25, or 50 wt.% PEG*n*.

^{1}H NMR was used to confirm successful incorporation of the two components into the final copolymers, as well as determine copolymer composition (**Figure 2.6**). End group analysis of the pendent chains within the copolymer structure was used to calculate the compositions of the final copolymers. The signal corresponding to the end chain methyl protons of the fatty acid chains ("p") from 2-VOES was used for normalization purposes. Using the ratio of the initial monomer feed, simple arithmetic was used to calculate the expected integral value of the end chain methyl protons ("r") from the pendent PEG*n* chains, assuming total incorporation of the two components. The experimentally integrated value of the "r" signal matched the theoretically calculated value, suggesting total incorporation of the two monomers into the final copolymer. From the integrated signals correlating to the end group methyl protons of both 2-VOES and PEG*n* components, it was determined that the amount of the components in the purified product matched the ratio of the original monomer feed.

Using the same technique as described above for poly(2-VOES), preservation of the unsaturation provided by the parent soybean oil throughout the copolymerization was investigated using integration of the signals correlating to the bis-allylic ("j"), allylic ("l"), and vinyl ("b") protons of the fatty acid portion of the polymers. The signal representing the end chain methyl protons ("p") of the 2-VOES fraction was used for normalization purposes. By comparing the normalized peak integration values for the poly(2-VOES-*ran*-PEG3) (85/15) (w/w) copolymer to the corresponding signals obtained from 2-VOES monomer, it was determined that approximately 10% of the unsaturation from the fatty acid chains was consumed during the polymerization. As mentioned above, the consumption of the unsaturation within the fatty acid chains could be a factor in the broader than expected molecular weights and PDI values that were observed for the copolymers used in this study.

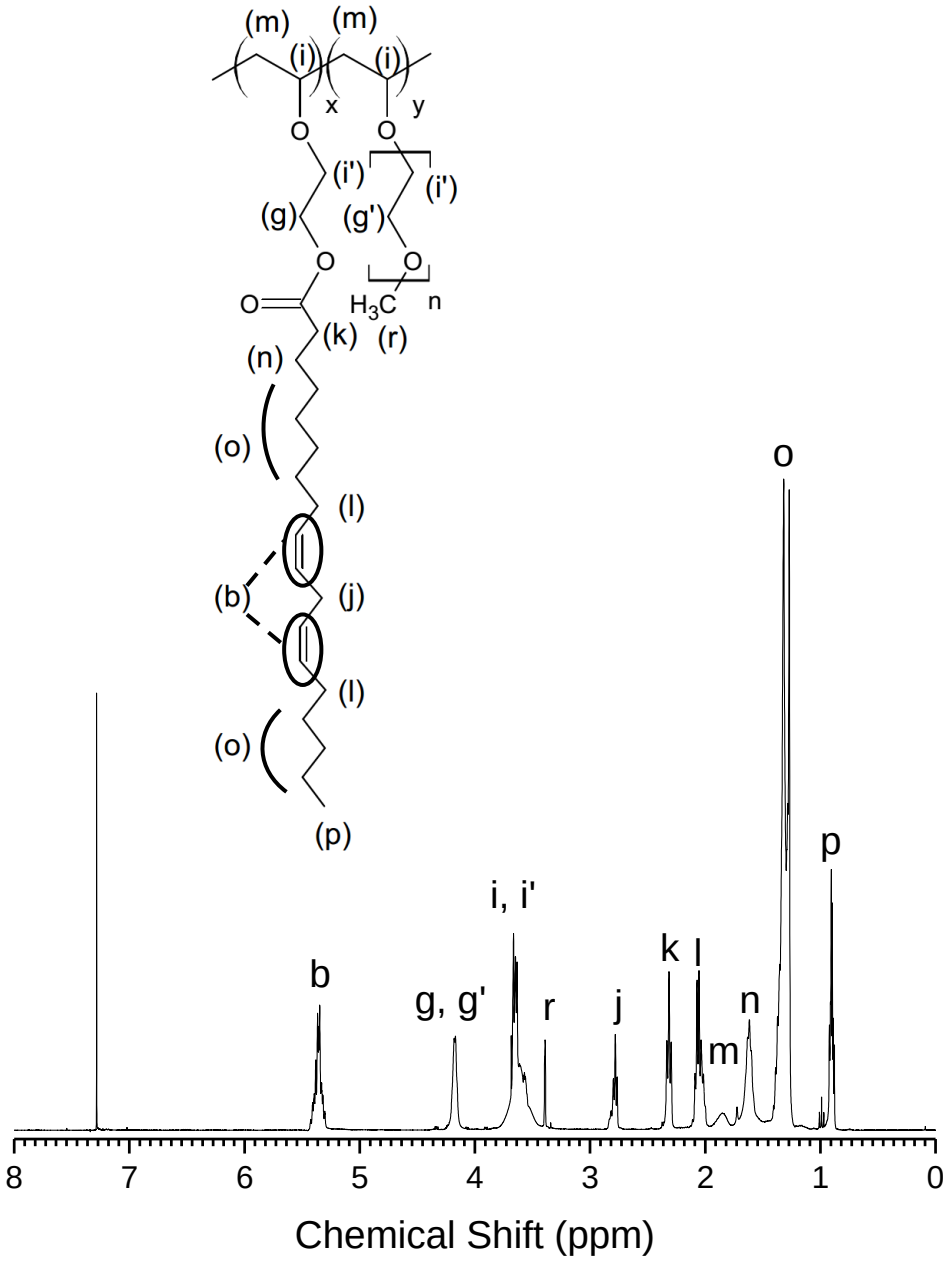

Figure 2.6. ^{1}H NMR spectrum of poly(2-VOES-ran-PEG3) (85/15) (w/w)

It was expected that by using the living cationic polymerization process, greater control of polymer molecular weight and molecular weight distributions would be attainable. As seen in **Table 2.3**, this control was not sustained for all copolymerization reactions. Of the 10 different polymers that were prepared, the final molecular weights were basically divided into two categories; “lower” molecular weight (~10 kDa) and “higher” molecular weight (~25 kDa).

Additionally, the molecular weight distributions were broader than expected (PDI > 2), compared to previously reported values[8]. The inconsistencies in final molecular weight between the 10 2-VOES-based samples may be due to the consumption of unsaturation of the fatty acid chains during the polymerization, as discussed above, and/or by improper ratios between the coinitiator (i.e. $Et_3Al_2Cl_3$) and the 2-VOES monomer[13]. These variations in molecular weight can be one of the factors used to explain discrepancies in coating properties such as crosslink density (XLD) and pendulum hardness.

Coatings from poly(2-VOES) homopolymer and the nine different copolymers were formed by a crosslinking mechanism through the unsaturation of the fatty acid pendent chains of 2-VOES. By controlling the concentration of monomer, as well as the ratio between monomer and coinitiator (i.e. $Et_3Al_2Cl_3$), it was expected that each synthesized copolymer would have comparable molecular weight and weight distribution using living cationic polymerization. This trait was desired in order to accurately compare changes in XLD as the composition of the copolymers was altered. If the molecular weights for all reactions were equivalent, it was expected that poly(2-VOES) would exhibit the highest XLD compared to coatings with greater amounts of PEG*n*. Based on the GPC results in **Table 2.3**, the two poly(vinyl ether) systems to use for comparative purposes can be poly(2-VOES) and PEG24 (15 wt.%) because they are similar in molecular weight and have relatively narrow molecular weight distribution.

Table 2.3. Molecular weight, hardness, and film thickness data for poly(2-VOES) and the different copolymers

	Poly(2-VOES)	PEG3			PEG5			PEG24	
Wt.%	-	15	25	50	15	25	50	15	25
M_n (kDa)	24	10.7	8.5	10.0	25.7	19.0	7.5	25.9	7.0
PDI	1.4	1.85	1.90	1.45	2.09	2.08	1.95	1.17	1.9
Pencil Hardness (gouge)	7H	3H	2H	6B	4H	3H	F	H	B
Thickness (μm)	158 ± 21.0	162 ± 16.1	142 ± 21.3	114 ± 7.23	169 ± 10.8	145 ± 17.6	134 ± 23.4	136 ± 8.3	130 ± 13.6

For coating systems like the ones evaluated in this study, the XLD was expected to be a determining factor in a number of physical properties as discussed in the following sections. For example, as seen in **Table 2.3**, the pencil hardness is a function of the amount of unsaturation present in the copolymer provided from the 2-VOES fatty acid chains. Poly(2-VOES) exhibits the hardest coating because the unsaturation can more easily form a crosslinked network. As portions of 2-VOES are replaced with PEG*n* fragments, the percentage of 2-VOES pendent chains that interact and form a crosslinked network is reduced, leading to a decrease in XLD and, ultimately, coating hardness.

Although the pencil hardness appears to be dependent on the amount of unsaturation present, the differences in molecular weight and weight distribution of the copolymers distorts this trend as can be seen when comparing the PEG3 and PEG5 copolymer series. Because of the shorter PEG chains in the PEG3 series, it was expected that these coatings would be harder than the coatings of the PEG5 series. However, the three copolymers in the PEG 3 series have much lower molecular weights compared to the copolymers of the PEG5 series. This reduced molecular weight correlates to lower amounts of unsaturation per molecule compared to their respective counterparts in the PEG5 series, which reduces the XLD and coating hardness.

2.4.3. Drying time measurements

An important property for polymer coatings that cure/crosslink by autoxidation is tack-free time (**Figure 2.7**). "Tack-free" times were determined according to ASTM D1640. A tack-tester was pressed against the surface of the coating with a 300 g load for five seconds before removing the load. If the coating was "tack-free", the tack-tester would release from the coating surface. Short tack-free times are desired for most coating applications. This helps reduce the chance of introducing surface defects by debris from the surrounding atmosphere and allows the coated substrates to be handled and/or used with less wait time.

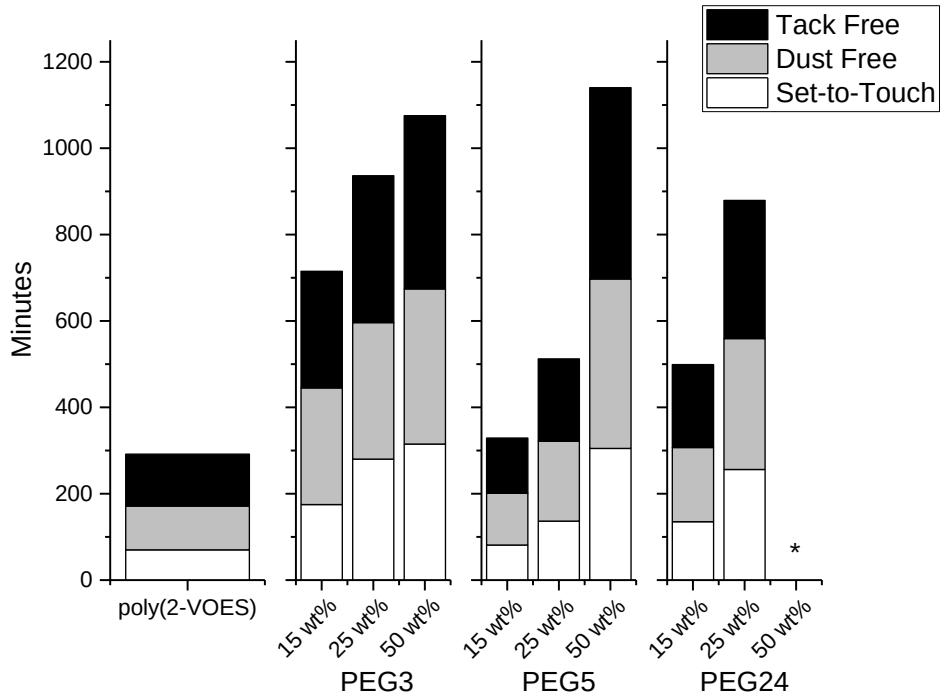

Figure 2.7. Drying times as a function of PEGn content within the copolymer (* PEG24 (50 wt.%) copolymer did not cure and remained tacky even after four weeks)

Coating systems that are derived from binders having glass transition temperatures (T_g) significantly above ambient temperature often correlate tack-free time to the rate of solvent evaporation. On the other hand, for binders that have T_g values well below ambient temperature, tack-free time is dependent on the rate of formation of a crosslinked network. For these alkyd-type

coatings, the crosslinked networks were formed *via* autoxidation of the unsaturation provided by the parent soybean oil fatty acid chains. Drying times for poly(2-VOES) and select 2-VOES-based copolymers can be seen in **Figure 2.7**. As expected, poly(2-VOES) became tack-free in the shortest amount of time due to the greatest amount of unsaturation present within the system. Coatings derived from the different 2-VOES-based copolymers required longer times to cure/crosslink as the unsaturation from 2-VOES was replaced with different weight percentages of the PEG methyl vinyl ether comonomers. Copolymer tack-free times increased with the percent of PEG comonomer present as such, 15 wt.% < 25 wt.% < 50 wt.%.

Longer tack-free times were observed for coatings containing PEG3 comonomer compared to their PEG5 analogs due to differences in molecular weight and PDI. The PEG3 copolymers all had molecular weight values around 10 kDa, whereas the PEG5 copolymers (specifically, 15 and 25 wt.%) had much higher molecular weight values between 20-25 kDa and larger PDI values around 2. The higher molecular weights correlate to larger amounts of unsaturation per molecule compared to the PEG3 copolymers. Even though it was expected the PEG3 series would become tack-free more quickly compared to the longer PEG5 series, the average concentration of unsaturation per polymer chain was lower, ultimately increasing the tack-free time.

The number average molecular weight (M_n) is not the only parameter useful for comparing the properties of the coatings. The copolymers of the PEG5 series have larger PDI values compared to their PEG3 counterparts. These higher PDI values correlate to larger fractions of higher molecular weight species within the 2-VOES-based copolymer samples, or greater amounts of unsaturation per molecule that can participate in autoxidation, compared to the copolymers within the PEG3 series. However, when M_n and PDI are similar for two different copolymers, such as poly(2-VOES) and PEG24 (15 wt.%), useful conclusions correlating tack-free time to copolymer

composition can be made. As expected, the presence of PEG24 (15 wt.%) extends the tack-free time as the amount of unsaturation from 2-VOES fatty acid chains available for autoxidation is reduced compared to poly(2-VOES).

The copolymer poly(2-VOES-*ran*-PEG24) (50/50) (w/w) was unable to cure/crosslink even after four weeks and the coating remained tacky. It is reasonable to say that curing was unable to occur in this system due to the longer PEG chains (n=24) which could impede interactions between the 2-VOES chains. With these fatty acid chains unable to interact, crosslinking was not able to proceed, and the coating remained tacky.

2.4.4. Viscoelastic properties of crosslinked free films

Free films from poly(2-VOES) and select 2-VOES-based copolymers were characterized by DMA to evaluate the viscoelastic properties. T_g values were determined as the peak maximums of the tan δ response (**Figure 2.8b, Table 2.4**). Poly(2-VOES) and the select 2-VOES-based copolymers exhibit glass transition temperatures below ambient temperature. From the data, a general trend can be observed in that as the chain length of the PEG vinyl ether comonomer increases (n=3<5<24), the T_g decreases due to the increased mobility of the pendent PEG vinyl ether chain segments that do not participate in forming a crosslinked network.

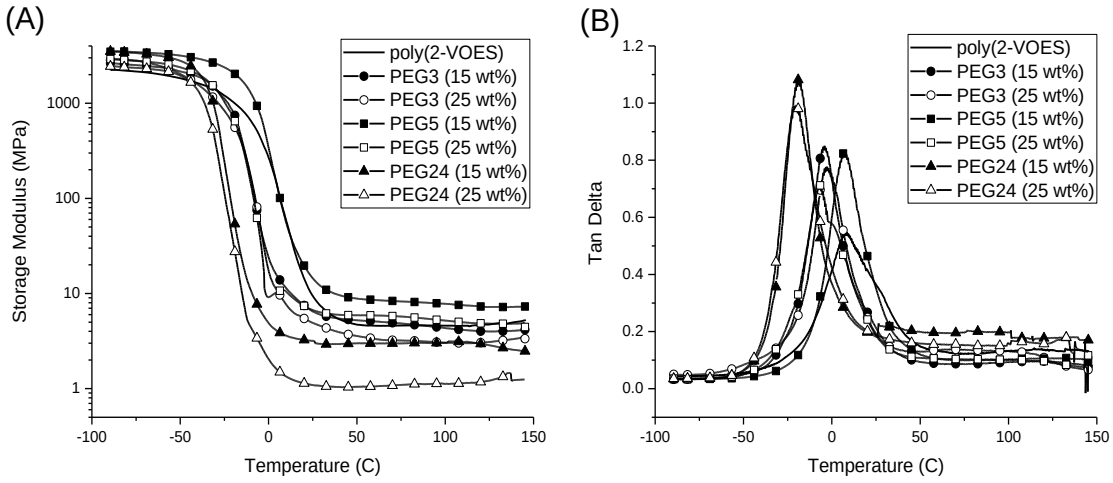

Figure 2.8. Viscoelastic properties a) storage modulus and b) tan δ of select crosslinked networks

For thermoset networks, an important parameter to consider is the crosslink density (XLD) as it affects many physical properties such as chemical resistance, hardness, and impact resistance. A convenient method to estimate XLD of theses networks is to evaluate the storage modulus at a temperature well above the temperature range associated with the T_g. Within this region, commonly referred to as the rubbery plateau, polymers exhibit long-range rubber elasticity, or the ability to return to their original shape after being distorted. For thermoset networks, the XLD largely determines the elastic response of the material. When the material is stretched, the crosslinks throughout the network prevent other polymer chains from slipping past one another, limiting the segmental motions that dissipate mechanical energy. More highly crosslinked networks restrict the dissipation of mechanical energy and exhibit increased values for storage modulus. Estimates for XLD of select 2-VOES-based free films were calculated using the theory of rubber elasticity, as described by the following equation:

$$\upsilon = E'/(3RT) \qquad \text{(Equation 2.1)}$$

where υ is the crosslink density defined as the moles of crosslinks per unit volume of material, *E'* is the storage modulus (MPa) in the rubbery plateau region, *R* is the gas constant (cm^3 MPa mol^{-1}

K^{-1}), and *T* is the temperature (K) corresponding to the storage modulus value. Using **Equation 2.1**, *E'* data at 80 °C were used to estimate the crosslink density of the select networks, and the results are shown in **Table 2.4**.

Table 2.4. Viscoelastic properties of select crosslinked networks determined from DMA measurements

	Wt. %	**M_n (kDa)**	**PDI**	**T_g (°C)†**	**Plateau Modulus (MPa)‡**	**XLD (mol cm^{-3})**
Poly(2-VOES)	--	24.0	1.4	8.00	4.62	5.25×10^{-4}
PEG3	15	10.7	1.85	-2.32	4.76	5.4×10^{-4}
	25	8.5	1.9	-2.57	3.18	3.61×10^{-4}
PEG5	15	25.7	2.09	7.75	8.17	9.28×10^{-4}
	25	19.0	2.08	-5.85	5.67	6.44×10^{-4}
PEG24	15	25.9	1.17	-17.43	3.02	3.43×10^{-4}
	25	7.0	1.9	-18.94	1.11	1.26×10^{-4}

†T_g was reported as the peak maximum of the tan δ response curve. ‡ Plateau modulus values for all coatings were determined in the rubbery plateau region at 80 °C.

As discussed above, it was expected that the XLD of poly(2-VOES) would be greater compared to copolymer networks where PEG vinyl ether comonomer replaced a portion of 2-VOES, assuming comparable molecular weights were achieved, since the crosslinking mechanism involves the bis-allylic and allylic protons present in the pendent fatty acid chains from 2-VOES. From **Figure 2.8a** and **Table 2.4**, the storage modulus responses of poly(2-VOES) and the 2-VOES-based copolymers can be seen. Similar to the discussions in previous sections, correlations between poly(2-VOES) and PEG24 (15 wt.%) can be made based on their similarities in molecular weight and PDI. Differences in XLD for these two systems can be explained by the reduced amount of unsaturation per polymer molecule, as portions of PEG24 are incorporated into the copolymer, compared to poly(2-VOES). In the PEG24 (15 wt.%) copolymer, there are fewer fragments (i.e. PEG24 pendent chains) participating in the crosslinking reaction, reducing the XLD. This result concurs with the trend observed in tack-free time measurements. On the other

hand, the XLD for the series of PEG5 copolymers was higher than poly(2-VOES) and the PEG3 copolymers since the PEG5 copolymers have a higher molecular weight and PDI, providing more unsaturation per molecule, which leads to a more highly crosslinked network. Furthermore, *E'* decreases when the fraction of the same PEG vinyl ether comonomer is increased (i.e. $E'_{15\ wt.\%} > E'_{25\ wt.\%}$). This result is consistent with expectations and the results of the drying time measurements.

2.4.5. Physical properties of coated substrates

According to ASTM D4366, pendulum hardness of a polymer coating is characterized by setting two ball bearings rocking on the surface of a coating *via* a pendulum. The rocking motion of the ball bearings will dissipate more rapidly for softer polymer coatings compared to harder coatings. For these crosslinked 2-VOES-based coatings, all of which have T_g values below ambient temperature, the pendulum hardness was expected to be largely dependent on the XLD that was achieved throughout the allotted curing time of four weeks. Pendulum hardness data were plotted in **Figure 2.9** as a function of PEG vinyl ether comonomer chain length and amount. Unlike expectations, and the results of the pencil hardness test (**Table 2.3**), it can be seen from the data that incorporation of the PEG vinyl ether comonomers enhanced the hardness of the copolymer coatings compared to coatings comprised of poly(2-VOES). The larger molecular weights and PDI for the copolymers in the PEG5 series represent a larger amount of unsaturation per polymer molecule compared to lower molecular weight copolymers in the PEG3 series. With this greater amount of unsaturation, a more highly crosslinked network was formed, providing increased pendulum hardness for the PEG5 series compared to their PEG3 counterparts. Based on XLD calculations (**Table 2.4**) it was expected that poly(2-VOES) pendulum hardness would be comparable to the PEG3 series of copolymers, and even outperform the PEG24 series. In fact,

poly(2-VOES) coatings exhibited the softest surfaces of all the 2-VOES-based coatings analyzed. Even when poly(2-VOES) is compared to PEG24 (15 wt.%), both with similar molecular weights and PDI, the homopolymer appears softer than when PEG24 is incorporated into the system. This suggests perhaps an underestimate for XLD values for the 2-VOES-based copolymers.

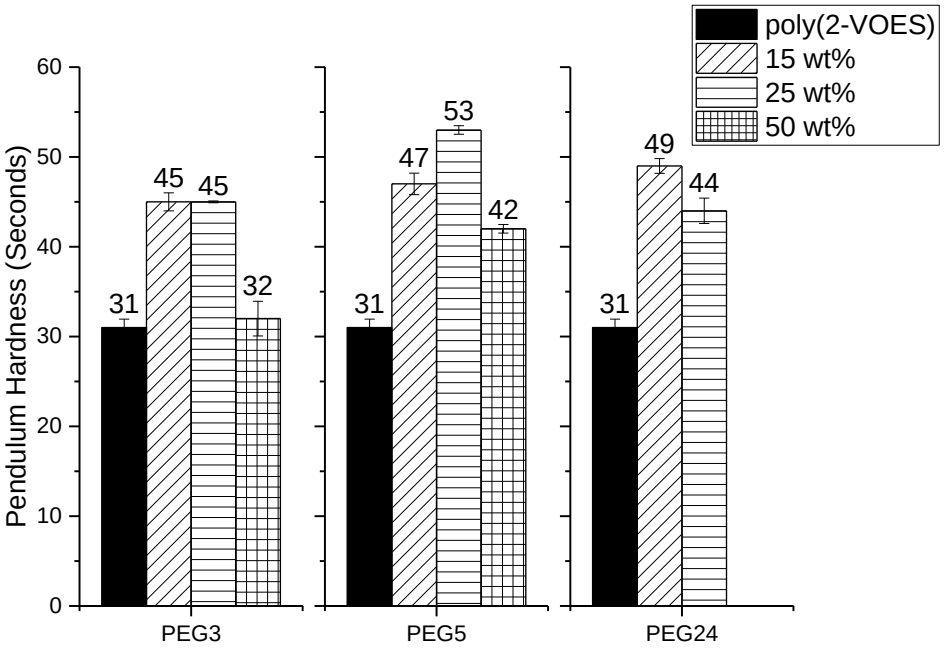

Figure 2.9. König pendulum hardness for 2-VOES-based crosslinked networks as a function of PEG*n* chain length and amount

Unlike pendulum hardness, a more distinct trend was observed when evaluating the solvent resistance of the crosslinked coatings. Solvent resistance, defined as the minimum number of MEK double rubs that resulted in visible changes to the coating surface, are largely dependent on XLD for thermoset coatings having T_g values below ambient temperature. Based on the calculated XLD values, it was expected that the solvent resistance of poly(2-VOES) would be comparable to, if not worse than, those of the PEG3/5 copolymers. Shown in **Figure 2.10**, the solvent resistance was plotted as a function of PEG vinyl ether comonomer chain length and amount. Solvent resistance decreased as the fraction of PEG*n* comonomer increased. One possible explanation for the better solvent resistance of poly(2-VOES) coatings is the efficiency of the crosslinking mechanism

during network formation compared to 2-VOES-based copolymers containing fractions of PEG*n*. Without the presence of PEG pendent chains, a higher percentage of fatty acid pendent chains from 2-VOES portions participate in the autoxidation process. This reduces the number of dangling chain ends that are not incorporated into the network, ultimately forming a more complete crosslinked network. Once again, the correlation between molecular weight and PDI to XLD and certain coating properties was observed when comparing the results for 2-VOES-based copolymers containing PEG3 and PEG5. With higher molecular weight and PDI, more unsaturation per polymer molecule was present in the PEG5 series, creating a more highly crosslinked network compared to the copolymers containing PEG3.

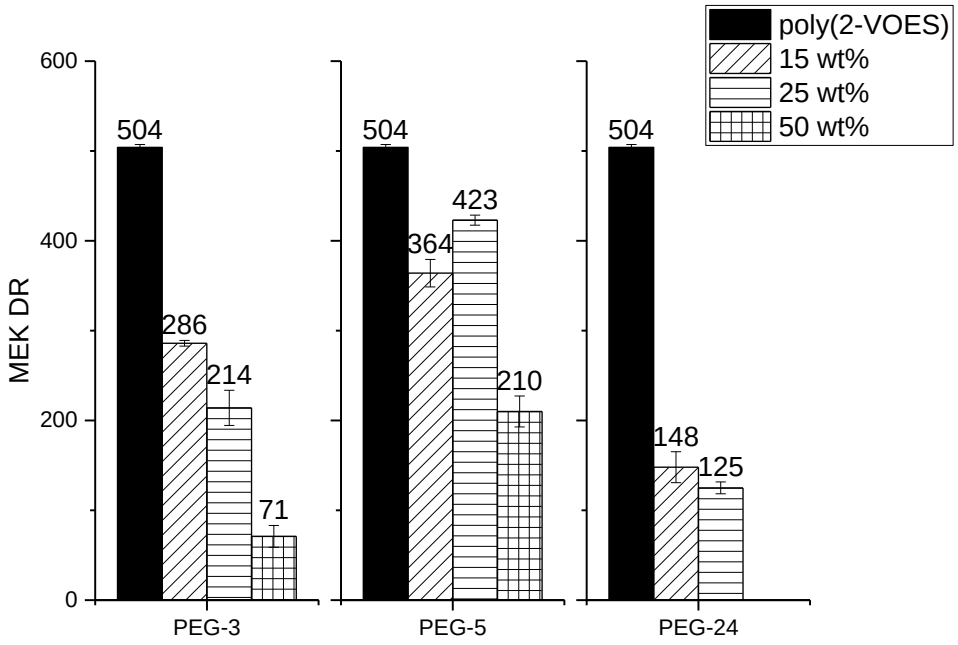

Figure 2.10. Solvent resistance of crosslinked networks as a function of PEG*n* chain length and amount

The flexibility of the coatings was evaluated by the mandrel bend test, as described by ASTM D522. The results of the mandrel bend test are plotted in **Figure 2.11**. Flexibility was greatly improved as larger fractions of PEG vinyl ether comonomers were incorporated into the 2-VOES-based copolymers. Rationale for this trend can be explained by the decreasing number of

chains that participate in network formation as the amount of PEG*n* increases. By not being incorporated into the elastic network, these dangling chains act as plasticizers within the coating. This effect was also shown in the DMA results when comparing the T_g of PEG24 (15 wt.%) to poly(2-VOES). The incorporation of the PEG24 fraction reduced not only the XLD, but the glass transition temperature as well. From **Figure 2.11**, this plasticizing effect was observed upon the addition of even 15 wt.% PEG*n*. All coatings that contained PEG*n* comonomer showed no cracking or delamination at 32% elongation, which was the highest strain associated with this test method.

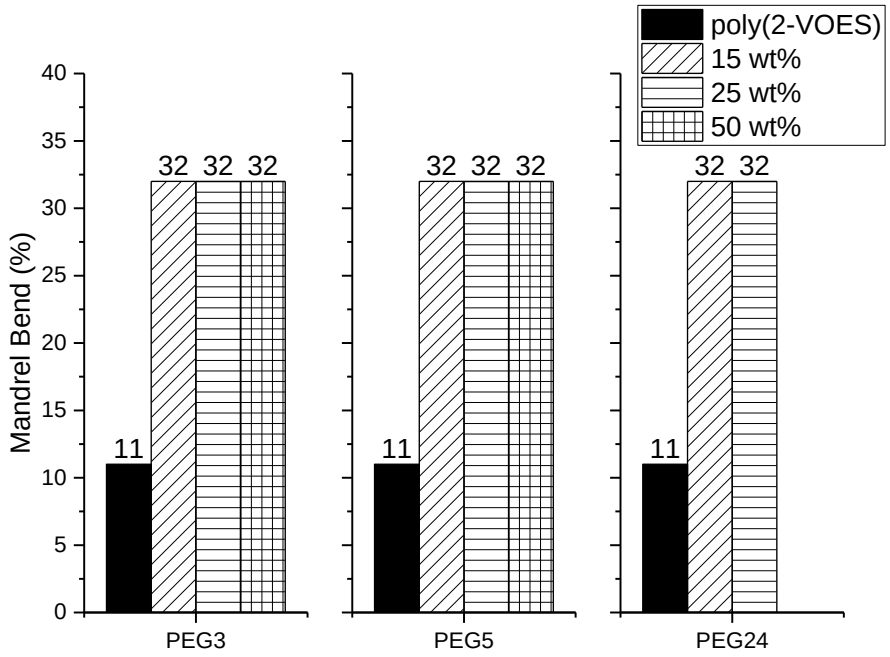

Figure 2.11. Flexibility of the crosslinked networks as a function of PEG*n* chain length and concentration

Using the guidelines described by ASTM D2794, the impact resistance of the crosslinked polymer coatings was characterized by impacting the uncoated side of the panels (i.e. reverse impact). In **Figure 2.12**, the impact resistance of the 2-VOES-based coatings was improved as amount of PEG*n* comonomers increased. As shown previously in **Figure 2.8b** and **Figure 2.11**, higher amounts of the PEG vinyl ether comonomers in the copolymers increases the number of

dangling chains that do not participate in network formation and increase the elasticity of the coating. From this information, it makes sense that poly(2-VOES) performs worst in terms of impact resistance. In general, as higher fractions of PEG*n* are incorporated into the 2-VOES-based copolymers, the impact resistance increases. When comparing the two "optimal" (i.e. similar in molecular weight with acceptable PDI values) compositions, poly(2-VOES) and PEG24 (15 wt.%), impact resistance increases in the presence of PEG24 comonomer. This result matches expectations and conforms with trends observed in previously shown coating properties. Due to the low molecular weights of the PEG3 copolymers, corresponding to fewer amounts of unsaturation per copolymer molecule, the impact resistance of this series vastly outperforms their counterparts in the PEG5 and PEG24 series. On the other hand, the higher molecular weight and PDI of 2-VOES-based copolymers in the PEG5 series yield relatively brittle coatings compared to the other 2-VOES-based copolymers due to the higher XLD, resulting from higher amounts of unsaturation present per copolymer molecule. Copolymers containing 50 wt.% PEG*n* vinyl ether exhibited the maximum resistance to impact available for this test method, 172 in lbs.

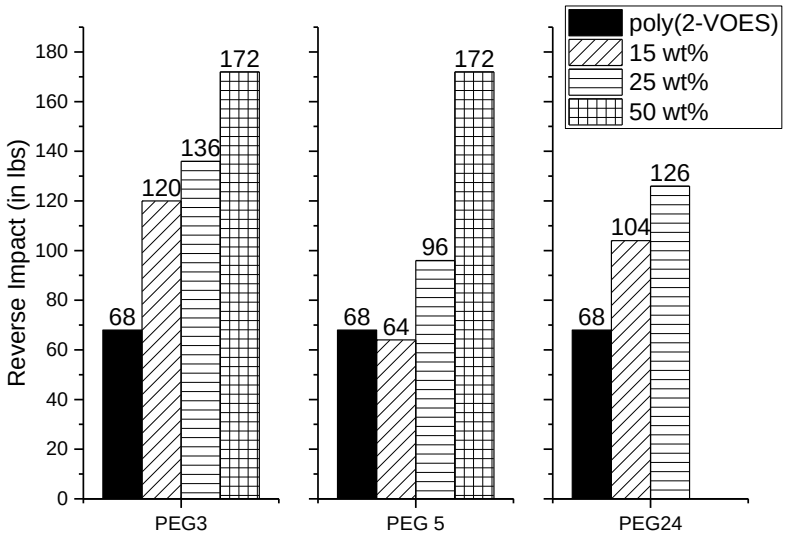

Figure 2.12. Reverse impact resistance of crosslinked networks as a function of PEG*n* chain length and amount

Changes in hydrophobicity of the crosslinked 2-VOES-based coatings were investigated by measuring changes in water contact angle over a period of five minutes. Improved hydrophobicity of coatings is crucial in protecting the substrate from water and other atmospheric contaminants that can degrade the underlying substrate. 2-VOES and other monomers derived from soybean oil are hydrophobic due to the long chain fatty acid moieties. Therefore, it was expected that coatings comprised of poly(2-VOES) would maintain increased hydrophobicity over the time period investigated. As the hydrophobic 2-VOES component of the copolymer was replaced with more hydrophilic PEG vinyl ether fragments, it was expected to see reductions in water contact angle, correlating to reductions in hydrophobicity of the copolymer coatings.

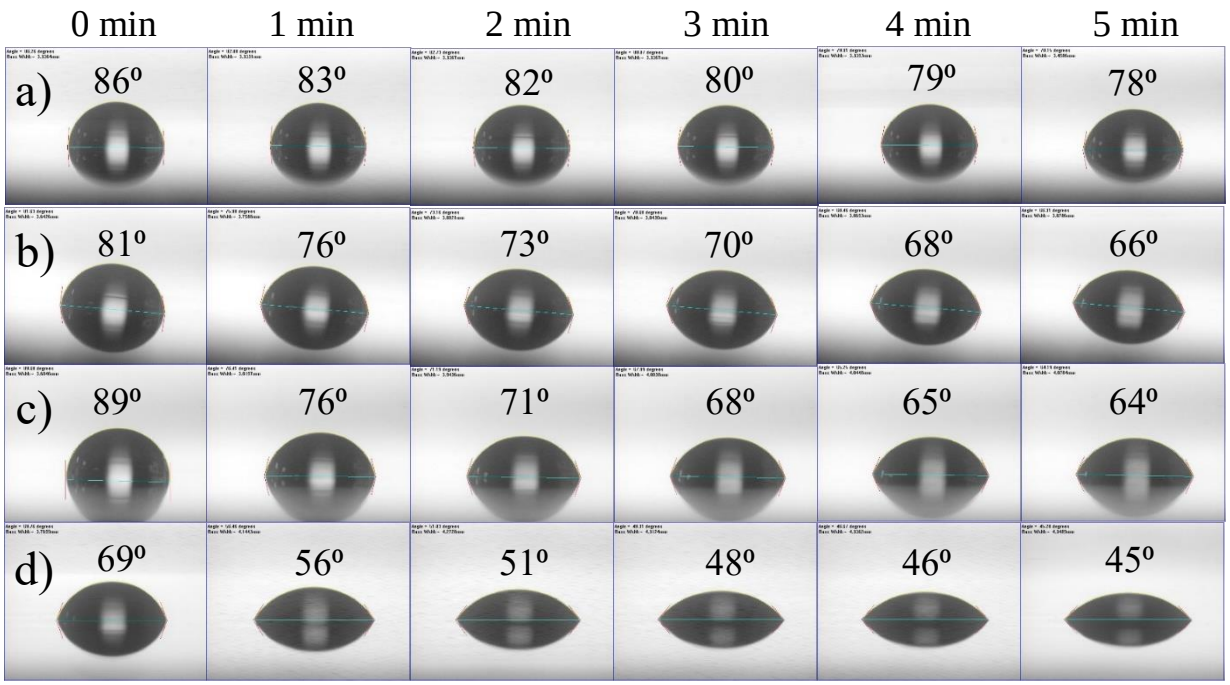

Figure 2.13. Changes in water contact angle as a function of time for a) poly(2-VOES), b) PEG3 (15 wt.%), c) PEG5 (15 wt.%), and d) PEG24 (15 wt.%)

As seen above in **Figure 2.13**, the water contact angle of a water droplet on the surface of the 2-VOES-based coatings was measured every minute for five minutes. Poly(2-VOES) (**Figure 2.13a**) maintains the highest contact angle throughout the time duration due to the hydrophobic

pendent fatty acid chains provided by the parent soybean oil. The water contact angle decreases more rapidly as the PEG chain length of the comonomer increases from 3 to 5 to 24, as seen in **Figure 2.13 b, c, and d**, respectively. This result concurred with expectations of increased wettability to the incorporation of more hydrophilic ethylene glycol repeat units[46].

Atomic force microscopy was utilized to examine the morphology of the coatings. As seen in **Figure 2.14a**, poly(2-VOES) coatings produced smooth, homogeneous surfaces. When 25 wt.% of PEG5 was incorporated into the copolymer (**Figure 2.14b**), the surface roughness increased (right) and phase separation (left and middle) between the hydrophobic 2-VOES fragments and the hydrophilic PEG vinyl ether counterparts was observed as a result of the incompatibility between the two components causing the PEG5 fragments to localize at the surface of the polymer coating. This phenomenon was further amplified when investigating the longer PEG comonomer comprised of 24 repeat units. Shown in **Figure 2.14c**, the phase separation of the longer chain PEG comonomer is even more pronounced, yielding a rather heterogeneous (left) and rough (right) coating surface due to the localization of the more hydrophilic PEG24 fragments at the surface.

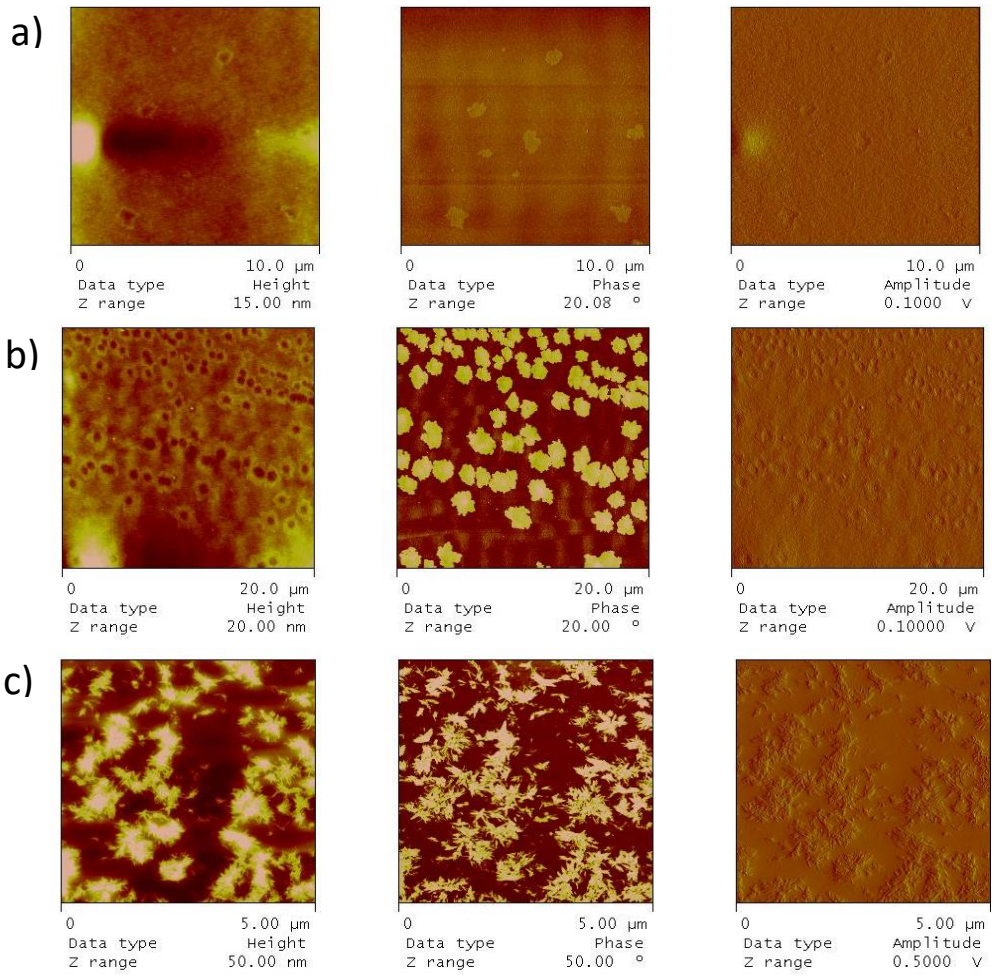

Figure 2.14. AFM images of coatings from a) poly(2-VOES), b) PEG5 (25 wt.%), and c) PEG24 (25 wt.%). Surface parameters such as height (left), phase (middle), and amplitude (right) were investigated.

2.4.6. Biocompatibility assays

Biocompatibility studies were conducted to test the feasibility of using 2-VOES-based polymer coatings on blood contact devices. First, protein adsorption was analyzed on crosslinked networks in a well plate and compared to a hydrophobic silicone standard with well-known high protein adsorption (**Figure 2.15**). Since this was simply a screening analysis, actual values of protein adsorption were not calculated, but general trends were determined. All 2-VOES-based coatings that were evaluated for protein adsorption performed better than the polystyrene and glass controls. Protein adsorption was reduced as the chain length and amount of PEG vinyl ether

comonomer presence in the 2-VOES-based copolymers increased. Low protein adsorption is well known for PEG-based coatings due to the hydrogen bonding between PEG and water molecules on the surface of the coatings. It is very difficult for the protein to overcome this hydrogen bonding and replace the water molecules, which allows PEG-based coatings to diminish or even repel protein adsorption[34-36]. These results concurred with expectations for polymer coatings containing PEG repeat units, as PEG functional units are commonly used in coatings for blood contact devices and other biomaterials, such as hydrogels, biosensors, stents, valves, and drug delivery systems[35, 37-41].

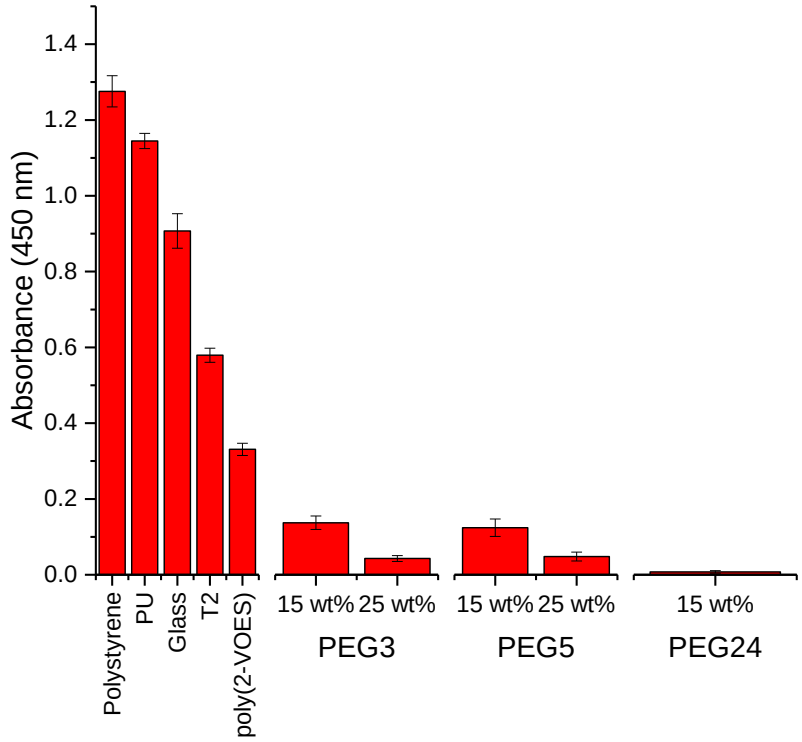

Figure 2.15. Protein absorption of crosslinked networks compared to the protein absorption of controls with known high protein absorption

In order to be considered for applications in blood contact devices, it is important the polymer coatings do not rupture (lyse) red blood cells that contact the coating. Using absorbance measurements, the release of hemoglobin was quantified for select 2-VOES-based coatings and compared to a number of known standards. Red blood cells (RBCs) suspended in a saline solution

were used as a negative control (i.e. minimal hemoglobin release), while RBCs suspended in DI water were used as the positive control (i.e. profound hemoglobin release). From the results in **Figure 2.16** all crosslinked 2-VOES-based polymer coatings performed similar to the positive control. The large amount of hemoglobin release after contacting the coatings suggests that they may not be suitable for application as coatings for blood contact devices. One plausible explanation for the high hemolytic activity of the 2-VOES-based coatings is the hydrophobicity of the coatings provided by the parent soybean oil of the 2-VOES fragments. It has been reported that hydrophobic surfaces might promote adverse reactions when blood comes into contact with them[42].

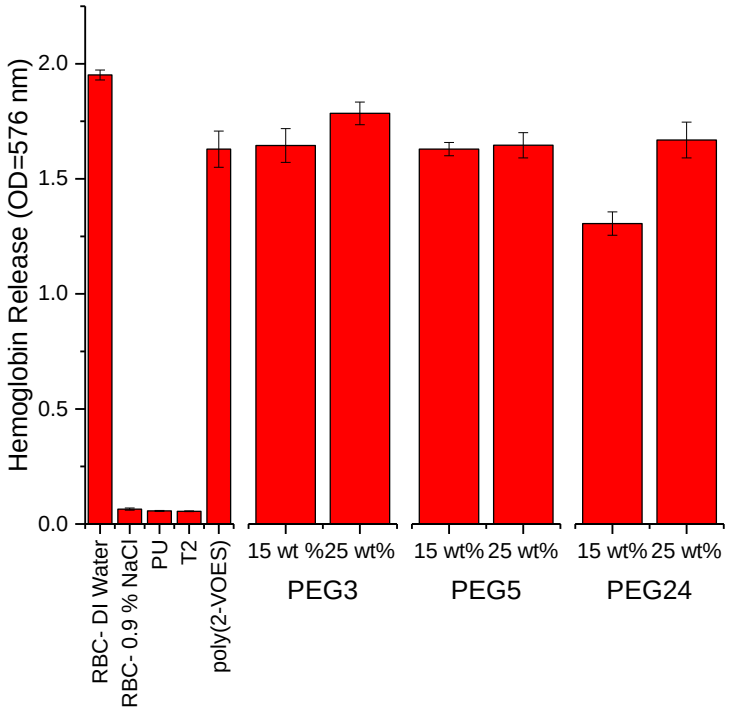

Figure 2.16. Hemolytic activity of select crosslinked networks compared to positive (RBC-DI water) and negative (RBC-saline solution) controls

2.5. Conclusions

A novel vinyl ether monomer, 2-VOES, was synthesized *via* direct transesterification of soybean oil with 2-vinyloxy ethanol. The composition of the fatty acid chains varied based on the parent soybean oil. Cationic polymerization was utilized to prepare the homopolymer, poly(2-

VOES), by polymerizing through the vinyl ether functional groups. The unsaturation of the pendent fatty acid chains remains available for post polymerization autoxidation, producing a crosslinked polymer network. Furthermore, copolymers of different weight ratios between 2-VOES and PEG*n* (n=3, 5, or 24) were also prepared *via* cationic copolymerization. Successful synthesis of the monomer, homopolymer, and 2-VOES-based copolymers was confirmed using ^{1}H NMR spectroscopy. Normalized integration values of end chain methyl groups of the 2-VOES and PEG*n* chains indicated successful incorporation of both components into the different resulting copolymers.

Cationic polymerization of 2-VOES monomer was expected to produce linear polymer chains with controlled molecular weight and narrow PDI by polymerizing exclusively through the vinyl ether functionality, due to the strong stabilizing effect of the oxygen atom next to the vinyl group. However, variations in the resulting copolymers might be explained by a couple different "synthetic imperfections" present during the reaction process. Therefore, the resulting copolymers were characterized into one of two weight classes; "lower" molecular weight (~10 kDa) and "higher" molecular weight (~25 kDa), and the PDI values were broader than expected. First, it was determined by ^{1}H NMR that approximately 10-15% of the unsaturation from the 2-VOES fragments was consumed throughout the polymerization. This consumption of unsaturation was thought to prohibit further propagation of the polymer chain due to degradative chain transfer reactions. Depending at what extent of monomer conversion this chain transfer occurred, the molecular weight distributions of the 2-VOES-based copolymers may become broader. The second explanation derives from possible inconsistencies in the monomer concentration as well as the ratio between the monomer concentration and the concentration of the coinitiator (i.e. $Et_3Al_2Cl_3$).

For this work, it was important to prepare 2-VOES-based copolymers with comparable molecular weights and narrow PDI through living cationic polymerization. By achieving this parameter, it would then be possible to study the impact of varying copolymer composition on coating properties such as XLD, T_g, hardness, solvent resistance, and flexibility. Based on the results of the GPC measurements for the various 2-VOES-based copolymers, it was determined that the most accurate conclusions could be made when comparing poly(2-VOES) and PEG24 (15 wt.%). These two coatings were chosen because of their similarities in average molecular weight and relatively narrow PDI values.

Coatings and free films of poly(2-VOES) and nine different synthesized copolymers were prepared by making drawdowns on glass, steel, and Teflon®-coated substrates. Crosslinked polymer networks were formed by autoxidation of the unsaturation provided by the pendent fatty acid chains of 2-VOES. Unlike soybean oil, poly(2-VOES) has a higher amount of unsaturation per molecule, therefore curing/crosslinking occurs at a faster rate. The tack-free times of the copolymers increased as the amount and chain length of the PEG vinyl ether comonomers increased. This trend followed expectations since the amount of unsaturation within the reactive system decreased. The longer PEG chains further increase the tack-free time by limiting the 2-VOES fatty acid chains from interacting with each other to form a crosslinked polymer network.

Using DMA, the viscoelastic properties of the 2-VOES-based coatings were characterized. In general, increasing the PEG chain length and amount reduced the T_g and the XLD of the resultant polymer networks. A clear trend was not observed due to the differences in final molecular weight and PDI, and thus different amounts of unsaturation per molecule, of the different samples. For thermoset coatings having T_g values at or below ambient temperature, the XLD largely determines the properties of the 2-VOES-based polymer coatings. Coating properties

were dependent on the molecular weight and PDI of the (co)polymers, average amount of unsaturation per polymer molecule, and presence of dangling chain ends that did not contribute to the formation of the elastic network (i.e. PEG*n* pendent chains). Increased chain length and amount of the PEG*n* comonomers resulted in decreased solvent resistance and more flexible coatings.

The surfaces of select 2-VOES-based coatings were analyzed by changes in water contact angle over time, atomic force microscopy, and in biocompatibility studies. The pendent fatty acid chains from 2-VOES provide the polymer coatings with hydrophobic fragments, capable of preventing water droplets to wet the surface. Increasing the amount and chain length of the PEG vinyl ether comonomers resulted in greater changes in water contact angle over five minutes as the coating was wetted by the water droplet. The increasing chain lengths of the PEG comonomers also resulted in increased phase separation and surface roughness, which was characterized by AFM. Unlike poly(2-VOES), which produced smooth and homogeneous coating surfaces, copolymers with PEG24 revealed heterogenous domains throughout the coating.

Investigations to use the synthesized copolymers as coatings for blood contact devices were carried out. First, protein adsorption studies determined that minimal protein amounts were adsorbed onto the surface of the crosslinked polymer networks. In fact, protein adsorption continued to diminish as the presence and chain length of the PEG vinyl ether comonomers increased. From this result, select polymer coatings were then tested for their propensity to rupture red blood cells. The results exhibited a large quantity of hemoglobin release, indicative of severe red blood cell hemolysis, possibly due to the highly hydrophobic nature of the 2-VOES fragments within the copolymers and performed similar to that of the positive control used. From these results, it was determined that these coatings may not be suitable for applications involving blood contact devices.

2.6. References

1. Lichtenthaler, F. W.; Peters, S., Carbohydrates as green raw materials for the chemical industry. *Comptes Rendus Chimie* **2004,** *7* (2), 65-90.
2. Güner, F. S.; Yağcı, Y.; Erciyes, A. T., Polymers from triglyceride oils. *Progress in Polymer Science* **2006,** *31* (7), 633-670.
3. Meier, M. A.; Metzger, J. O.; Schubert, U. S., Plant oil renewable resources as green alternatives in polymer science. *Chemical Society Reviews* **2007,** *36* (11), 1788-1802.
4. Lu, Y.; Larock, R. C., Novel polymeric materials from vegetable oils and vinyl monomers: preparation, properties, and applications. *ChemSusChem: Chemistry & Sustainability Energy & Materials* **2009,** *2* (2), 136-147.
5. Biermann, U.; Bornscheuer, U.; Meier, M. A.; Metzger, J. O.; Schäfer, H. J., Oils and fats as renewable raw materials in chemistry. *Angewandte Chemie International Edition* **2011,** *50* (17), 3854-3871.
6. Demchuk, Z.; Shevchuk, O.; Tarnavchyk, I.; Kirianchuk, V.; Lorenson, M.; Kohut, A.; Voronov, S.; Voronov, A., Free-Radical Copolymerization Behavior of Plant-Oil-Based Vinyl Monomers and Their Feasibility in Latex Synthesis. *ACS Omega* **2016,** *1* (6), 1374-1382.
7. de Espinosa, L. M.; Meier, M. A., Plant oils: The perfect renewable resource for polymer science?! *European Polymer Journal* **2011,** *47* (5), 837-852.
8. Kalita, H.; Selvakumar, S.; Jayasooriyamu, A.; Fernando, S.; Samanta, S.; Bahr, J.; Alam, S.; Sibi, M.; Vold, J.; Ulven, C., Bio-based poly (vinyl ether) s and their application as alkyd-type surface coatings. *Green Chemistry* **2014,** *16* (4), 1974-1986.

9. Teeter, H.; Dufek, E.; Coleman, C.; Glass, C.; Melvin, E.; Cowan, J., Reactions of unsaturated fatty alcohols. I. Preparation and properties of some vinyl ethers. *Journal of the American Oil Chemists Society* **1956,** *33* (9), 399-404.

10. Gast, L.; Schneider, W. J.; Teeter, H., Reactions of unsaturated fatty alcohols. III. Viscosity and molecular weight studies on some vinyl ether polymers. *Journal of the American Oil Chemists Society* **1957,** *34* (6), 307-310.

11. Schneider, W. J.; Gast, L.; Melvin, E.; Glass, C.; Teeter, H., Reactions of unsaturated fatty alcohols. II. Polymerization of vinyl ethers and film properties of polymers. *Journal of the American Oil Chemists' Society* **1957,** *34* (5), 244-247.

12. Aoshima, S.; Higashimura, T., Living cationic polymerization of vinyl monomers by organoaluminum halides. 3. Living polymerization of isobutyl vinyl ether by ethyldichloroaluminum in the presence of ester additives. *Macromolecules* **1989,** *22* (3), 1009-1013.

13. Chernykh, A.; Alam, S.; Jayasooriya, A.; Bahr, J.; Chisholm, B. J., Living carbocationic polymerization of a vinyl ether monomer derived from soybean oil, 2-(vinyloxy) ethyl soyate. *Green Chemistry* **2013,** *15* (7), 1834-1838.

14. Satoh, K., Controlled/living polymerization of renewable vinyl monomers into bio-based polymers. *Polymer Journal* **2015,** *47* (8), 527.

15. Sadahito, A.; Shinji, S.; Mitsuhiro, S.; Shokyoku, K., Synthesis and Self-Association of Stimuli-Responsive Diblock Copolymers by Living Cationic Polymerization. *Macromolecular Symposia* **2004,** *215* (1), 151-164.

16. Aoshima, S.; Kanaoka, S., A Renaissance in Living Cationic Polymerization. *Chemical Reviews* **2009,** *109* (11), 5245-5287.

17. Kanazawa, A.; Kanaoka, S.; Aoshima, S., Major Progress in Catalysts for Living Cationic Polymerization of Isobutyl Vinyl Ether: Effectiveness of a Variety of Conventional Metal Halides. *Macromolecules* **2009,** *42* (12), 3965-3972.

18. Chisholm, B. J.; Bezbaruah, A.; Kalita, H., Vegetable oil-based polymers for nanoparticle surface modifcation. Google Patents: 2013.

19. Alam, S.; Chisholm, B. J., Coatings derived from novel, soybean oil-based polymers produced using carbocationic polymerization. *J Coat Technol Res* **2011,** *8* (6), 671-683.

20. Alam, S.; Kalita, H.; Kudina, O.; Popadyuk, A.; Chisholm, B. J.; Voronov, A., Soy-based surface active copolymers as a safer replacement for low molecular weight surfactants. *ACS Sustainable Chemistry & Engineering* **2012,** *1* (1), 19-22.

21. Alam, S.; Kalita, H.; Jayasooriya, A.; Samanta, S.; Bahr, J.; Chernykh, A.; Weisz, M.; Chisholm, B. J., 2-(Vinyloxy) ethyl soyate as a versatile platform chemical for coatings: An overview. *European Journal of Lipid Science and Technology* **2014,** *116* (1), 2-15.

22. Kalita, H.; Alam, S.; Kalita, D.; Chernykh, A.; Tarnavchyk, I.; Bahr, J.; Samanta, S.; Jayasooriyama, A.; Fernando, S.; Selvakumar, S.; Popadyuk, A.; Wickramaratne, D. S.; Sibi, M.; Voronov, A.; Bezbaruah, A.; Chisholm, B. J., Synthesis and Characterization of Novel Soybean Oil-Based Polymers and Their Application in Coatings Cured by Autoxidation. In *Soy-Based Chemicals and Materials*, American Chemical Society: **2014**; Vol. 1178, pp 371-390.

23. Kalita, H.; Jayasooriyamu, A.; Fernando, S.; Chisholm, B. J., Novel high molecular weight polymers based on palm oil. *J. Oil Palm Res.* **2015,** *27* (March), 39-56.

24. Kalita, D. J. Polymers and Coatings Derived from Novel Bio-Based Vinyl Ether Monomers. Ph.D., North Dakota State University, Ann Arbor, 2018.

25. Skorokhodov, S. S., Cationic polymerization of vinyl ethers as synthetic path to diphylic polymers and potential complexants. *Makromol. Chem., Macromol. Symp.* **1986,** *3,* 153-62.

26. Deffieux, A.; Schappacher, M., Linear and macrocyclic poly(vinyl ethers) with functional side groups. *Macromol. Rep.* **1994,** *A31* (Suppl. 6&7), 699-706.

27. Goethals, E. J.; Reyntjens, W.; Lievens, S., Poly(vinyl ethers) as building blocks for new materials. *Macromol. Symp.* **1998,** *132* (International Symposium on Ionic Polymerization, 1997), 57-64.

28. Ken-Ichi, S.; Akiko, D.; Shokyoku, K.; Sadahito, A., Synthesis and solution properties of poly(vinyl ether)s with long alkyl chain, biphenyl, and cholesteryl pendants. *Journal of Polymer Science Part A: Polymer Chemistry* **2008,** *46* (13), 4392-4406.

29. Hiroaki, S.; Shokyoku, K.; Sadahito, A., Precise synthesis of end-functionalized thermosensitive poly(vinyl ether)s by living cationic polymerization. *Journal of Polymer Science Part A: Polymer Chemistry* **2012,** *50* (19), 4137-4144.

30. Jin, M.; Taketo, I.; Masahiko, M., Stimuli-responsive brush-shaped conjugated polymers with pendant well-defined poly(vinyl ether)s. *Journal of Polymer Science Part A: Polymer Chemistry* **2016,** *54* (20), 3318-3325.

31. Hawkins, M. L.; Schott, S. S.; Grigoryan, B.; Rufin, M. A.; Ngo, B. K. D.; Vanderwal, L.; Stafslien, S. J.; Grunlan, M. A., Anti-protein and anti-bacterial behavior of amphiphilic silicones. *Polymer chemistry* **2017,** *8* (34), 5239-5251.

32. Zhang, Q.; Wang, C.; Babukutty, Y.; Ohyama, T.; Kogoma, M.; Kodama, M., Biocompatibility evaluation of ePTFE membrane modified with PEG in atmospheric pressure glow discharge. *Journal of biomedical materials research* **2002,** *60* (3), 502-509.

33. Duan, Y.; Nie, Y.; Gong, T.; Wang, Q.; Zhang, Z., Evaluation of blood compatibility of MeO-PEG-poly (d, l-lactic-co-glycolic acid)-PEG-OMe triblock copolymer. *Journal of applied polymer science* **2006,** *100* (2), 1019-1023.

34. Bernhard, C.; Roeters, S. J.; Franz, J.; Weidner, T.; Bonn, M.; Gonella, G., Repelling and ordering: the influence of poly(ethylene glycol) on protein adsorption. *Physical Chemistry Chemical Physics* **2017,** *19* (41), 28182-28188.

35. Xu, L. C.; Siedlecki, C. A., Protein adsorption, platelet adhesion, and bacterial adhesion to polyethylene-glycol-textured polyurethane biomaterial surfaces. *Journal of Biomedical Materials Research Part B: Applied Biomaterials* **2017,** *105* (3), 668-678.

36. Jeong, H.; Hwang, J.; Lee, H.; Hammond, P. T.; Choi, J.; Hong, J., In vitro blood cell viability profiling of polymers used in molecular assembly. *Scientific Reports* **2017,** *7* (1), 9481.

37. Hoffman, A. S., Hydrogels for biomedical applications. *Advanced Drug Delivery Reviews* **2002,** *54* (1), 3-12.

38. Baroli, B., Hydrogels for tissue engineering and delivery of tissue-inducing substances. *Journal of pharmaceutical sciences* **2007,** *96* (9), 2197-2223.

39. Censi, R.; Di Martino, P.; Vermonden, T.; Hennink, W. E., Hydrogels for protein delivery in tissue engineering. *Journal of Controlled Release* **2012,** *161* (2), 680-692.

40. Vashist, A.; Vashist, A.; Gupta, Y.; Ahmad, S., Recent advances in hydrogel based drug delivery systems for the human body. *Journal of Materials Chemistry B* **2014,** *2* (2), 147-166.

41. Stevens, K. R.; Miller, J. S.; Blakely, B. L.; Chen, C. S.; Bhatia, S. N., Degradable hydrogels derived from PEG-diacrylamide for hepatic tissue engineering. *J. Biomed. Mater. Res., Part A* **2015,** *103* (10), 3331-3338.

42. Wu, W.-I.; Sask, K. N.; Brash, J. L.; Selvaganapathy, P. R., Polyurethane-based microfluidic devices for blood contacting applications. *Lab on a Chip* **2012,** *12* (5), 960-970.

CHAPTER 3. THE FEATURES OF EMULSION COPOLYMERIZATION FOR PLANT OIL-BASED VINYL MONOMERS AND STYRENE[1]

3.1. Abstract

Vinyl monomers from plant oils that have different degrees of unsaturation, soybean (SBM) and olive (OVM) oil, were copolymerized in emulsion with styrene to investigate the kinetic features and feasibility of latex formation. In the presence of up to 20 wt.% of SBM/OVM in the initial feed, the order of reaction with respect to the emulsifier and initiator do not depend on the plant oil-based monomers' unsaturation degree. Reaction kinetics agree with the Smith-Ewart theory, predicting that the number of nucleated latex particles is proportional to the surfactant and initiator concentration to the powers 0.6 and 0.4, respectively. Copolymerization of styrene with plant oil-based monomers follows the typical phenomenology for emulsion polymerization of hydrophobic monomers with a micellar nucleation mechanism. Nevertheless, based on experimentally obtained latex particle size and number, evidence for a mixed mode of nucleation (both micellar and homogeneous) was observed in this research. Mixed nucleation can be explained by the potential surface-active properties of plant oil-based monomer molecules containing polar acryloylamino "head," CH_2=CH-C(O)-NH- and hydrophobic "tail," C_{17}).

Because of the effect of degradative chain transfer on the plant oil-based monomer, the molecular weight of the resulting macromolecules decreases as the monomer degree of unsaturation and monomer fraction in the initial mixture increases. This feature can be used for

[1] The material in this chapter was co-authored by Kyle Kingsley, Oleh Shevchuk, Zoriana Demchuk, Stanislav Voronov, and Andriy Voronov. Kyle Kingsley had the primary responsibilities of synthesizing and characterizing polymer latexes and determining reaction orders with respect to emulsifier and initiator. Kyle Kingsley was involved in drafting and revising all versions of this chapter. Oleh Shevchuk and Andriy Voronov helped express relationships between particle number and reaction mechanism using data collected by Kyle Kingsley. Published article can be found at https://doi.org/10.1016/j.indcrop.2017.08.043.

controlling the molecular weight of latex polymers that come from plant oil-based monomers by varying the content and nature of bio-based monomer in the feed. The thermomechanical properties of latex films depend considerably on the nature and amount of incorporated plant oil-based fragments. Their presence lowers T_g (more than 40 °C difference) and provides some flexibility and toughness as compared to the normally rigid and brittle polystyrene.

3.2. Introduction

Polymer latexes are one of the most advanced polymeric materials and are widely used for making coatings and paints[1]. The chemical process for producing latexes is a free radical polymerization in emulsion that involves the emulsification of monomers (or monomer mixtures) and (co)polymerization, resulting in the formation of latex particles in an aqueous medium[2-3]. Because of the highly hydrophobic nature of triglyceride molecules, using plant and vegetable oils in emulsion polymerization (including commercial latex polymerization) and incorporating them at high levels in bio-based latexes remains a challenge[4-5]. Finite levels of aqueous solubility are required for monomers to be diffused from the emulsified droplets, a process which is done through the aqueous phase, into growing polymer particles during polymerization[6]. The extremely low solubility of plant oil-derived hydrophobic monomers in water limits their transport and incorporation into the resulting (co)polymers[4]. Additional limitations are associated with the presence of allylic protons in triglyceride molecules, in which hydrogen easily abstracts and formed in such a way radical can take part in chain transfer reactions, thus terminating the kinetic chain, reducing the polymerization rate, and lowering the molecular weight[7-8].

Chen and Bufkin used the reaction of fatty alcohols with acryloyl chloride for synthesis of fatty acrylates (including oleyl acrylate, lauryl acrylate, linolenyl acrylate, and linoleyl acrylate). After determining the fatty acrylates' reactivity in copolymerization with ethyl acrylate and methyl

methacrylate, high conversion (>98%) crosslinkable emulsion polymers were synthesized and characterized in terms of their molecular weight, glass transition temperature, and crosslinking mechanisms[7-8]. Thames et al. reported the synthesis of vegetable oil macromonomers (VOMMs)[4-5] using a two-step process of oil amidation and further acrylation of the resulting oil amide (exemplified with soybean oil)[9]. Latexes with varying amounts of soybean oil-based macromonomers were synthesized in copolymerization with methyl methacrylate to determine the effect of bio-based content on the resulting latexes' properties and coatings performance[10]. Moreno et al. incorporated methacrylic functionality into linoleic acid and successfully polymerized the resulting monomer via miniemulsion polymerization[11]. The synthesized waterborne polymers (latexes) based on plant oil ingredient were investigated for their potential applications as coatings. Tang et al. recently described the synthesis of new monomers derived from high oleic soybean oil (HOSO) and demonstrated their ability to yield thermoplastic polymers in free-radical polymerization in a solution[12]. Macromolecules with a wide range of glass transition temperatures (more than 100 °C difference) and physical properties (materials with viscoelastic and thermoplastic behaviors) were synthesized from a library of HOSO-based (meth)acrylate monomers[13].

Despite these advances and the relative simplicity of the emulsion process, it is currently not widely employed for making industrial coatings based on polymers and copolymers from plant and vegetable oils, mainly because of the limited availability of the respective monomers derived for free radical polymerization[14-20]. Also, the influence of hydrophobicity of plant oil-derived monomers and taking part in the chain transfer of allylic protons on the overall polymerization kinetics and latex particle formation in emulsion remain largely unexplored.

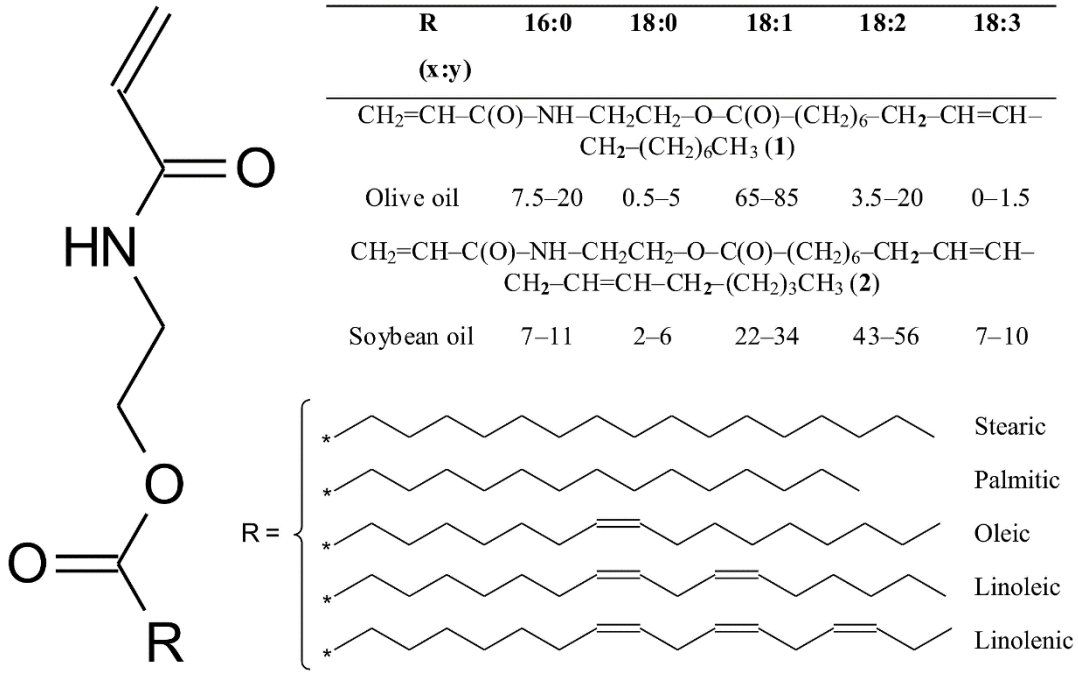

R (x:y)	16:0	18:0	18:1	18:2	18:3
CH_2=CH–C(O)–NH–CH_2CH_2–O–C(O)–$(CH_2)_6$–CH_2–CH=CH–CH_2–$(CH_2)_6CH_3$ (**1**)					
Olive oil	7.5–20	0.5–5	65–85	3.5–20	0–1.5
CH_2=CH–C(O)–NH–CH_2CH_2–O–C(O)–$(CH_2)_6$–CH_2–CH=CH–CH_2–CH=CH–CH_2–$(CH_2)_3CH_3$ (**2**)					
Soybean oil	7–11	2–6	22–34	43–56	7–10

Figure 3.1. Typical chemical compositions of the plant oils used in this study in percentages and the molecular structure of (acryloylamino)ethyl linoleate in SBM (1) and (acryloylamino)ethyl oleate in OVM (2). R (x:y) is the structure of the fatty acids (x is the number of carbon atoms in the fatty acid chain and y is the number of double bonds in the fatty acid).

Recently, our group developed a one-step method of plant oil direct transesterification, and we synthesized vinyl monomers from sunflower, linseed, soybean, and olive oil[21-23]. As expected, their homopolymerization rate depends on the monomer chemical structure, where chain propagation coexists with chain transfer reaction, which is determined by the degree of unsaturation in the monomers[22]. To characterize the monomers' reactivity in radical copolymerization, they were copolymerized with conventional petroleum-based counterparts (methyl methacrylate, MMA, and vinyl acetate, VA) in solution. The reaction rate, conversion and molecular weight of the resulting copolymers depended on the plant oil-based monomers' degree of unsaturation[23].

In the next step, stable latexes containing up to 50 wt.% of bio-based content were synthesized using emulsion and miniemulsion copolymerization of plant oil-based monomers with

MMA or VA[23]. Inspired by previous findings, here we report on emulsion polymerization of plant oil-based monomers from soybean (SBM) and olive (OVM) oils with widely used in plastics and rubber industry styrene (St). SBM and OVM possess remarkably different compositions of fatty acids in the triglycerides of the plant oils (**Figure 3.1**). The degree of unsaturation in the triglycerides' fatty acids was utilized as a criterion in studying copolymerization kinetics, as well as for showing the feasibility of bio-based latex synthesis and preparing films from latexes.

The features of the kinetics and latex particle formation in the emulsion process were investigated with respect to changing SBM/OVM content in the reaction feed. Replacing some petroleum-based components in latexes with a natural renewable ingredient can be beneficial for a broad variety of applications of polymeric materials. The latter is a major long-term goal of the current research study.

3.3. Experimental

3.3.1. Materials

Soybean oil (Crisco; The J.M. Smucker Company, Orville, OH), olive oil (Bertolli; Houston, TX), sodium dodecyl sulfate (SDS, VWR; Solon, OH), and ammonium persulfate (APS, VWR; Solon, OH) were used as received. Styrene (Sigma-Aldrich; St. Louis, MO) was distilled under vacuum to remove the inhibitor and was then stored in a refrigerator. All solvents that we used were reagent grade or better and were used as received. Deionized water was used for all reactions (MilliQ, 18 MΩ).

3.3.2. Synthesis of plant oil-based latexes using emulsion copolymerization

The synthesis of plant oil-based acrylic monomers (POBM) from olive and soybean oils with N-(hydroxyethyl) acrylamide (OVM and SBM, respectively) was previously reported from the current research group[21-23]. In the current study, plant oil-based latexes were synthesized using

a batch emulsion process and formulated to a final solids content of approximately 30 wt.%. First, the aqueous phase was prepared in a 25-mL single-neck round bottom flask equipped with a magnetic stirrer by dissolving 2.5–10 wt.% SDS (per oleo phase) in 10.2 g water under continuous purging with argon.

Table 3.1. Used recipes to investigate POBM/St emulsion copolymerization

	Wt.%	Wt.% per oleo phase	Mass, g
Oleo phase	30		4.8
POBM, SBM or OVM		5–40	0.24–1.92
Styrene		60–95	2.88–4.56
Aqueous phase	70		11.2
Emulsifier, SDS, $C_{12}H_{25}SO_4Na$, % per oleo phase		2.5–10	0.12–0.48
Initiator, APS, $(NH_4)_2\ S_2O_8$, % per oleo phase		1–2.5	0.048–0.12
Total	100		16

The oleo phase was prepared separately by dissolving 5–40 wt.% POBM (per oleo phase) in styrene before being charged to the reaction vessel while simultaneously being purged with argon. Emulsion was formed at room temperature for 5 minutes before being transferred to a pre-heated water bath at 60 °C, where emulsion formation was continued for an additional 5 minutes to reach bath temperature under an argon blanket. Polymerization was started by charging 1.0–2.5 wt.% APS (per oleo phase), which was dissolved in 1.0 g of water. The recipes used to investigate emulsion copolymerization of POBM with St can be seen in **Table 3.1**.

3.3.3. Characterization of plant oil-based latexes

Kinetic curves were recorded by taking aliquots from the reaction mixture at various time intervals and then determining the monomer conversion. Samples were reprecipitated in methanol three times before being dried at 110 °C, producing the constant final mass. Three distinct intervals of emulsion polymerization were observed by plotting monomer conversion as a function of time. The reaction rate was determined from the slope of the second interval of the conversion-time

curve that corresponded to the pseudo steady-state rate of polymerization, as described by the Smith-Ewart theory of emulsion polymerization.

The particle size distribution was determined by a submicron particle sizer (PSS NICOMP Particle Sizing Systems; Santa Barbara, CA) using a monochromatic light with wavelength of approximately 250 nm and a temperature of 25 °C. Samples were prepared by diluting one drop of latex in approximately 7 mL of water. To simplify these calculations, it was assumed that the latex particles were of a spherical morphology. The particle number was calculated using the following equation:

$$N_p = \frac{3 \cdot m_o \cdot S}{4 \cdot 100 \cdot \rho \cdot \pi r^3 \cdot V} \qquad \text{(Equation 3.1)}$$

where m_o (g) is the total mass of oleo phase in the feed, S (%) is the monomer conversion, ρ (g/mL) is the density of the polymer, r (cm) is the radius of the latex particle, and V (mL) is the total volume of the reaction mixture.

Samples were prepared for additional characterization; this was done by reprecipitating the samples three times in methanol before drying them in an inert atmosphere, producing a constant final mass. Latex polymer composition was determined by ^{1}H NMR spectroscopy on an AVANCE III HDTM 400 MHz high-performance digital NMR spectrometer (Bruker; Billerica, MA) using $CDCl_3$ as a solvent (spectrum not shown). The integral of the triplet at δ 0.92 ppm, corresponding to the end-chain methyl protons of POBM (a), was normalized for all formulations. The aryl protons (b) of styrene were then integrated in the region of δ 7.25–6.3 ppm. The resulting peak ratios, along with the molar masses of the POBMs and styrene, were used to determine the final POBM content in the final latex copolymer.

Copolymer molecular weight averages were determined by gel permeation chromatography (GPC) using a Waters Corporation modular chromatograph consisting of a

Waters 515 HPLC pump, a Waters 2410 Refractive Index Detector, and a set of two 10 μm PL-gel mixed-B columns. The column temperature was set to 40 °C. THF was used as the carrier solvent.

The glass-transition (T_g) temperature of the resulting latex polymers was determined via differential scanning calorimetry (DSC) using a TA Instruments Q1000 calorimeter. Dry nitrogen was purged through the sample at a flow rate of 50 mL/min. The samples were subjected to a heat–cool–heat process using temperatures ranging from -30–150 °C with heating and cooling rates of 5 °C/min. The T_g was determined at the midpoint of the inflection region that was observed in the second heating cycle.

Latex films were prepared using a draw-down bar that was 8 mm thick; the bar was cleaned by acetone prior to application on glass substrates. Films were cured at 150 °C for up to 5 h, depending on latex composition. Higher amounts of OVM monomer in the final latex required longer cure times because of the lower degree of unsaturation available for crosslinking compared to latex copolymers with an SBM monomer, which were cured after 3 hours. The dynamic mechanical behavior of the latex films was determined using a dynamic mechanical analyzer (TA Instruments Q800) with tensile mode and a heating rate of 5 °C/min. Samples of films with a typical size of 14 mm X 5 mm (length X width) were used.

The mechanical properties of the latex films were determined using an Instron testing machine 2710-004 with a crosshead speed of 5 mm/min and a maximal load of 500 N. Rectangular samples with a size of approximately 25 mm X 5 mm (length X width) were used. At least five replicates of each latex sample were used to obtain an average value.

3.4. Results and discussion

3.4.1. Copolymerization kinetics

A typical emulsion polymerization process involves three phenomenological stages: (1) the nucleation of the latex particles, (2) particle growth proportional to monomer conversion, and (3) the growing latex particles becoming monomer-starved because of the decreasing monomer concentration at the polymerization loci that continues toward the end of reaction[6]. The Smith–Ewart kinetics theory of emulsion polymerization assumes that particle nucleation occurs in monomer-swollen emulsifier micelles (formed above the emulsifier critical micelle concentration, CMC) by capturing waterborne free radicals generated by molecules of a water-soluble initiator[24-25]. As a consequence, the micelles transform into particle nuclei that continue to grow (polymerize). According to the Smith-Ewart theory, the polymerization rate and kinetic chain length are determined by the free radicals' ability to penetrate the micelles. To this end, the rate of polymerization, R_p, is proportional to the concentration of monomer (or monomers in copolymerization), *[M]*, in the particles, average number of free radicals per particle (n), and number of particles nucleated per unit volume of water, N_p. Proposed by Harkins[26-28] and Smith and Ewart[25, 29] and modified by Gardon[30-31], the *micelle nucleation* model indicates that a large surface area of micelles strictly controls (by the population of particles available for consuming monomer) the emulsion polymerization of hydrophobic monomers, such as styrene (aqueous solubility is limited to 0.029% at 20 °C). An alternative mode is called the *homogeneous nucleation* of latex particles, where waterborne free radicals first polymerize with dissolved in water monomer molecules. Formed in this way insoluble oligoradicals coil up into small particle nuclei that aggregate into primary particles that are stabilized by surfactant molecules[32]. This nucleation mode is more typical for the emulsion polymerization of monomers that have a higher aqueous solubility.

The Smith-Ewart theory is based on some assumptions, however; one such assumption is that at any moment, each monomer-swollen particle contains either 0 or 1 free radical, resulting in an average number of free radicals per particle *n* equal to 0.5[24-25, 29]. Furthermore, the Smith-Ewart theory predicts that N_p is proportional to the surfactant concentration *[S]* and initiator concentration *[I]* to the powers of 0.6 and 0.4, respectively, showing the essential importance of *[S]* in the particle nucleation process.

$$R_p = K\,[I]^{0.4}[S]^{0.6}[M]\text{, where } K \text{ is a constant} \qquad \text{(Equation 3.2)}$$

Calculations based on the Smith-Ewart theory result in a simple expression (**Equation 3.2**) of the rate of emulsion polymerization of hydrophobic monomers at a given temperature and for initiators generating free radicals in the aqueous phase, such as potassium persulfate, $K_2S_2O_8$[33].

It is generally accepted that micellar nucleation predominates in the emulsion polymerization of hydrophobic monomers, such as styrene, at a surfactant (emulsifier) concentration above CMC[34]. Nevertheless, a detailed understanding of the particle formation mechanisms for each new monomer is crucial to control the final latex particles' size and number.

In the current study, the practical goal was to determine the kinetic features for emulsion copolymerization of highly hydrophobic SBM/OVM (their aqueous solubility is in the range of 10^{-3} wt.%[22] with styrene (St) and investigate the process of latex particles formation.

To the best of our knowledge, there is no report in the literature on the effect of triglyceride-based monomers' hydrophobic nature, as well as such monomers chain transfer reaction on the overall emulsion copolymerization kinetics and latex particle formation. For this purpose, the surfactant (sodium dodecyl sulfate, SDS) and initiator (ammonium persulfate, APS) reaction orders were determined first in reaction of St with SBM or OVM at 5 and 20 wt.% of POBM in a monomer mixture. **Table 3.1** gives the used recipes to investigate copolymerization kinetics. To

determine the effect of surfactant concentration, the course of copolymerization initiated by 1.5 wt.% of APS per total concentration of monomer at 60 °C was followed by measuring monomer conversion *vs* time and calculating the rate of polymerization R_p at different concentrations of SDS.

Selected plots that demonstrate the effect of SDS concentration in terms of conversion versus time profiles for various monomer ratios in feed (including homopolymerization of St) are shown in **Figure 3.2**. One can see that when 20 wt.% of POBM was added to the initial feed, the reaction rate dropped significantly (**Fig. 3.2** *5,6*) at both concentrations of SDS compared to the homopolymerization of St (**Fig. 3.2** *1,2*). This retardation can be explained by the effect of the degradative chain transfer on the monomer (allylic termination) because of the presence of allylic protons in unsaturated acyl fragments of plant oil-based monomer[22-23]. Chain transfer is more pronounced for reactions with more unsaturated SBM (**Fig. 3.2 B**) compared to OVM (**Fig. 3.2 A**). In our previous work, we showed that SBM molecules indeed undergo chain transfer reactions more readily (C_M (SBM) = 0.026, C_M (OVM) = 0.015)[22-23].

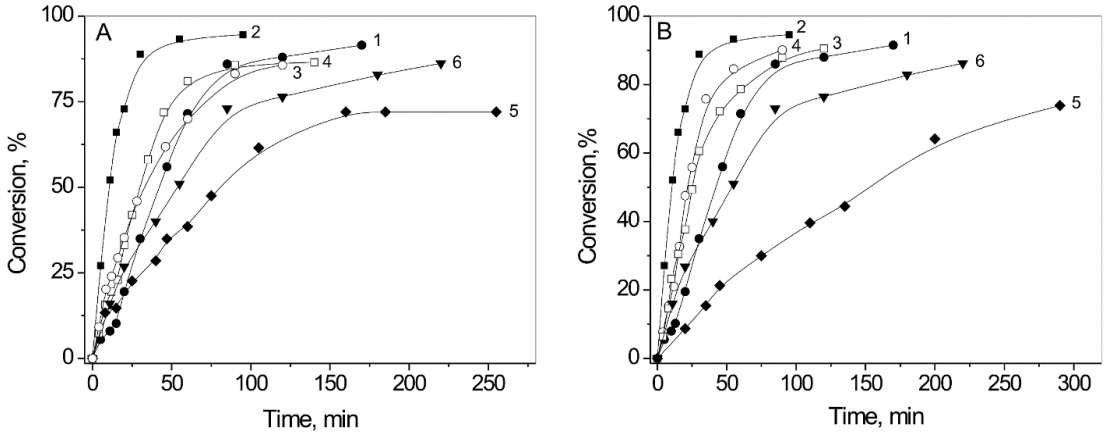

Figure 3.2. Conversion–time changes in emulsion copolymerization of St with 5 (3,4) and 20 wt.% (5,6) of OVM (**A**) and SBM (**B**) at 2.5% (3,5) and 5% (4,6) of SDS. Graphs 1,2 show conversion versus time curves in St homopolymerization at 2.5% and 5% of SDS, respectively.

The effect of retardation is less noticeable at 5 wt.% of plant oil-based monomer in the reaction feed (**Fig. 3.2** *3,4*). This can be explained by the fact that in the copolymerization of St

with SBM (monomer reactivity ratios r_1=1.11, r_2=0.35), as well as with OVM (r_1=1.19, r_2=0.39), macroradicals of POBM interact with St molecules much quicker[22-23]. Because of two simultaneously occurring reactions, higher rate of cross-propagation, and retardation due to the chain transfer, the overall copolymerization rate changes only slightly at 5 wt.% of POBM in the feed. However, chain transfer dominates at 20 wt.% of POBM in the monomer mixture, and copolymerization slows down.

From conversion–time plots (**Fig. 3.2**), the rates of copolymerization (first derivative of the conversion–time curves) were estimated for each reaction (**Fig. 3.3**). The copolymerization rate is lower for reactions with higher concentrations of SBM/OVM because of the retardation effect described above. As expected, this effect is more pronounced for St copolymerization with more unsaturated SBM compared to OVM. Nevertheless, all graphs in **Fig. 3.3** clearly follow three typical phenomenological intervals in the emulsion process, that is, latex particles' nucleation (up to about 20% monomer conversion), propagation (growth) at an almost steady copolymerization rate, and the final stage when the rate decreases toward end copolymerization reaction.

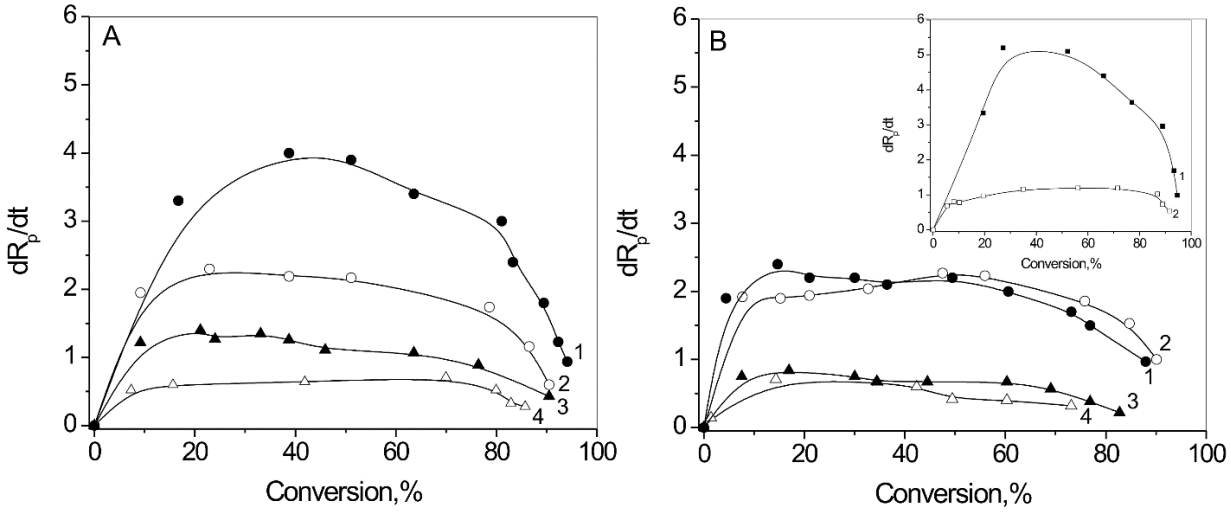

Figure 3.3. Rate of St copolymerization with 5% (1,2) and 20% (3,4) of OVM (**A**) and SBM (**B**) at 2.5% (2,4) and 5% (1,3) of SDS. B shows the rate of St homopolymerization in the presence of 2.5% (2) and 5% (1) of SDS.

Using the obtained kinetic data, the reaction orders with respect to the emulsifier and initiator were calculated for copolymerization and compared to the homopolymerization of St. For this purpose, conversion as a function of time plots for emulsion copolymerization of St with SBM/OVM at various concentrations of SDS and APS were used to calculate R_p. **Figure 3.4 A** shows that the reaction orders with respect to the surfactant obtained in reaction of St with OVM/SBM (in the range of 0.58–0.65) are similar to St homopolymerization, where this value is 0.59 (as predicted by the Smith-Ewart theory). This indicates that at least for the monomer mixtures containing up to 20 wt.% of SBM/OVM, the copolymerization follows the Smith-Ewart theory. Adding POBM does not change an effect of the emulsifier concentration on the copolymerization rate.

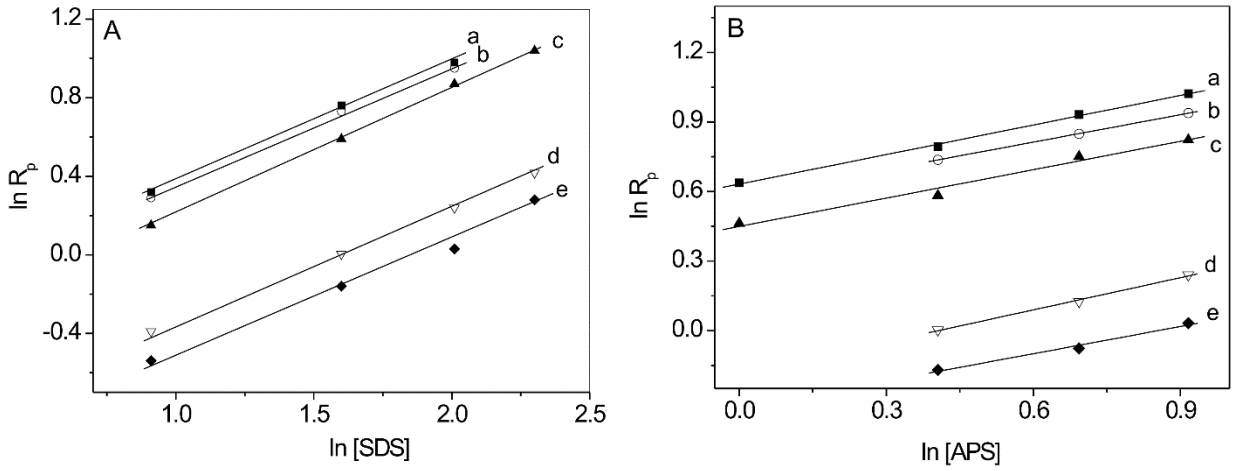

Figure 3.4. Log–log plots of the rate of emulsion polymerization of styrene (a) and plant oil-based monomers [OVM, b-(5%), d-(20%) and SBM, c-(5%), e-(20%)] versus [SDS] at 60 °C and 1.5% APS (**A**) and versus [APS] at 60 °C and 5% of SDS (**B**)

From the plots seen in **Fig. 3.4 B**, for the homopolymerization of St initiated by APS at 60 °C, the reaction order with respect to the initiator is 0.42. When SBM/OVM are presented in a reaction mixture, no significant differences were observed for this kinetic parameter. In the copolymerization of St with SBM/OVM, the comparable values of 0.39–0.46 were obtained.

Both obtained kinetics parameters show that the copolymerization of St with up to 20 wt.% OVM/SBM follows **Eq. 3.1**, which predicted that that number of nucleated latex particles N_p is proportional to the *[S]* and *[I]* to the 0.6 and 0.4 powers, conforming to the Smith-Ewart theory. Although such dependence is widely considered as proof of micellar nucleation mechanism[25], Roe demonstrated that the same exponents can also be found using a homogeneous nucleation model[35]. The latter work was followed by Fitch and Gardon's studies that experimentally demonstrated both exponents in a wider range[30-31, 36].

3.4.2. Latex particle formation

Understanding the formation of latex particles is crucial for controlling final polymer material performance and quality. Particle nucleation and growth kinetics impact their size distribution, as well as latex stability, transportation, storage, and scaling up in an industrial process[1, 34]. It is not always straightforward to determine experimentally if micellar nucleation is dominant in a particular emulsion polymerization of hydrophobic monomers. To distinguish the features of latex formation in the presence of SBM/OVM, the number of particles during copolymerization, and final particle size, copolymer composition, and molecular weight were determined for latexes from St and 5% or 20 wt.% of POBM at 2.5% or 5% of SDS.

In the emulsion process, N_p is conventionally controlled by the mechanism of particle formation. Examining this parameter as a function of surfactant concentration is a good tool for testing particle nucleation. Unless secondary processes occur, the N_p remains constant after the nucleation stage ends and until the end of the reaction. The evolution of the resulting latex particle number with total monomer conversion in this study is shown in **Fig. 3.5**. In general, the N_p shows close values at both concentrations of emulsifier (regardless of POBM unsaturation degree and content). Obviously, the N_p is higher in reactions at 5% SDS because more micelles are available

for particle nucleation. However, one noticeable change was observed with the progress of copolymerization in the presence of POBM. Although N_p slightly decreases toward the end of copolymerization at 2.5% of SDS, conversely, the number of latex particles grows almost linearly at 5% of emulsifier (**Fig. 3.5**).

Judging from the data and taking into account the potential surface-active properties of SBM/OVM molecules (in particular, because of polar acryloylamino "head," CH_2=CH-C(O)-NH- and hydrophobic "tail," C_{17}), a mixed mode (micellar and homogeneous) of particle nucleation can be proposed for the emulsion copolymerization of St with POBM. This nucleation mode has been reported as possible for the emulsion homopolymerization of hydrophobic styrene at surfactant concentrations above CMC (the same surfactant concentration regime was used in this work). According to Priest[32] and Fitch and Tsai[36-37] waterborne free radicals from the initiator can polymerize with monomer molecules dissolved in water and form insoluble (at some critical chain length) hydrophobic oligomeric radicals. Subsequently, those radicals may twist into small particle nuclei that undergo further flocculation and form the primary particles that are stabilized by surfactant molecules. The number of nucleated in this way primary particles is controlled by the amount of surfactant available for stabilizing the generated interfacial area.

Assuming the surface-active properties of POBM and its very limited aqueous solubility, homogeneous nucleation (in addition to micellar) seems to be a possible mode for particle formation in copolymerization of styrene with SBM/OVM in the presence of SDS molecules. Based on these assumptions, a mixed mode of particle nucleation can be an explanation for what is shown in **Fig. 3.5** regarding the differences of N_p change with the progress of polymerization at SDS 2.5% and 5%. At a lower concentration, there is not enough emulsifier molecules provided to stabilize all the particles formed in the homogeneous nucleation mode coexisting with micellar

mode. Consequently, the coagulation of some particles leads to decreasing N_p during polymerization (**Fig. 3.5**). Contrarily, at higher concentrations of surfactant, the stabilizing power is sufficient for all particles nucleated in a homogeneous mechanism. Homogeneous nucleation takes place continuously during polymerization and leads to a growing N_p. (**Fig. 3.5, inset**).

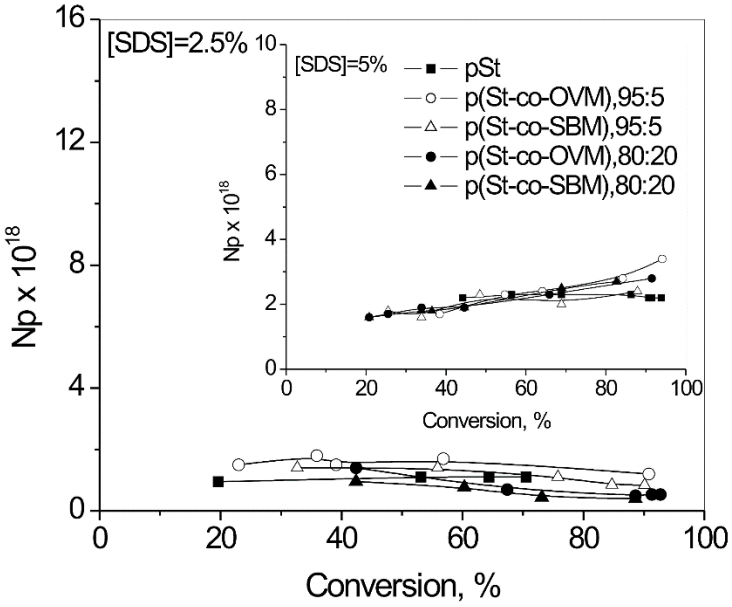

Figure 3.5. Latex particles' number change versus conversion in emulsion polymerization of St and SBM/OVM at 2.5% and 5% (inset) of SDS

According to Chern and Lin, quantitative determination of a polystyrene latex fraction formed by homogeneous nucleation is challenging and has not been successful[38]. **Table 3.2** shows that the results of particle size of final latexes are in agreement with the concept of a mixed-nucleation mechanism. In experiments with 2.5% SDS, the latex particle size increases (compared to St homopolymerization) due to the coagulation of some particles; thus, the remaining particles have larger diameters. In the case of a higher surfactant concentration, latex particle diameters decrease due to the fact that more particles nucleate and become smaller in size.

Table 3.2. Characteristics of latex particles from styrene and plant oil-based monomers

Bio-based content (feed), wt.%	Bio-based content (polymer), wt.%	Conversion, %	Latex solid content, %	Latex particles size, nm	M_w/M_n x10^3	T_g, °C
[SDS] = 2.5%						
St only	-	91.5	27.5	71 ± 17	1,216/367	110
5OVM	3.3	90.8	27.2	70 ± 14	1,027/303	104
20OVM	18.8	87.0	25.5	85 ± 17	549/257	88
5SBM	3.0	87.0	26.1	81 ± 19	892/288	103
20SBM	14.1	73.2	21.9	95 ± 22	384/120	86
[SDS] = 5%						
St only	-	97.8	29.4	72 ± 18	1,365/395	110
5OVM	2.9	94.1	28.2	52 ± 12	1,237/376	104
20OVM	18.5	91.5	27.4	54 ± 14	626/251	89
5SBM	2.3	87.8	26.4	50 ± 12	863/236	102
20SBM	14.5	82.8	24.8	52 ± 13	486/121	87

3.4.3. Latex properties

As expected, the molecular weight of the final latex polymers decreases as the degree of unsaturation and fraction of POBM increases in the initial monomer mixture (**Table 3.2**). A decreasing molecular weight can be explained by the effect of degradative chain transfer on either SBM or OVM, which was reported recently in our previous study[22-23]. The obtained data are in agreement with the previously described, more extensive chain transfer effect caused by a higher unsaturation degree of SBM compared to OVM (**Figure 3.1**).

In terms of the thermomechanical properties, showing the plasticization effect of oil-based fragments in latex copolymers was targeted in the current work. The function of a plasticizer is to reduce the forces between the macromolecules, thereby increasing chain mobility and leading to polymer softening, which may facilitate better material processing. To demonstrate that POBM monomers with differing levels of unsaturation can act as modifiers of polymer thermomechanical properties, T_g was determined for each synthesized latex polymer. Determining the glass transition temperature, T_g, is the most conventional and important method to estimate chain mobility[39]. Our

expectation was that even with a small amount of POBM fragments in the macromolecules, the plasticizing effect would be noticeable.

The obtained data (**Table 3.2**) indicate that T_g decreases for copolymers with incorporated plant oil-based fragments compared to latexes from polystyrene that were synthesized (T_g = 110 °C). A variation of oil-based monomer content changes the T_g (and, thus, the thermal properties) of the resulting latex polymers for all synthesized compositions. Even a small fraction of POBM fragments makes the macromolecules more flexible, as indicated by decreasing T_g.

Table 3.2 shows that the incorporation of 3–18 wt.% of SBM/OVM fragments in the copolymer changes the T_g of latex films about 25 °C. A decrease of T_g corresponds to the bio-based content in the resulting macromolecules and is more pronounced for the latexes that contain more plant oil-based fragments.

The efficiency of the plasticizer can also be determined in dynamic mechanical tests (DMA) by measuring the material response to a periodic force and material deformation at this force. To provide further insights into the plasticizing effect of oil-based fragments, the tensile properties of films from the latexes synthesized from styrene and SBM were evaluated at room temperature. For this experiment, additional latex compositions were synthesized in an emulsion copolymerization of St with 30 and 40 wt.% of SBM, respectively. For testing the tensile properties of the resulting material, latex films were prepared.

Table 3.3 shows that although Young's moduli and tensile stresses decreased by increasing the bio-based content in copolymers with St, elongation at break increased significantly for films made from copolymers with incorporated POBM. The results indicate that although polystyrene is a rigid and brittle material with limited ability for elongation, the presence of the bio-based fragments makes the latex films much softer and increases the material's toughness. The

thermomechanical properties of latex films can vary by changing the content of the incorporated POBM fragments.

Table 3.3. Tensile properties (at room temperature) of latex films from SBM copolymerized with St**.**

Bio-based content (feed), wt.%	Bio-based content (polymer), wt.%	T_g, °C	$G'(\omega)$, MPa	E, MPa	σ, MPa	ε_b, %	Toughness, x 10^{-4}, J/m^3
20SBM	14.1	87.3	1673	681 ± 84	6.7	1.9	13.3
30SBM	19.0	79.4	530	457 ± 22	6.3	3.5	25.7
40SBM	36.2	64.3	295	177 ± 13	2.7	81.8	38.6

where $G'(\omega)$ is the storage modulus, E is Young's modulus, σ is the tensile strength at break, and ε_b is the elongation at break.

3.5. Conclusions

Vinyl monomers from plant oils (soybean (SBM) and olive (OVM) oil) that have different degrees of unsaturation were copolymerized in emulsion with styrene to investigate the copolymerization kinetic features and the feasibility of latex formation with respect to the nature of POBM (degree of unsaturation in plant oil) and its content in the initial feed. Copolymerization of St with up to 20 wt.% of POBM follows the Smith-Ewart theory, predicting that latex particles are formed by micellar nucleation and the number of nucleated particles is proportional to the surfactant and initiator concentration to the powers 0.6 and 0.4, respectively. Both the initiator (0.39–0.46) and emulsifier (0.58–0.65) reaction order do not depend on the POBM unsaturation degree and content in a copolymerization reaction.

Although the experimental data showed that copolymerization of St with POBM follows a typical phenomenology for the emulsion process of hydrophobic monomers, experimental proof of a mixed mode of nucleation (micellar and homogeneous) was observed by determining latex particle size and number. Considering the possible surface activity of POBM molecules (due to polar acryloylamino "head," CH_2=CH-C(O)-NH- and hydrophobic "tail," C_{17}), homogeneous

nucleation seems to be a possible operative mode (in addition to micellar) in the copolymerization of POBM with St.

Molecular weight of the latex copolymers (M_n=120,000–380,000) decreases by increasing the degree of POBM unsaturation and content in the reaction mixture; this is because of the effect of degradative chain transfer on the monomer. This feature can be used for controlling the molecular weight of latex polymers from plant oil-based monomers by varying the content of bio-based monomers in the feed. The thermomechanical properties of latex films depend considerably on the amount of incorporated plant oil-based fragments. Their presence lowers T_g (more than 40 °C difference) and provides some flexibility and toughness as compared to the normally rigid and brittle polystyrene. The results indicate that POBM can be good candidates for the internal plasticizing and formation of thermo-reactive crosslinked polymer coatings.

3.6. References

1. Chern, C., Emulsion polymerization mechanisms and kinetics. *Progress in polymer science* **2006,** *31* (5), 443-486.
2. Blackley, D. C., *Emulsion polymerisation: theory and practice*. Applied science publishers London: 1975.
3. Eliseeva, V. I.; Ivanchev, S.; Kuchanov, S.; Lebedev, A., *Emulsion polymerization and its applications in industry*. Springer Science & Business Media: 2012.
4. Booth, G.; Delatte, D. E.; Thames, S. F., Incorporation of drying oils into emulsion polymers for use in low-VOC architectural coatings. *Industrial Crops and Products* **2007,** *25* (3), 257-265.

5. Quintero, C.; Delatte, D.; Diamond, K.; Mendon, S.; Rawlins, J.; Thames, S., Reaction calorimetry as a tool to determine diffusion of vegetable oil macromonomers in emulsion polymerization. *Progress in organic coatings* **2006,** *57* (3), 202-209.

6. Ugelstad, J.; Hansen, F., Kinetics and mechanism of emulsion polymerization. *Rubber chemistry and technology* **1976,** *49* (3), 536-609.

7. Chen, F. B.; Bufkin, B. G., Crosslinkable emulsion polymers by autoxidation. II. *Journal of applied polymer science* **1985,** *30* (12), 4551-4570.

8. Chen, F. B.; Bufkin, B. G., Crosslinkable emulsion polymers by autoxidation. I. Reactivity ratios. *Journal of applied polymer science* **1985,** *30* (12), 4571-4582.

9. Delatte, D.; Kaya, E.; Kolibal, L. G.; Mendon, S. K.; Rawlins, J. W.; Thames, S. F., Synthesis and characterization of a soybean oil-based macromonomer. *Journal of Applied Polymer Science* **2014,** *131* (10).

10. Kaya, E.; Mendon, S. K.; Delatte, D.; Rawlins, J. W.; Thames, S. F. In *Emulsion Copolymerization of Vegetable Oil Macromonomers Possessing both Acrylic and Allylic Functionalities*, Macromolecular Symposia, Wiley Online Library: **2013;** pp 95-106.

11. Moreno, M.; Miranda, J. I.; Goikoetxea, M.; Barandiaran, M. J., Sustainable polymer latexes based on linoleic acid for coatings applications. *Progress in Organic Coatings* **2014,** *77* (11), 1709-1714.

12. Yuan, L.; Wang, Z.; Trenor, N. M.; Tang, C., Robust Amidation Transformation of Plant Oils into Fatty Derivatives for Sustainable Monomers and Polymers. *Macromolecules* **2015,** *48* (5), 1320-1328.

13. Yuan, L.; Wang, Z.; Trenor, N. M.; Tang, C., Amidation of triglycerides by amino alcohols and their impact on plant oil-derived polymers. *Polymer Chemistry* **2016,** *7* (16), 2790-2798.

14. Bailey, A. E., *Industrial oil and fat products*. Interscience Publishers, Inc.; New York: 1945.

15. Johnson, R. W.; Fritz, E., *Fatty acids in industry*. M. Dekker: 1989.

16. Lligadas, G.; Ronda, J. C.; Galia, M.; Cádiz, V., Plant oils as platform chemicals for polyurethane synthesis: current state-of-the-art. *Biomacromolecules* **2010,** *11* (11), 2825-2835.

17. Raquez, J.-M.; Deléglise, M.; Lacrampe, M.-F.; Krawczak, P., Thermosetting (bio) materials derived from renewable resources: a critical review. *Progress in polymer science* **2010,** *35* (4), 487-509.

18. Pan, X.; Sengupta, P.; Webster, D. C., High biobased content epoxy–anhydride thermosets from epoxidized sucrose esters of fatty acids. *Biomacromolecules* **2011,** *12* (6), 2416-2428.

19. Wang, Z.; Zhang, X.; Wang, R.; Kang, H.; Qiao, B.; Ma, J.; Zhang, L.; Wang, H., Synthesis and characterization of novel soybean-oil-based elastomers with favorable processability and tunable properties. *Macromolecules* **2012,** *45* (22), 9010-9019.

20. Türünç, O.; Meier, M. A., The thiol-ene (click) reaction for the synthesis of plant oil derived polymers. *European journal of lipid science and technology* **2013,** *115* (1), 41-54.

21. Tarnavchyk, I.; Popadyuk, A.; Popadyuk, N.; Voronov, A., Synthesis and free radical copolymerization of a vinyl monomer from soybean oil. *ACS Sustainable Chemistry & Engineering* **2015,** *3* (7), 1618-1622.

22. Demchuk, Z.; Shevchuk, O.; Tarnavchyk, I.; Kirianchuk, V.; Kohut, A.; Voronov, S.; Voronov, A., Free Radical Polymerization Behavior of the Vinyl Monomers from Plant Oil Triglycerides. *ACS Sustainable Chemistry & Engineering* **2016**.

23. Demchuk, Z.; Shevchuk, O.; Tarnavchyk, I.; Kirianchuk, V.; Lorenson, M.; Kohut, A.; Voronov, S.; Voronov, A., Free-Radical Copolymerization Behavior of Plant-Oil-Based Vinyl Monomers and Their Feasibility in Latex Synthesis. *ACS Omega* **2016,** *1* (6), 1374-1382.

24. Smith, W. V., The Kinetics of Styrene Emulsion Polymerization1a. *Journal of the American Chemical Society* **1948,** *70* (11), 3695-3702.

25. Smith, W. V.; Ewart, R. H., Kinetics of emulsion polymerization. *The journal of chemical physics* **1948,** *16* (6), 592-599.

26. Harkins, W. D., A general theory of the reaction loci in emulsion polymerization. *The Journal of Chemical Physics* **1945,** *13* (9), 381-382.

27. Harkins, W. D., A general theory of the reaction loci in emulsion polymerization. II. *The Journal of Chemical Physics* **1946,** *14* (1), 47-48.

28. Harkins, W. D., A general theory of the mechanism of emulsion polymerization1. *Journal of the American Chemical Society* **1947,** *69* (6), 1428-1444.

29. Smith, W. V., Chain initiation in styrene emulsion polymerization. *Journal of the American Chemical Society* **1949,** *71* (12), 4077-4082.

30. Gardon, J., Emulsion polymerization. II. Review of experimental data in the context of the revised Smith-Ewart theory. *Journal of Polymer Science Part A-1: Polymer Chemistry* **1968,** *6* (3), 643-664.

31. Gardon, J. L., Emulsion polymerization. I. Recalculation and extension of the Smith-Ewart theory. *Journal of Polymer Science Part A-1: Polymer Chemistry* **1968,** *6* (3), 623-641.

32. Priest, W., Partice growth in the aqueous polymerization of vinyl acetate. *The Journal of Physical Chemistry* **1952,** *56* (9), 1077-1082.

33. Erbil, Y. H., *Vinyl acetate emulsion polymerization and copolymerization with acrylic monomers*. CRC press: 2000.

34. Thickett, S. C.; Gilbert, R. G., Emulsion polymerization: State of the art in kinetics and mechanisms. *Polymer* **2007,** *48* (24), 6965-6991.

35. Roe, C. P., Surface chemistry aspects of emulsion polymerization. *Industrial & Engineering Chemistry* **1968,** *60* (9), 20-33.

36. Fitch, R.; Tsai, C., Polymer Colloids, ed. RM Fitch. New York, London: Plenum) p: 1971.

37. Fitch, R. M., The homogeneous nucleation of polymer colloids. *British polymer journal* **1973,** *5* (6), 467-483.

38. Chern, C.-S.; Lin, C.-H., Using a water-insoluble dye to probe the particle nucleation loci in styrene emulsion polymerization. *Polymer* **1999,** *40* (1), 139-147.

39. Immergut, E. H.; Mark, H. F., Principles of plasticization. *Plasticization and plasticizer processes* **1965,** *48*, 1-26.

CHAPTER 4. EFFECT OF HIGHLY HYDROPHOBIC PLANT OIL-BASED MONOMERS ON MICELLIZATION OF SODIUM DODECYL SULFATE[1]

4.1. Abstract

The effect of highly hydrophobic olive oil-based (OVM) and high oleic soybean oil-based (HO-SBM) acrylic monomers on micellization of sodium dodecyl sulfate (SDS) was examined at different surfactant and monomer concentrations by determining micellar parameters, size and structure, as well as surface tension measurements. The obtained results indicate the ability of SDS to solubilize sparingly soluble-in-water plant oil-based monomer (POBM) molecules and facilitate the formation of mixed (SDS/POBM) micelles. Surface activity of a surfactant/monomer mixture varies by adding the POBM and is generally higher than for SDS. Comprehensive trends were observed for micellar aggregation number and number of micelle-bound monomer molecules demonstrating that POBM molecules replace SDS counterparts in the mixed micelles. Based on dynamic light scattering measurements (DLS), we hypothesized that incorporation of POBM into the mixed micelles promotes micellar association and formation of 25-30 nm size structures, also detected using transmission electron microscopy (TEM). The practical importance of these findings is the fact that solubilization of POBM by surfactant molecules can have an impact on reaction kinetics and mechanism of emulsion polymerization, as well as affect latex particle formation and, respectively, resulting particle morphology.

[1] The material in this chapter was co-authored by Kyle Kingsley, Oleh Shevchuk, Stanislav Voronov, and Andriy Voronov. Kyle Kingsley had the primary responsibilities of preparing micellar solutions for steady-state fluorescence experiments and TEM analysis. Kyle Kingsley was also charged with characterizing the mixed-micelle solutions by fluorescence spectroscopy, DLS, and surface energy measurements, as well as performing all calculations in this chapter. Kyle Kingsley was involved in drafting and revising all versions of this chapter. Oleh Shevchuk and Andriy Voronov checked the calculations performed by Kyle Kingsley. Published article can be found at https://doi.org/10.1016/j.colsurfa.2019.02.013.

4.2. Introduction

Using plant and vegetable oils in emulsion polymerization, and their incorporation at high levels in bio-based latexes (including commercial latexes), is challenging because of the highly hydrophobic nature of main oil constituents, triglycerides (esters derived from glycerol and fatty acids)[1-4]. Being emulsified into the droplets, the monomer's ability to diffuse through the aqueous phase and enter the growing polymer-monomer particles to be polymerized is essential for emulsion polymerization[5]. For this process to take place, the monomer has to be soluble in water at some finite level[6-8]. Because of the highly hydrophobic nature of triglyceride molecules, plant oil-derived hydrophobic monomers possess only very limited aqueous solubility[4] restricting their transport and incorporation into the resulting emulsion polymers (latexes)[9-10]. Besides, the presence of allylic protons in fatty acid fragments of triglyceride molecules leads to additional limitations in terms of using such monomers in emulsion polymerization. Allylic hydrogen can be easily abstracted from monomer molecules during the polymerization process to form a radical that terminates the kinetic chain, reduces rate of polymerization, and essentially lowers the molecular weight of polymer by taking part in chain transfer reactions[11-12].

Currently, emulsion polymerization is not extensively applied in synthesizing industrial polymer materials based on plant and vegetable oils, in part due to the limited availability of free radical polymerization monomers derived from oil triglycerides[13-19]. In this regard, the synthesis of new monomers derived from high oleic soybean oil (HOSO) was recently reported, as well as the ability to polymerize such monomers in free-radical polymerization in a solution to yield thermoplastic polymers[20]. From a library of HOSO-based (meth)acrylate monomers, polymers with a broad range of glass transition temperatures and physical properties were synthesized[21]. Using the one-step method of plant oil direct transesterification developed in our group, vinyl

monomers from sunflower, linseed, soybean, and olive oil have been recently synthesized[22-23]. The resultant plant oil-based monomers (POBM) have different amount of unsaturation in fatty acid fragments presented in each POBM structure (**Figure 4.1**).

In our previous work, unsaturation amount was used as a criterion in studying the kinetics of free radical solution polymerization, as well as for demonstrating the feasibility of bio-based latex synthesis and preparing films from latexes[22-24]. It was shown that reaction rate, monomer conversion, and molecular weight of the resulting polymers and copolymers all depend on POBM structure and are determined by chain transfer reaction (due to the allylic hydrogen atoms in POBM fatty acid fragments) coexisting with chain propagation[23-24].

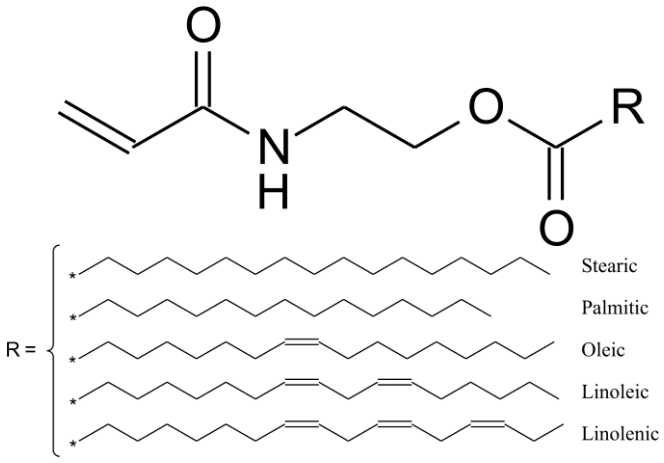

Figure 4.1. Chemical composition of plant oil-based monomers

As it is mentioned above, very high hydrophobicity of vinyl plant oil-based monomers (their aqueous solubility was shown to be in a range of 10^{-3} wt.%)[22] limits POBM transport from monomer droplets through the aqueous phase into the growing particles, thus impacting kinetic features and the process of latex particle formation in conventional emulsion polymerization.

Recently our group reported that the emulsion copolymerization of up to 20 wt.% of POBM (soybean and olive oil-based monomers) with styrene, in general, follows the Smith-Ewart kinetic theory, most often used to describe the polymerization of hydrophobic monomers in emulsion

(Chapter 3)[25]. Experimentally determined emulsifier (sodium dodecyl sulfate, SDS) and initiator reaction orders (0.58-0.65 and 0.39-0.46, respectively) indicate that latex particles are mainly formed by micellar nucleation. The number of nucleated particles almost does not depend on the POBM chemical structure (unsaturation amount) and its content in a copolymerization reaction. However, although the obtained results showed that the reaction follows a typical phenomenology for the emulsion process for hydrophobic monomers, mixed mode of nucleation (both micellar and homogeneous) was observed by measuring latex particle size and calculating their number. This mode of mixed nucleation was explained by the possible interactions between amphiphilic molecules of POBM (containing polar acryloylamino "head," CH_2=CH-C(O)-NH- and long hydrophobic "tail" with an average 17 carbon atoms) and SDS. During emulsion polymerization, these interactions can facilitate higher POBM availability (through monomer solubilization) in polymerization loci, either in the aqueous phase or in the micelles (and growing particles). This is why, in addition to micellar nucleation, homogeneous nucleation seems to be the possible operative mode in the copolymerization of POBM.

Here we report on studying intermolecular interactions between two different plant oil-based monomers from those synthesized in our group's POBM library, olive oil-based (OVM) and high oleic soybean oil-based (HO-SBM), with SDS. The features of the micelles formed by SDS in the presence of OVM and HO-SBM were investigated in respect to changing OVM/HO-SBM content and SDS/OVM (HO-SBM) ratio in the aqueous medium. For this purpose, micellar aggregation number (using steady state fluorescence quenching), micellar size (by dynamic light scattering) and surface tension were measured to determine the effect of POBMs on micellar formation and, thus, illustrate that potential effects of surfactant-monomer interactions on

polymerization kinetics and latex particle formation (nucleation mechanism) during conventional emulsion polymerization process exists.

It is assumed that replacing petroleum-based components in latexes with a natural, renewable POBM ingredient can be beneficial for a broad variety of applications of polymeric materials. It is a major long-term goal of the current research study.

4.3. Experimental

4.3.1. Materials

Olive oil (Bertolli; Houston, TX), high oleic soybean oil (Perdue AgriBusiness LLC; Salisbury, MD), sodium dodecyl sulfate (SDS, VWR; Solon, OH), pyrene (Alfa Aesar, Ward Hill, MA), and cetylpyridinium chloride (TCI, Portland, OR) were used as received. All other solvents used were reagent grade or better and used as received. The water used for all reactions was deionized water (MilliQ, 18MΩ).

4.3.2. Sample preparation

Synthesis of plant oil-based acrylic monomers (POBM) from olive and high oleic soybean oils with N-(hydroxyethyl) acrylamide (OVM and HO-SBM, respectively) has been previously reported from this research group[23-24]. A $1x10^{-3}$ M stock solution of pyrene in ethanol was first prepared due to pyrene's poor solubility in water. A small aliquot of the stock solution was then transferred to a 20 mL vial with water where the ethanol was allowed to evaporate under nitrogen. 10 mL aqueous solutions containing pyrene ($1.9x10^{-5}$ M), SDS (0.104 M or 0.26 M (to be used in emulsion polymerization process)), and appropriate amounts of OVM/HO-SBM were prepared and stirred via magnetic stir bar.

Once homogeneous, samples were prepared by transferring 1 mL of the pyrene/SDS/POBM solutions to a small vial before charging appropriate volumes of

cetylpyridinium ion (quencher) aqueous solution ($8.7x10^{-4}$ M). All mixtures were then diluted with water to a final volume of 5 mL. The final concentrations in the working samples were [pyrene] = $3.8x10^{-6}$ M and [SDS] = 0.0208 M or 0.052 M. POBM concentrations are listed in **Table 4.1**. The different concentrations of quencher used in this study can be seen in **Figure A1** in **Appendix A**.

4.3.3. Steady-state fluorescence quenching

Fluorescence spectra were recorded using a Fluoromax-3 spectrofluorimeter (Jobin Yvon Inc., Edison, NJ) at room temperature. An excitation wavelength of 337 nm and emission wavelength recorded from 350 to 500 nm with a step of 1 nm were used to obtain the experimental fluorescence spectra. Emission and excitation slit widths were fixed at 2.5 and 2.5 nm, respectively. Measured intensities of quenched (I) and unquenched (I_0) solution fluorescences were determined using the maximum height of the fourth peak (394 nm). Fluorescence spectra for a complete series of solutions can be seen in **Figure A1**. As the concentration of quencher increases, the relative intensities of the solutions decrease.

4.3.4. Micelle characterization

Micelle size distributions were recorded using a Zetasizer Nano-ZS90 (Malvern, Worcestershire, U.K.) at 25 °C using a single scattering angle of 90°. The reported values are the average of 5 measurements compiled of 10 runs per measurement. Surface tension values were determined by the pendant drop method using a contact angle/surface tension analyzer (First Ten Angstroms, Portsmouth, VA). Average surface tension values were determined from five measurements. Transmission election microscopy (TEM) was used to confirm size and study the morphology of the micelles using a JEM-100CX II (JEOL, Peabody, MA) tungsten-filament 100 kV transmission electron microscope at room temperature.

4.3.5. Calculations

First developed by Turro and Yekta[26], fluorescence quenching measures changes in intensity of fluorescent probes (pyrene) upon the addition of quencher molecules (cetylpyridinium ion). Due to the nature of both the probe and quencher, it is assumed that both species will be found in the micelle. Low concentrations are required in order to assume random association with micelles as described by Poisson distributions[27]. It is also assumed that the presence of one quencher molecule will deactivate all fluorescent probes located within that micelle[26-27].

If the concentration of micelles [M] and concentration of quencher [Q] are known and assumed to exhibit Poisson distributions, **Equation 4.1** can be derived relating the ratio between I and I_0 to [M] and [Q].

$$\frac{I}{I_0} = e^{-\frac{[Q]}{[M]}} \qquad \text{(Equation 4.1)}$$

Furthermore, the concentration of micelles can be calculated in terms of aggregation number N_{agg}, bulk concentration of surfactant [S] and concentration of free surfactant [S_F]. By assuming that $S_F \approx CMC$[27-28], the [M] can be calculated using **Equation 4.2**.

$$[M] = \frac{[S]-CMC}{N_{agg}} \qquad \text{(Equation 4.2)}$$

From this, **Equation 4.1** becomes:

$$\ln\left(\frac{I_0}{I}\right) = \frac{[Q]N_{agg}}{[S]-CMC} \qquad \text{(Equation 4.3)}$$

As seen in **Figure 4.2**, plotting $\ln(I_0/I)$ as a function of [Q] produces a straight line with a best fit equation equal to that seen in **Equation 4.3**. As long as the CMC of the surfactant is known, the aggregation number can be calculated as the slope of the best fit line.

Calculating the number of additive molecules per micelle N_{add} can be done using **Equation 4.4**:

$$N_{add} = \frac{k[C_A]_T}{(1+k)[M]}, \quad \text{(Equation 4.4)}$$

where $[C_A]_T$ is the total additive concentration and k is the partition coefficient, given by **Equation 4.5**:

$$k = \frac{[C_A]_{mic}}{[C_A]_{aq}}, \quad \text{(Equation 4.5)}$$

where $[C_A]_{mic}$ and $[C_A]_{aq}$ are the concentrations of additive in the micellar and aqueous phases, respectively. In order to calculate k, the aqueous solubility of the POBMs (~$1x10^{-3}$ %) was used, making the partition coefficient much larger than 1. This reduced **Equation 4.4** to:

$$N_{add} = \frac{[C_A]_T}{[M]} \quad \text{(Equation 4.6)}$$

4.4. Results and discussion

The micelle aggregation number corresponds to the number of surfactant molecules making the micelle and is affected by nature of surfactant and temperature[29-30], but also the concentration and nature of additives in the solution[31-32]. The value of aggregation number provides important information for practical applications, such as micellar shape and size, and can be related to stability of the micelles[29, 32].

In determination of physical properties in micellar systems, including their aggregation number, fluorescence quenching is considered as the most widespread method[26, 33]. In brief, this method involves labeling micelles with a fluorescent probe and measuring the signal before and after adding quencher molecules which interact with a probe and deactivate its excited molecules. Various probe/quencher systems can be used to determine micellar aggregation number in aqueous solution with the assumption that both probe and quencher are located in the same environment of the micelles[34].

In this work, the probe is polycyclic hydrocarbon pyrene (apolar) and the quencher, cetylpyridinium ion, possessing a long, hydrophobic fragment. Both have been often used for

characterizing physical properties of various micellar systems[27] and undergo preferential localization in the micelles upon addition into micellar systems[35]. To determine the micellar aggregation number, N_{agg}, fluorescent intensity I should be measured at various concentrations of quencher [Q] with fixed concentrations of surfactant and pyrene. Provided the CMC of the surfactant is known, the N_{agg} can be calculated by plotting $\ln(I_0/I)$ against [Q], where I_0 *i*s the intensity in the absence of quencher. **Figure 4.2** shows plots of $\ln(I_0/I)$ vs. [Q] obtained at two different SDS concentrations (0.02 M and 0.05 M, both above CMC of the SDS, 0.008 mol/L) in the presence of various amounts of high oleic soybean oil- and olive oil-based monomers. From the slope of each line, aggregation number in each experiment was determined (**Figure 4.3, Table 4.1**).

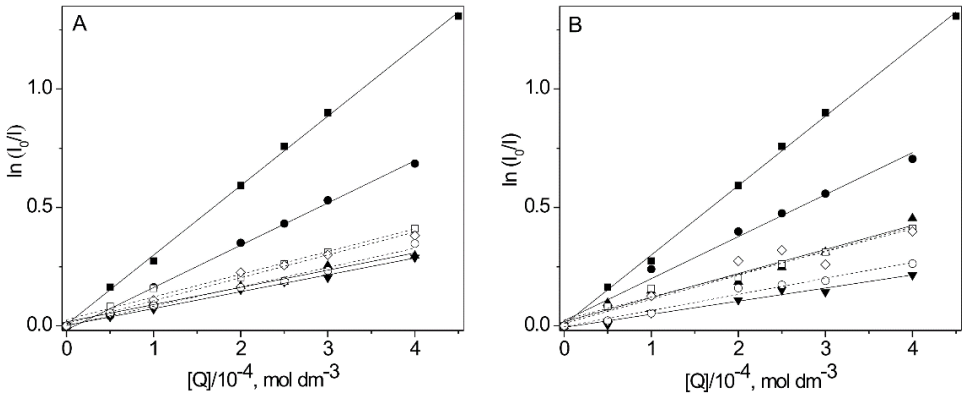

Figure 4.2. Plots of $\ln(I_0/I)$ vs. [Q] obtained at SDS concentration of ■ - 0.02 M in the presence of ● - 0.01M, ▲- 0.02M, ▼ - 0.04M**,** and at SDS concentration of □ - 0.05 M in the presence of ◊ - 0.02M, ○ - 0.04 M of HO-SBM (**A**) and OVM (**B**).

Table 4.1. Micellar parameters for SDS and POBM at different concentrations

SDS + POBM (x, mol : y, mol)	N_{agg}*	N_{POBM}	I_1/I_3	d, nm	PDI	γ, mN/m
SDS at 0.02 M	41	0	1.04	3.1	0.01	36.2
+ HO-SBM 0.01 M	25	20	0.94	18.2	0.02	34.1
0.02 M	15	25	0.94	23.3	0.05	31.2
0.04 M	12	39	0.92	25.4	0.04	30.4
SDS at 0.05 M	57	0	1.03	1.7	0.008	34.9
+ HO-SBM 0.02 M	46	22	0.96	27.3	0.03	31.5
0.04 M	38	34	0.95	28.5	0.05	29.8
SDS at 0.02 M	41	0	1.04	3.1	0.01	36.2
+ OVM 0.01 M	27	22	0.95	22.6	0.06	32.4
0.02 M	19	31	0.93	28.7	0.04	31.1
0.04 M	10	33	0.93	37.8	0.04	30.1
SDS at 0.05 M	57	0	1.03	1.7	0.008	34.9
+ OVM 0.02 M	48	23	0.95	28.2	0.02	32.6
0.04 M	31	28	0.94	33.9	0.04	30.2

***** uncertainty for N_{agg} is determined by the accuracy of linear fit of the obtained points (**Fig. 4.1**), r^2 varies in a range 0.96-0.98

It is evident from **Figure 4.3** and **Table 4.1** that there is an interaction between the surfactant and plant oil-based monomer affecting the resulting micellar aggregation number. N_{agg} of SDS molecules in the micelle decreases with increasing concentration of added HO-SBM and OVM. The obtained results indicate the ability of SDS to solubilize sparingly soluble plant oil-based monomer molecules and facilitate their incorporation into aggregated phase, thus, formation of mixed (SDS/POBM) micelles. Such effects have been observed by various authors when solubilization of various polar and non-polar additives (including medium chain length alcohols and aliphatic ketones) in micelles of different surfactants (including SDS) was investigated[28].

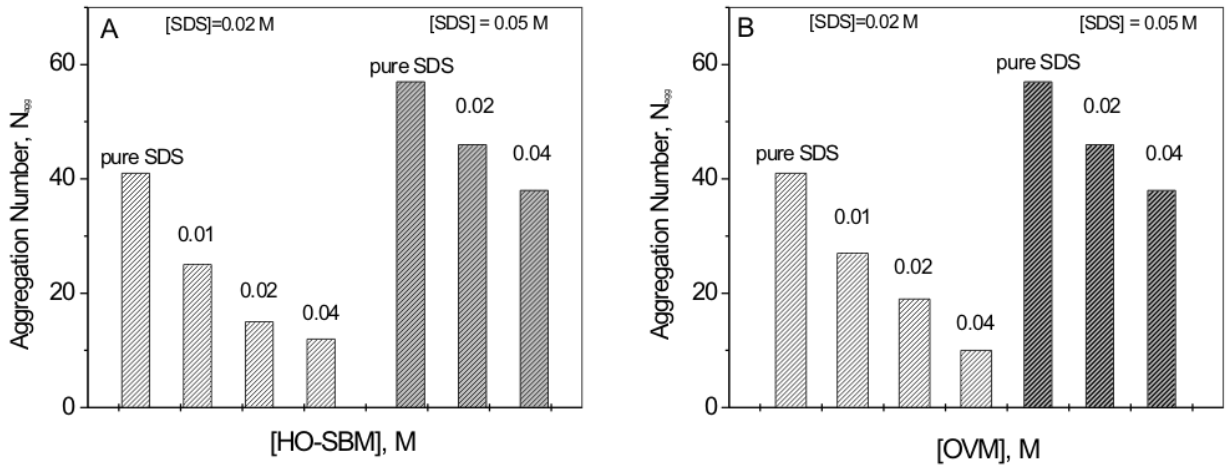

Figure 4.3. Values of aggregation number for SDS in the presence of various amounts of HO-SBM (**A**) and OVM (**B**)

Solubilization is determined by various physical parameters of additives such as polarity, molar concentration, charge, configuration etc. In this communication, our main interest is focused on POBM effect on surfactant micellization, emulsion formation and further, on polymerization mechanism and latex particle nucleation and growth. To this end, in this study we determined how the presence of HO-SBM or OVM changes micellar aggregation number, number of micelle-bound monomer molecules and surface tension in the presence of various amount of POBM, as well as mixed micelles size.

While decreasing micellar aggregation number confirms surfactant and monomer interaction, evidence for site of POBM solubilization in the mixed micelles can be found using fluorescence spectra recorded for determining N_{agg}. In this regard, the ratio between the first and third peaks of pyrene fluorescence (see plots in **Appendix A**) can be used to identify the polarity of the microenvironment of the fluorophore (knowing that pyrene molecules reside in the micellar interior)[28] and monitor changes of pyrene localization in the presence of hydrophobic POBM molecules. In this study, the I_1/I_3 value for SDS at both experimental concentrations is equal to 1.03-1.04 which corresponds to published data[28]. As it is seen from **Table 4.1**, the I_1/I_3 is affected

by solubilization of either HO-SBM or OVM in the mixed micelles. This value decreases for various ratios of monomer and surfactant and ranges from 1.04 to 0.92 for HO-SBM and from 1.04 to 0.93 for OVM. Those changes might be caused by partial quenching of pyrene probe fluorescence upon solubilization of plant oil-based monomer. This is evident from the changing value I_1/I_3 that most probable localization site of POBM molecules is close to the place where pyrene probe molecules are located.

To further confirm intermolecular interactions between SDS molecules and plant oil-based monomers, the surface activity of SDS/POBM mixtures was determined using surface tension measurements. The surface tension data showed that with increasing concentration of POBM in the mixture with SDS (above CMC), the surface tension values decrease, thus surface activity of the mixture becomes higher in comparison to pure SDS (**Table 4.1**). This finding confirms that there is an interaction between SDS and POBM in aqueous solutions, resulting in changing surface activity of SDS by adding the POBM already at low concentration.

In order to provide more insights about mixed micellar composition, we determined another micellar parameter, the number of plant oil-based monomer molecules per micelle, N_{POBM} (**Table 4.1**). As expected, this number systematically increases as the concentration of POBM increases, with the rise of N_{POBM} being more pronounced when HO-SBM was added. The latter fact can be qualitatively explained by slightly higher aqueous solubility of HO-SBM as compared to OVM. The obtained data clearly indicate that being solubilized by surfactant, molecules of plant oil-based monomers take part in the micellization process, thus mixed species from SDS and POBM are yielded. **Figure 4.4** presents DLS data on particle size distribution for the mixed micelles formed from two SDS concentrations in a presence of different amounts of OVM and HO-SBM, along with the size of SDS only micelles (**Figure 4.4 A**, inset).

The plots indicate that micellar diameter grows, and size distribution becomes increasingly broader when plant oil-based monomers are mixed with SDS in solution. The maximum was detected at about 18 - 38 nm for the measurements performed on surfactant-monomer mixtures, while characteristic size of the SDS micelles is about 2 – 3 nm, that is in agreement with literature data[36]. It is evident that while $N_{agg} + N_{POBM}$ in POBM/SDS micelles does not increase significantly (**Table 4.1**), size of the micelles essentially grows once POBM is added at different concentrations.

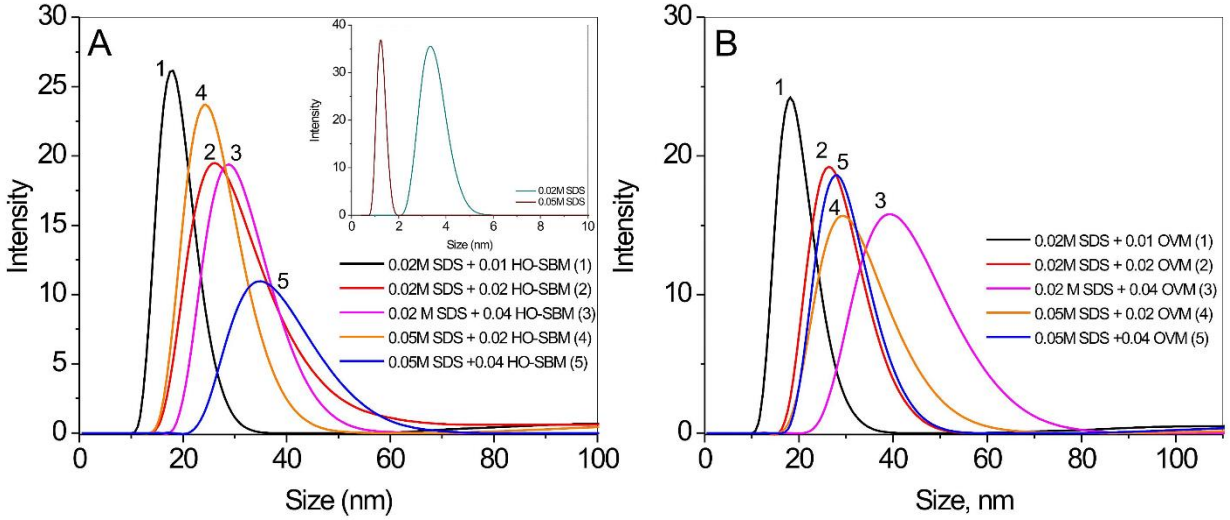

Figure 4.4. Size distribution of micelles prepared from SDS (A, inset), SDS mixed with HO-SBM (**A**) and OVM (**B**) at different concentrations

Selected samples of mixed micelles from plant oil-based monomers and surfactant have been studied using TEM. **Figure 4.5** shows the TEM micrograph of the micelles prepared by mixing SDS and HO-SBM. A thin film was fabricated using the blotting technique. The picture indicates that the average diameter of the micelles is approximately 25 - 35 nm. Therefore, the obtained results determined by TEM confirm the mixed micelles DLS size measurements.

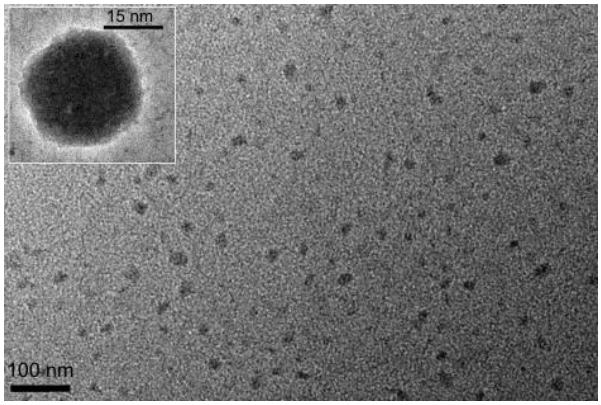

Figure 4.5. TEM micrograph of micelles prepared by mixing SDS (0.02 M) and HO-SBM (0.01 M). Inset shows morphology of selected individual micelle.

Assuming that solubilization of POBM amphiphilic molecules by SDS and their incorporation into the micelles can facilitate higher availability of plant oil-based monomer in the emulsion polymerization process, and impact latex particle nucleation modes, we addressed formation of mixed micelles and micellar size increases in the following way.

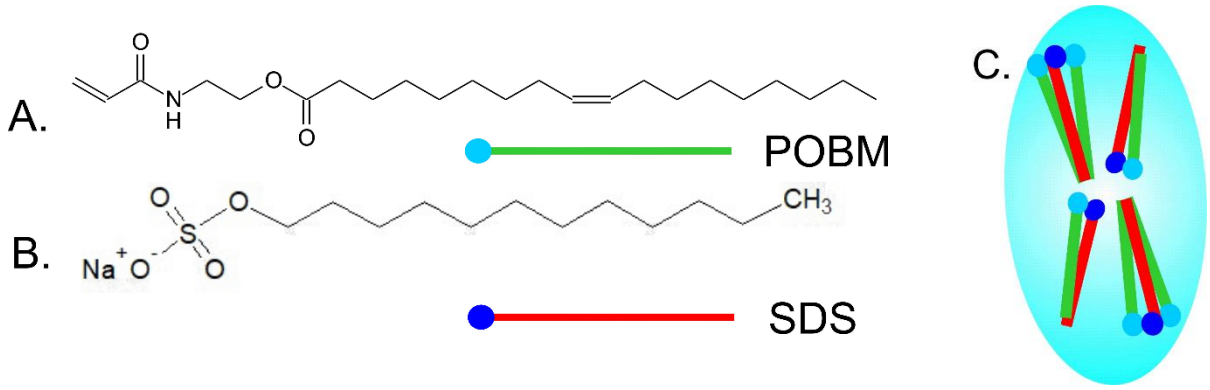

Figure 4.6. Chemical structure of plant oil-based monomer (**A**), surfactant (**B**), and schematic of POBM solubilization by SDS molecules (**C**)

Due to similarity of POBM (**Figure 4.6 A**) and SDS (**Figure 4.6 B**) molecular composition (both molecules have polar "head" and long hydrophobic "tail" with an average 17 carbon atoms in POBM and 12 carbon atoms in SDS), POBM molecules are solubilized by the much more soluble in water SDS counterparts once they both are presented in solution at the same time. It seems obvious that the most realistic way for POBM and SDS physical association in water is when "head-to-head" and "tail-to-tail" interactions act synergistically (**Figure 4.6 C**), followed by

micellization and POBM incorporation into the mixed micelles. Experimentally confirmed fact of POBM incorporation into the micelles with SDS can help in explaining the micellar size increase in the presence of plant oil-based monomer.

We hypothesize that polar "heads" of the solubilized into micellar exterior POBM can interact not only with polar "heads" of SDS molecules within the individual micelle, but also form physical bonds with counterparts localized in other neighboring micelles, thus causing their overall destabilization and promoting some level of aggregation in the micellar solution (**Figure 4.7**). As a result, stable micellar aggregates are formed consisting from several mixed micelles as it is shown in **Figure 4.7 C**.

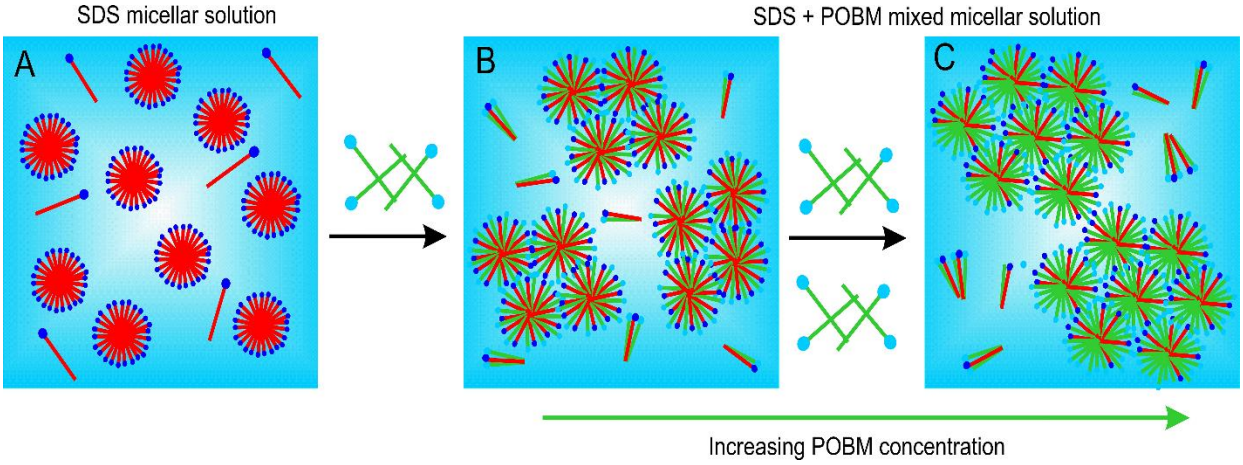

Figure 4.7. Formation of SDS/POBM mixed micelles in aqueous medium by increasing concentration of plant oil-based monomers

Summarizing the obtained findings in a connection with phenomenology and basics of emulsion polymerization, one can almost certainly expect the effect of plant oil-based monomers solubilization by surfactant molecules on reaction kinetics, latex particle formation mechanisms and, respectively, particle morphology. An extensive study of those aspects is currently on its way in our research group.

4.5. Conclusions

The effect of highly hydrophobic olive oil-based (OVM) and high oleic soybean oil-based (HO-SBM) acrylic monomers on micellization of sodium dodecyl sulfate (SDS) was studied at different concentrations of monomers and surfactant. Chemical composition of plant oil-based monomer (POBM) and SDS molecules is similar. They both have a polar "head" and long hydrophobic "tail" with an average 17 (POBM) and 12 (SDS) carbon atoms. The obtained results indicate that SDS molecules solubilize sparingly soluble-in-water plant oil-based monomer (POBM) counterparts, thus facilitating formation of mixed (SDS/POBM) micelles. It is our assumption that intermolecular interactions occur through physical association of both molecular "heads" and "tails" in water. The data show that surface activity of a surfactant/monomer mixture is generally higher than for SDS and varies by adding the POBM. Additionally, micellar parameters, size and structure, observed changes upon the addition of POBM.

A similar effect of POBM presence in a mixture with SDS was shown for micellar aggregation number and number of micelle-bound monomer molecules demonstrating that plant oil-based molecules do replace SDS counterparts in mixed micelles.

Being incorporated into the micellar exterior, the polar "heads" of POBM interact between each other, not only within an individual micelle, but also with neighboring micelles, thus promoting some level of micellar association. Based on dynamic light scattering measurements (DLS), we observed the formation of 25-30 nm sized micellar structures, also detected using transmission electron microscopy (TEM). The practical importance of these findings is in fact that solubilization of POBM by surfactant molecules can have an impact on reaction kinetics and mechanism of emulsion polymerization, as well as affect latex particle formation and, respectively, resulting particle morphology.

4.6. References

1. Thames, S. In *Solventless emulsion polymers for coatings*, Proceedings of the Twenty-Fifth International Waterborne, High-Solids, and Powder Coatings Symposium, New Orleans, LA, **1998;** pp 305-320.
2. Williams, C.; Mendon, S.; Rogers, M.; Thames, S. In *Emulsion polymerization of hydrophobic monomers*, Proceedings of 30th International Waterborne, High-Solids, and Powder Coatings Symposium, New Orleans, LA, **2003;** pp 199-216.
3. Quintero, C.; Delatte, D.; Diamond, K.; Mendon, S.; Rawlins, J.; Thames, S., Reaction calorimetry as a tool to determine diffusion of vegetable oil macromonomers in emulsion polymerization. *Progress in organic coatings* **2006,** *57* (3), 202-209.
4. Booth, G.; Delatte, D. E.; Thames, S. F., Incorporation of drying oils into emulsion polymers for use in low-VOC architectural coatings. *Industrial Crops and Products* **2007,** *25* (3), 257-265.
5. Ugelstad, J.; Hansen, F., Kinetics and mechanism of emulsion polymerization. *Rubber chemistry and technology* **1976,** *49* (3), 536-609.
6. Joseph Schork, F.; Back, A., Inhibition effects in emulsion and miniemulsion polymerization of monomers with extremely low water solubility. *Journal of applied polymer science* **2004,** *94* (6), 2555-2557.
7. Chai, X.-S.; Schork, F.; DeCinque, A.; Wilson, K., Measurement of the solubilities of vinylic monomers in water. *Industrial & engineering chemistry research* **2005,** *44* (14), 5256-5258.
8. Tauer, K.; Ali, A. I.; Yildiz, U.; Sedlak, M., On the role of hydrophilicity and hydrophobicity in aqueous heterophase polymerization. *Polymer* **2005,** *46* (4), 1003-1015.

9. Leyrer, R. J.; Mächtle, W., Emulsion polymerization of hydrophobic monomers like stearyl acrylate with cyclodextrin as a phase transfer agent. *Macromolecular Chemistry and Physics* **2000,** *201* (12), 1235-1243.

10. Lau, W. In *Emulsion polymerization of hydrophobia monomers*, Macromolecular Symposia, Wiley Online Library: **2002;** pp 283-289.

11. Chen, F. B.; Bufkin, B. G., Crosslinkable emulsion polymers by autoxidation. II. *Journal of applied polymer science* **1985,** *30* (12), 4551-4570.

12. Chen, F. B.; Bufkin, B. G., Crosslinkable emulsion polymers by autoxidation. I. Reactivity ratios. *Journal of applied polymer science* **1985,** *30* (12), 4571-4582.

13. Bailey, A. E., *Industrial oil and fat products*. Interscience Publishers, Inc.; New York: 1945.

14. Johnson, R. W.; Fritz, E., *Fatty acids in industry*. M. Dekker: 1989.

15. Lligadas, G.; Ronda, J. C.; Galia, M.; Cádiz, V., Plant oils as platform chemicals for polyurethane synthesis: current state-of-the-art. *Biomacromolecules* **2010,** *11* (11), 2825-2835.

16. Raquez, J.-M.; Deléglise, M.; Lacrampe, M.-F.; Krawczak, P., Thermosetting (bio) materials derived from renewable resources: a critical review. *Progress in polymer science* **2010,** *35* (4), 487-509.

17. Pan, X.; Sengupta, P.; Webster, D. C., High biobased content epoxy–anhydride thermosets from epoxidized sucrose esters of fatty acids. *Biomacromolecules* **2011,** *12* (6), 2416-2428.

18. Wang, Z.; Zhang, X.; Wang, R.; Kang, H.; Qiao, B.; Ma, J.; Zhang, L.; Wang, H., Synthesis and characterization of novel soybean-oil-based elastomers with favorable processability and tunable properties. *Macromolecules* **2012,** *45* (22), 9010-9019.

19. Türünç, O.; Meier, M. A., The thiol-ene (click) reaction for the synthesis of plant oil derived polymers. *European journal of lipid science and technology* **2013,** *115* (1), 41-54.

20. Yuan, L.; Wang, Z.; Trenor, N. M.; Tang, C., Robust Amidation Transformation of Plant Oils into Fatty Derivatives for Sustainable Monomers and Polymers. *Macromolecules* **2015,** *48* (5), 1320-1328.

21. Yuan, L.; Wang, Z.; Trenor, N. M.; Tang, C., Amidation of triglycerides by amino alcohols and their impact on plant oil-derived polymers. *Polymer Chemistry* **2016,** *7* (16), 2790-2798.

22. Tarnavchyk, I.; Popadyuk, A.; Popadyuk, N.; Voronov, A., Synthesis and free radical copolymerization of a vinyl monomer from soybean oil. *ACS Sustainable Chemistry & Engineering* **2015,** *3* (7), 1618-1622.

23. Demchuk, Z.; Shevchuk, O.; Tarnavchyk, I.; Kirianchuk, V.; Kohut, A.; Voronov, S.; Voronov, A., Free Radical Polymerization Behavior of the Vinyl Monomers from Plant Oil Triglycerides. *ACS Sustainable Chemistry & Engineering* **2016**.

24. Demchuk, Z.; Shevchuk, O.; Tarnavchyk, I.; Kirianchuk, V.; Lorenson, M.; Kohut, A.; Voronov, S.; Voronov, A., Free-Radical Copolymerization Behavior of Plant-Oil-Based Vinyl Monomers and Their Feasibility in Latex Synthesis. *ACS Omega* **2016,** *1* (6), 1374-1382.

25. Kingsley, K.; Shevchuk, O.; Demchuk, Z.; Voronov, S.; Voronov, A., The features of emulsion copolymerization for plant oil-based vinyl monomers and styrene. *Industrial Crops and Products* **2017,** *109* (Supplement C), 274-280.

26. Turro, N. J.; Yekta, A., Luminescent probes for detergent solutions. A simple procedure for determination of the mean aggregation number of micelles. *Journal of the American Chemical Society* **1978,** *100* (18), 5951-5952.

27. Flor Rodríguez Prieto, M.; Ríos Rodríguez, M. C.; Mosquera Gonzílez, M.; Ríos Rodr'guez, A. M.; Mejuto Fernández, J. C., Fluorescence quenching in microheterogeneous media: a laboratory experiment determining micelle aggregation number. *Journal of Chemical Education* **1995,** *72*, 662.

28. Malliaris, A., Solubilization of organic molecules in SDS micelles studied by static fluorescence methods. *Advances in colloid and interface science* **1987,** *27* (3-4), 153-168.

29. Tanford, C., *The hydrophobic effect: formation of micelles and biological membranes 2d ed*. J. Wiley.: 1980.

30. Walstra, P., *Physical chemistry of foods*. CRC Press: 2002.

31. Lianos, P.; Lang, J.; Strazielle, C.; Zana, R., Fluorescence probe study of oil-in-water microemulsions. 1. Effect of pentanol and dodecane or toluene on some properties of sodium dodecyl sulfate micelles. *The Journal of Physical Chemistry* **1982,** *86* (6), 1019-1025.

32. Rosen, M. J.; Kunjappu, J. T., *Surfactants and interfacial phenomena*. John Wiley & Sons: 2012.

33. Yekta, A.; Aikawa, M.; Turro, N. J., Photoluminescence methods for evaluation of solubilization parameters and dynamics or micellar aggregates. Limiting cases which allow estimation of partition coefficients, aggregation numbers, entrance and exit rates. *Chemical Physics Letters* **1979,** *63* (3), 543-548.

34. Rodenas, E.; Perez-Benito, E., Sizes and aggregation numbers of SDS reverse micelles in alkanols obtained by fluorescence quenching measurements. *The Journal of Physical Chemistry* **1991,** *95* (11), 4552-4556.

35. Kalyanasundaram, K., *Photochemistry in microheterogeneous systems*. Elsevier: 2012.

36. Duplatre, G.; Ferreira Marques, M.; da Graça Miguel, M., Size of sodium dodecyl sulfate micelles in aqueous solutions as studied by positron annihilation lifetime spectroscopy. *The Journal of Physical Chemistry* **1996,** *100* (41), 16608-16612.

CHAPTER 5. EMULSION COPOLYMERIZATION OF VINYL MONOMERS FROM SOYBEAN AND OLIVE OILS: EFFECT OF COUNTERPART AQUEOUS SOLUBILITY[1]

5.1. Abstract

Highly hydrophobic vinyl monomers from soybean (SBM) and olive (OVM) oils with different amounts of unsaturation were copolymerized in emulsion with significantly more soluble-in-water comonomers, methyl methacrylate (MMA), vinyl acetate (VA), and methyl acrylate (MA). Our intention was to demonstrate that higher aqueous solubility of the comonomer impacts the mechanism of the emulsion process by balancing latex particle homogeneous and heterogeneous (micellar) nucleation.

Using an experimental method based on water insoluble dye Blue 70, it is shown that particle nucleation indeed depends to a great extent on aqueous solubility of the comonomer, along with the plant oil-based monomer (POBM) content in the feed. Upon addition of POBM into the monomer mixture with MMA (aq. solubility 1.5 wt.%), the latex polymer particles originating from micellar nucleation essentially increased. In copolymerization of POBM with MA (aqueous solubility 4.9 wt.%), this effect is even more pronounced. Those findings clearly indicate that copolymerization loci change when monomer feed hydrophobicity increases, and the magnitude of this effect is dependent on the comonomer aqueous solubility.

[1] The material in this chapter was co-authored by Kyle Kingsley, Oleh Shevchuk, Stanislav Voronov, and Andriy Voronov. Kyle Kingsley had the primary responsibilities of synthesizing and characterizing polymer latexes and determining reaction orders with respect to emulsifier and initiator. Kyle Kingsley was also responsible for conducting reactions involving Dye Blue 70 and quantifying modes of particle nucleation. Kyle Kingsley was involved in drafting and revising all versions of this chapter. Oleh Shevchuk and Andriy Voronov help explain trends in reaction order and checked calculations performed by Kyle Kingsley.

Experimentally established nucleation loci using Blue 70 dye were confirmed by a method of kinetic study. Reaction orders with respect to emulsifier and initiator confirm that a balance between latex particle homogeneous and heterogeneous (micellar) nucleation depends on comonomer aqueous solubility. Overall, the portion of latex particles originating through micellar nucleation is higher in the copolymerization of more unsaturated SBM (with both MMA and MA) in comparison to OVM. No impact of POBM content on the reaction kinetics was observed in copolymerization with VA (aq. solubility 2.5 wt.%). Here, high reactivity of growing PVA radicals in chain transfer reactions makes the presence of POBM in monomer feed kinetically irrelevant.

5.2. Introduction

Some of the most widely used polymeric materials in coatings and paints industries are polymer latexes[1]. Numerous reviews evidence that the most commonly applied process for producing latexes (latex polymers) is a free radical polymerization in emulsion that involves the emulsification of monomers (or monomer mixtures) and further (co)polymerization, resulting in the formation of latex particles in an aqueous medium[2-4].

A general theory of emulsion polymerization, as well as its mechanism, including discussions on polymerization loci, has been introduced by Harkins[5-9], and modified by Gardon[10-11]. According to this theory, formation of radicals by decomposition of water-soluble initiator is considered to be a starting point for the polymerization. Once the radicals are formed, latex particle nucleation and growth can proceed through two different mechanisms. The latter is based on monomers' aqueous solubility (hydrophobicity) determining the surface activity of growing macroradicals and their ability to enter the organic phase (the emulsified micellar monomer)[12].

If the surface activity of macroradicals is sufficient, they come into the micelles where latex particle formation proceeds, a mode known as *heterogeneous (micellar)* nucleation. In this

case, reaction rate is controlled by surface area of micelles available for adsorption and consuming the monomer. If the (co)monomer is less hydrophobic (better water-soluble) and the surface activity of macroradicals is lower, the propagation reaction can also occur in the aqueous phase, a process known as *homogeneous* nucleation. Here, formed-in-water macroradical species can further coil up into small particulate nuclei that aggregate into primary particles which are stabilized by available emulsifier[13].

However, both modes can be running simultaneously in any emulsion polymerization process, but one of them usually tends to dominate, based on (co)monomers' aqueous solubility. In this regard, monomers with relatively higher solubility in water (vinyl acetate, methyl methacrylate, methyl acrylate) polymerize more readily through the homogeneous nucleation mode, while the heterogeneous mechanism is preferential in emulsion polymerization of more hydrophobic (styrene, butyl acrylate) monomers.

Since monomer diffusion through the aqueous phase into the growing polymer particles determines the emulsion process, polymerization of highly hydrophobic monomers is challenging and accompanied with low total monomer conversion and large amount of coagulum[14-16]. Different approaches have been used to overcome the monomer diffusion limitations including miniemulsification[17], in situ formation of emulsifier at the oil-water interface[18], adding ingredients with a hydrophobic cavity for monomer localization[19] or improving the monomer solubility[20].

Recently, our group developed a one-step method of plant oil direct transesterification to synthesize vinyl monomers from a range of oils, including sunflower, linseed, soybean, olive oil etc. with a goal to produce plant oil-based latexes in emulsion polymerization[21-23]. Because of the highly hydrophobic nature of plant and vegetable oils, their latex polymerization and incorporation

at high levels in latexes is challenging because of the very low solubility of plant oil-derived monomers in water, which limits their transport during the emulsion process[24-25].

In the previous study, we reported that emulsion copolymerization of up to 20 wt.% of soybean and olive oil-based comonomers with styrene, overall follows the general kinetic Smith–Ewart theory (Chapter 3)[26]. Experimentally determined kinetic parameters (emulsifier and initiator reaction orders) indicate that latex particles are mainly formed by micellar nucleation mode. However, although the obtained results show that reactions follow a typical phenomenology for the emulsion process of hydrophobic monomers, mixed modes of nucleation (both micellar and homogeneous) were also observed.

In the current study, our goal was to determine how the aqueous solubility of comonomers can impact emulsion copolymerization loci of highly hydrophobic plant oil-based monomers as a function of the latex particle nucleation modes. For this purpose, kinetic features for emulsion copolymerization of monomers from soybean oil (SBM) and olive oil (OVM) (aqueous solubility of both monomers is in the range of 10^{-3} wt.%[22] with methyl methacrylate (MMA), vinyl acetate (VA) and methyl acrylate (MA) were investigated. Our intention was to choose comonomer counterparts with significantly higher aqueous solubility, 1.5 wt.% for MMA, 2 wt.% for VA, and 4.9 wt.% for MA, and compare to previously investigated more hydrophobic styrene comonomer (aqueous solubility 0.03 wt.%).

We hypothesize that higher aqueous solubility of the comonomer can impact the mechanism of emulsion process by enhancing plant oil-based monomer availability in the copolymerization reaction, as well as by balancing heterogeneous and homogeneous particle nucleation mechanisms. To the best of our knowledge, there is no report in the literature on the effect of plant oil-based

monomers' hydrophobic nature in emulsion copolymerization with comonomers having different aqueous solubility on the overall reaction kinetics and latex particle formation.

5.3. Materials and methods

5.3.1. Materials

Soybean oil (Crisco; The J.M Smucker Company, Orville, OH), olive oil (Bertolli; Houston, TX), sodium docedyl sulfate (SDS, VWR; Solon, OH), sodium acetate (NaAc, VWR; Solon, OH), and ammonium persulfate (APS, VWR; Solon, OH) were used as received. Methyl methacrylate (MMA, Alfa-Aesar; Ward Hill, MA), vinyl acetate (VA, Alfa-Aesar; Ward Hill, MA), and methyl acrylate (MA, Alfa-Aesar; Ward Hill, MA) were distilled under vacuum to remove the inhibitor and stored in a refrigerator. All other solvents used were reagent grade or better and used as received. The water used for all reactions was Millipore water.

5.3.2. Synthesis of plant oil-based latexes using batch emulsion copolymerization

The synthesis of plant oil-based monomers (POBMs) from olive and soybean oils (OVM and SBM, respectively) with N-(hydroxyethyl) acrylamide was previously reported from the current research group[21-23]. In the current study, reaction kinetics were evaluated using a batch emulsion process. Plant oil-based latexes were formulated to a final solids content of approximately 30 wt.%. First, the aqueous phase was prepared in a 25-mL, single-neck round bottom flask equipped with a magnetic stirrer by dissolving 0.75-6.0 wt.% SDS (per oleo phase) in 9.2 g of water under continuous purging with argon. A buffer solution containing 0.2 wt.% NaAc (per aqueous phase) in 1.0 g of water was then charged to the reaction flask.

The oleo phase was prepared separately by dissolving 2.5-20 wt.% POBM (per oleo phase) in MMA, VA, or MA before being charged to the reaction vessel while being purged with argon. Emulsion was formed at room temperature for 20 minutes before being transferred to a pre-heated

water bath at 60-70 °C, where emulsion formation continued for an additional 5 minutes to reach bath temperature. Polymerization was started by charging 1.0-2.5 wt.% APS (per oleo phase) in 1.0 g of water. The recipes used to investigate reaction kinetics of POBMs with petroleum-based comonomers by batch emulsion copolymerization can be seen in **Table 5.1**.

Table 5.1. Used recipes to investigate POBM/comonomer batch emulsion polymerization

	Wt.%	Wt.% per oleo phase	Mass, g
Oleo phase	30		4.8
POBM, SBM or OVM		2.5-20	0.12-0.96
MMA, VAc, or MA		80-97.5	3.84-4.68
Aqueous phase	70		11.2
Emulsifier, SDS		0.75-6.0	0.036-0.288
Buffer, NaAc*		0.2	0.0224
Initiator, APS		1.0-2.5	0.048-0.12
Total	100		16

* - % per aqueous phase

5.3.3. Characterization of plant oil-based latexes

Kinetic curves were recorded by taking aliquots from the reaction vessel at various time intervals and determining the monomer conversion. The samples were reprecipitated in methanol three times before being dried at 110 °C, producing a constant final mass. Monomer conversion was then plotted as a function of time. The reaction rate, corresponding to the pseudo steady-state rate of polymerization, was determined from the slope of the second interval of the conversion-time plots. Using the obtained kinetic data, the reaction order with respect to the emulsifier and initiator were calculated for copolymerization.

Particle size distributions of the latex polymer particles were determined by a submicron particle sizer (PSS NICOMP Particle Sizing Systems; Santa Barbara, CA) using a monochromatic light with wavelength of approximately 250 nm and a temperature of 25 °C. Samples were prepared by diluting one drop of latex in approximately 7 mL of water. The particle number was calculated using the following equation:

$$N_p = 3 \cdot m_o \cdot S/4 \cdot 100 \cdot \pi\rho r^3 \cdot V, \qquad \text{(Equation 5.1)}$$

where m_0 (g) is the total mass of the oleo phase in the feed, S (%) is the monomer conversion, ρ (g/mL) is the density of the polymer, r (cm) is the radius of the latex particle, and V (mL) is the total volume of the reaction mixture.

Samples were also prepared for additional characterization by reprecipitation in methanol three times before drying in an inert atmosphere until a constant mass was achieved. Latex copolymer composition was determined by ^{1}H NMR spectroscopy using an AVANCE III HDTM 400 MHz high-performance digital NMR spectrometer (Bruker; Billerica, MA). $CDCl_3$ was used as the deuterated solvent.

Copolymer molecular weight averages were determined by gel permeation chromatography (GPC) using a Waters Corporation modular chromatograph consisting of a Waters 515 HPLC pump, a Waters 2410 Refractive Index Detector, and a set of two 10 μm PL-gel mixed B columns. The column temperature was set to 40 °C. THF was used as the carrier solvent.

5.3.4. Evaluating the modes of particle nucleation of plant oil-based latexes using semi-batch process of emulsion copolymerization

Particle nucleation (micellar or homogeneous) modes for monomer mixtures with varying hydrophilicity were evaluated using a procedure described by Chern[27-28]. A water insoluble dye was used as a probe in the semi-batch emulsion copolymerization of POBM with MMA or MA. Typical recipes used for the semi-batch process are shown in **Table 5.2**. Plant oil-based latexes were formulated to a final solids content of approximately 20 wt.%. Polymerization was conducted in a 50-mL, three-neck round bottom flask equipped with a reflux condenser, addition funnel, and magnetic stirrer. First, the initial reactor charge comprised of 1.425 wt.% SDS (per oleo phase)

and 0.02 wt.% NaAc (per aqueous phase) dissolved in 32 g of water was charged to the reaction vessel before being purged with argon for 15 minutes while the reactor temperature was brought to 70 °C. Next, the initial monomer charge of 0.15 wt.% insoluble blue dye (per oleo phase) in 5 wt.% monomer mixture [0-20 wt.% POBM (per oleo phase) and 80-100 wt.% MMA or MA (per oleo phase)] was charged to the reactor. Emulsion was formed over 30 minutes at a stirring rate of 450 rpm. Polymerization was initiated upon the addition of 0.625 wt.% APS (per oleo phase) in 1.0 g of water. After 15 minutes, the remaining monomer mixture was added dropwise over 90 minutes using an addition funnel. Following the completion of the monomer feed, polymerization was continued for an additional 150 minutes at 70 °C.

Following polymerization, the reactor system was cooled to room temperature. The latex product was filtered through Whatman filter paper followed by a second filtration through a syringe equipped with a cotton ball lodged between the syringe tip and needle. The filtered latex was stored in a glass vial where it would not be disturbed for up to three weeks. Final conversion was determined by reprecipitation in methanol three times and drying at 110 °C until a constant final mass was achieved. Particle size distribution of the latex polymer particles was analyzed in the same manner as described above.

Table 5.2. Used recipes to investigate nucleation modes of POBM/comonomer semi-batch emulsion copolymerization

	Wt.%	Wt.% per oleo phase	Mass, g
Oleo phase	20		8
POBM, SBM or OVM		0-20	0-1.6
MMA or MA		80-100	6.4-8
Insoluble blue dye		0.15	0.012
Aqueous phase	80		33
Emulsifier, SDS		1.425	0.114
Buffer, NaAc*		0.022	0.0073
Initiator, APS		0.625	0.05
Total	100		41

* - % per aqueous phase

Ultraviolet absorbance (Cary 5000 UV-vis-NIR; Santa Clara, CA) was used to calculate the percentage of insoluble blue dye present in the latex polymer particles (P_{dye}). A solution of poly(methyl methacrylate) and blue dye in acetone exhibits a distinct peak at 670 nm. Without the blue dye present in the solution, no absorbance was detected at this wavelength. Therefore, the presence of latex in the sample does not alter the UV absorbance of the blue dye at 670 nm. Calibration curves for MMA and MA were constructed by dissolving 2 g of PMMA or PMA and a known quantity of blue dye in 20 mL of acetone. The extinction coefficients (mL g^{-1} cm^{-1}) were determined by the slope of the calibration straight line. Samples for UV absorbance were prepared by dissolving 0.5 mL of latex sample, pipetted from the middle portion of the emulsion, in 5 mL of acetone. Changes in peak absorbance values (and therefore P_{dye}) are known to become insensitive to sampling time. Thus, fresh samples were prepared every few days until no change in absorbance was detected, which typically occurred after 12-15 days.

5.4. Results and discussion

Motivated by previous findings and results (Chapter 3)[26], here we report on the kinetics and features for emulsion copolymerization of monomers from soybean (SBM) and olive (OVM) oils with commercially used methyl methacrylate (MMA), vinyl acetate (VA) and methyl acrylate (MA) monomers. SBM and OVM possess different compositions of fatty acids in the triglycerides of the plant oils, with OVM being significantly less unsaturated (**Table 5.3**). The amount of unsaturation in the triglycerides' fatty acids was utilized as a criterion in studying the effect of monomers' aqueous solubility on latex polymerization kinetics and latex polymer properties.

The practical importance of this study is in the fact that hydrophilicity of monomer counterpart molecules can have an impact on reaction kinetics and mechanism of emulsion

polymerization, as well as affect latex particle formation and, respectively, resulting particle morphology.

Table 5.3. The chemical structure of triglyceride and compositions of plant oils used in this study in percentages. R (x:y) is the structure of the fatty acids (x is the number of carbon atoms in the fatty acid chain and y is the number of double bonds in the fatty acid).

R (x:y)	16:0	18:0	18:1	18:2	18:3
Soybean oil	7–11	2–6	22-34	43–56	7-10
Olive oil	8–20	1–5	65-85	4–20	1–2

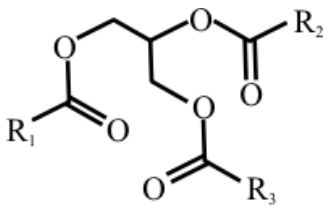

5.4.1. Study of latex particle nucleation in POBM emulsion copolymerization with monomers of various aqueous solubility

To determine the latex particle nucleation loci, and if their nucleation mechanism changes by changing aqueous solubility of counterpart monomer in POBM copolymerization, an experimental method based on water insoluble blue dye (Blue 70) was used in accordance with a procedure described by Chern[27-28]. Chern and Lin[28] illustrated a mixed mode of particle nucleation (micellar and homogeneous) for the emulsion homopolymerization of MMA at surfactant concentration higher than the CMC (8.2 mM for SDS). In their work, the portion of the latex particles formed *via* micellar nucleation was about 16% while no significant changes were observed with the varying emulsifier concentration. Our results (**Figure 5.1**) obtained for the emulsion homopolymerization of MMA at the [SDS] = 12 mM indicate that about 21% of latex particles are formed via micellar nucleation, which is in a good agreement with the Chern and Lin data.

Upon adding POBMs into the monomer mixture with MMA, the portion of the latex particles formed through micellar nucleation increases dramatically up to about 74% and 87% for 20 wt.% of added OVM and SBM, respectively **(Fig. 5.1**) The latter finding clearly indicates that

emulsion copolymerization loci change essentially when monomer feed hydrophobicity increases due to the POBM presence. As a result, significantly more latex polymer particles undergo micellar nucleation.

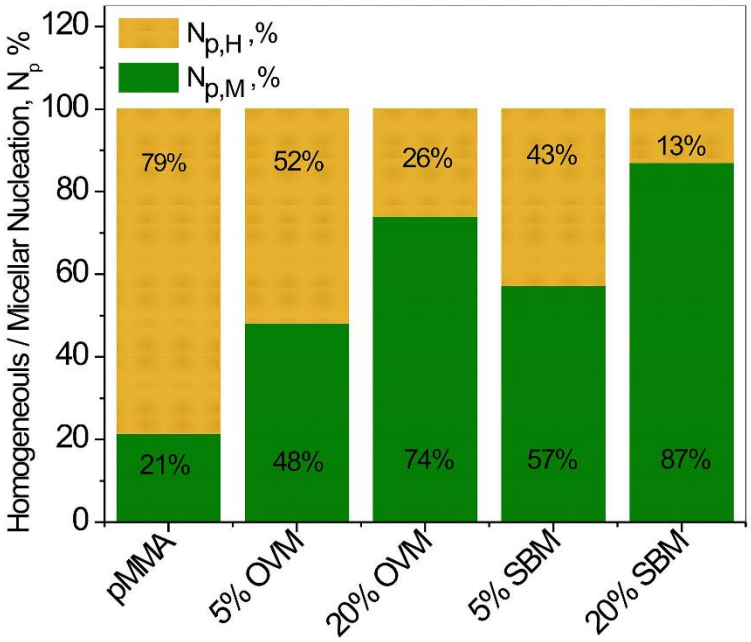

Figure 5.1. Dependence of latex polymer particles originated from micellar ($N_{p,M}$) and homogeneous ($N_{p,H}$) nucleation on the POBM nature and content in copolymerization with MMA

To determine if aqueous solubility of the comonomer also affects latex particle nucleation in reactions with POBM, methyl acrylate (~5% solubility in water, more than 3 times higher than MMA) was chosen for emulsion copolymerization with SBM and OVM. In the emulsion homopolymerization of MA, homogeneous nucleation is greatly enhanced in the continuous aqueous phase yielding over 90% of latex particles (**Fig. 5.2**) if compared to homopolymerization of MMA. It is evident that higher MA aqueous solubility leads to the more dominant homogeneous nucleation during emulsion homopolymerization. Similar to the experiments carried out with MMA, adding POBMs into the reaction mixture with MA enhances the portion of the latex particles formed through micellar nucleation, as it is seen in **Fig. 5.2**.

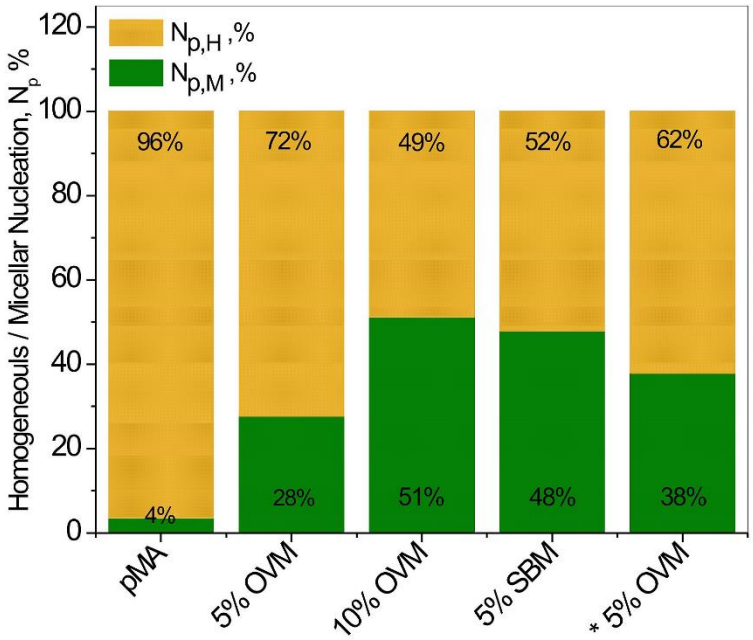

Figure 5.2. Dependence of latex polymer particles originated from micellar ($Np,_M$) and homogeneous ($Np,_H$) nucleation on the POBM nature and content, and [SDS] in copolymerization with MA (C_{SDS}= 1.4% per oleophase, *[SDS]= 4.2%)

It is noticeable that the increase in micellar nucleation with POBM introduction is much more pronounced for MA copolymerization, as compared with the reactions where MMA was used as a counterpart monomer. At 5 wt.% of OVM, the portion of the particles formed *via* micellar nucleation multiplies by 2.2 times for the emulsion copolymerization of MMA and by 7.7 times for MA, while the absolute value stays higher for more hydrophobic MMA (**Figs. 5.1** and **5.2**). A plausible explanation for that is the higher water solubility of MA compared to MMA. This occurs due to the fact that, upon the addition of POBM to MA system, there is a larger change in hydrophobicity compared to changes in hydrophobicity when POBMs are added to the originally more hydrophobic MMA.

The other noteworthy experimental observation here is the increase in the portion of particles formed through micellar nucleation in the case of copolymerization of SBM in comparison to OVM. As it was already mentioned above, during the emulsion polymerization of more hydrophilic monomers, like MMA or MA, a significant portion of latex particles can be

formed *via* homogeneous nucleation due to the growth in size of oligomeric radicals in the aqueous phase. The oligomeric radicals may at some critical chain length become water-insoluble (for MMA, n = 4-5)[29], coil up and form particle nuclei in the aqueous phase. Being adsorbed on the particulate surfaces, surfactant molecules stabilize these primary particles.

Taking into account the similarity between the POBM and SDS molecular composition (both molecules have a polar "head" and a long hydrophobic "tail") (**Fig. 5.3**), formation of mixed micelles from both SDS and POBM molecules was assumed and demonstrated in our previous work (Chapter 4)[30].

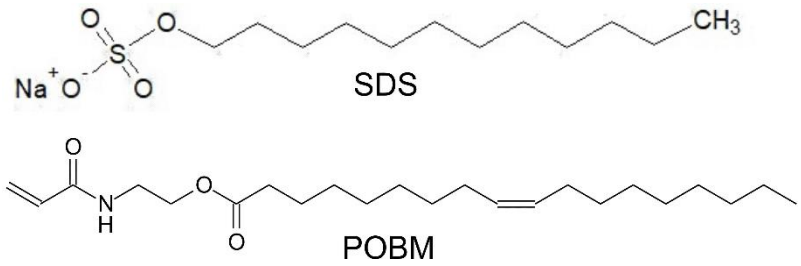

Figure 5.3. Chemical structure of surfactant (SDS) and plant oil-based monomer (POBM)

Due to the interactions between the molecules of POBM and SDS taking place, diffusion of POBM/SDS associates to the polymerization loci and their participation in the polymerization process in the continuous aqueous phase become more likely. SBM is more unsaturated by comparison with OVM, hence, chain-breaking transfer reactions are more common for the former, as it was demonstrated in our work previously[22]. For the emulsion copolymerization of MA and MMA with SBM, the growing oligomeric radicals terminate more frequently without reaching a critical length to become water-insoluble and form particle nuclei. The lifetime of such oligomeric chains in the aqueous phase and, therefore, the probability to enter the monomer-swollen micelles and then continue to propagate by reacting with the monomer molecules therein increase for SBM-based oligomeric radicals. It results in the lower portion of the particles formed through

homogeneous nucleation in emulsion copolymerization of SBM in comparison with OVM, as our results show.

In fact, interactions between SDS and POBM molecules can also explain an experimental fact that the portion of the latex particles formed through homogeneous nucleation is proportional to the concentration of both the emulsifier and POBM (**Figs. 5.1** and **5.2**). The latter indicates that the number of SDS/POBM mixed micelles evidently grows as the SDS and POBM concentrations increase. Solubilizing a water-soluble monomer (either MMA or MA), these mixed micelles become the loci of particle nucleation where the polymerization process occurs further.

Hence, these experimental findings indicate that the mode of latex particle nucleation depends to a great extent on the POBM content and nature along with the aqueous solubility of the acrylate comonomer (MMA and MA, in this study). We hypothesized that both factors might also impact copolymerization kinetics, as well as latex copolymer properties, in particular molecular weight and further determined kinetic features of POBM copolymerization with monomers of various aqueous solubility.

5.4.2. Study of POBM copolymerization kinetics with monomers of various aqueous solubility

For a better understanding of the effect of comonomer aqueous solubility on the nucleation mechanism in emulsion copolymerization with the highly hydrophobic POBMs (OVM and SBM), a method of kinetic study was used to determine the polymerization loci and a balance between latex particle homogeneous and heterogeneous (micellar) nucleation. To this end, orders of reaction with respect to the emulsifier and initiator were experimentally assessed. We hypothesized that in copolymerization of POBMs with MMA, VA and MA, orders of reaction with respect to the emulsifier and initiator might have distinct features because of differences in comonomer aqueous solubility, which need to be experimentally established.

Using the obtained kinetic data, the reaction orders with respect to the emulsifier and initiator were calculated for emulsion copolymerization of various concentrations of SBM/OVM with MMA, VA and MA and compared to the homopolymerization kinetics. For the emulsion homopolymerization of MMA, we determined the initiator and emulsifier reaction orders of 0.54 and 0.34 (**Fig. 5.4**), respectively, both implying expected deviations from the classic Smith-Ewart theory (predicting values of 0.4 and 0.6, respectively). These experimentally observed deviations for MMA homopolymerization are in good agreement with the literature data, where it was shown that the reaction order with respect to initiator increases and the emulsifier reaction order decreases when the aqueous solubility of monomers rises, indicating the increase of the fraction of the homogeneous nucleation mode[31-32].

Upon addition of highly hydrophobic SBM and OVM into the monomer mixture, the initiator reaction order increases with an increasing POBM content. This increase can be explained by the premature termination of the growing PMMA radicals by the transfer of the allylic hydrogen to them from the POBM molecules[33] (**Fig. 5.4 A**). The emulsifier reaction order increases considerably with the increasing POBM concentration and reaches 0.64 and 0.70 for monomer mixtures with 20 wt.% of OVM and SBM, respectively (**Fig. 5.4 B**). Thus, upon increasing the POBM content in the monomer feed, the kinetic parameters tend to approach the Smith-Ewart theory of the emulsion polymerization of hydrophobic monomers and more expressed micellar nucleation mechanism. The latter observation is consistent with the experimental data on the study of particle nucleation using the water insoluble blue dye (**Figs. 5.1** and **5.2**).

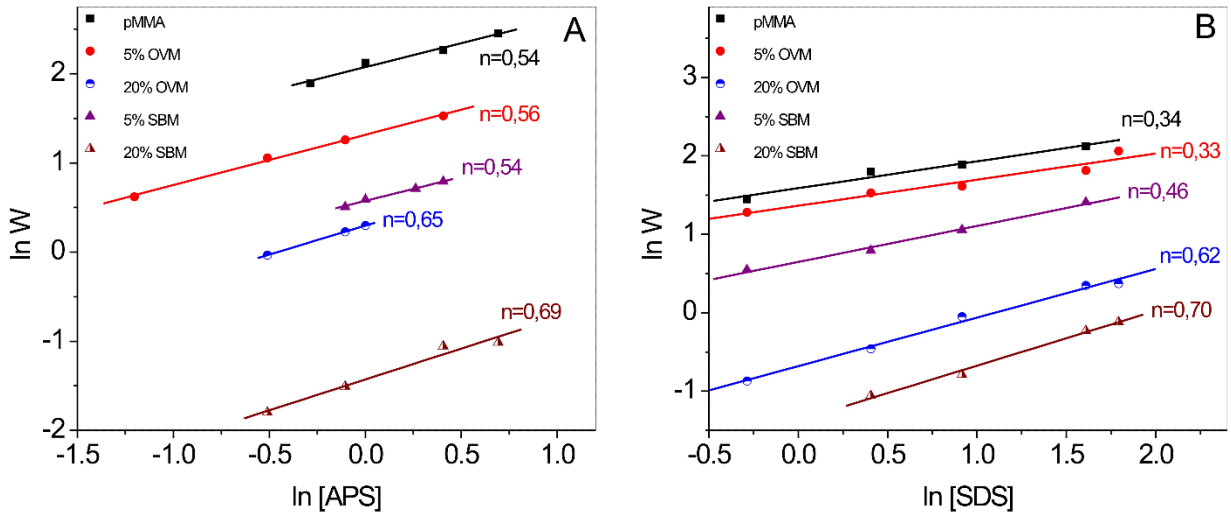

Figure 5.4. Log–log plots of the rate of emulsion (co)polymerization of MMA and POBMs vs. [APS] at 1.5% of SDS (**A**), and vs. [SDS] at 1.5% APS (**B**)

To further determine how the aqueous solubility of the comonomer contributes to kinetics of POBM copolymerization, we chose vinyl acetate possessing higher solubility in water (2.5 wt.%) in comparison with MMA, as a comonomer. For the emulsion homopolymerization of VA, the obtained value of initiator reaction order is higher (**Fig. 5.5 A**) and the order of reaction with respect to the emulsifier (**Fig. 5.5 B**) is lower (0.80 and 0.38, respectively) than those predicted by the Smith-Ewart theory and in agreement with literature data[34-36]. Nevertheless, no significant impact of POBM on the order of reaction with respect to both emulsifier and initiator was observed. Evidently, the reason for this is very high reactivity of radicals generated by VA in copolymerization reaction stages, and, particularly, their tendency to undergo chain transfer reactions[37-38]. As a result, multiple competing radical reactions can proceed in the monomer mixture at different stages of the polymerization (*i.e.*, initiation, propagation, and termination) that primarily determine reaction kinetics, while making POBM presence kinetically irrelevant.

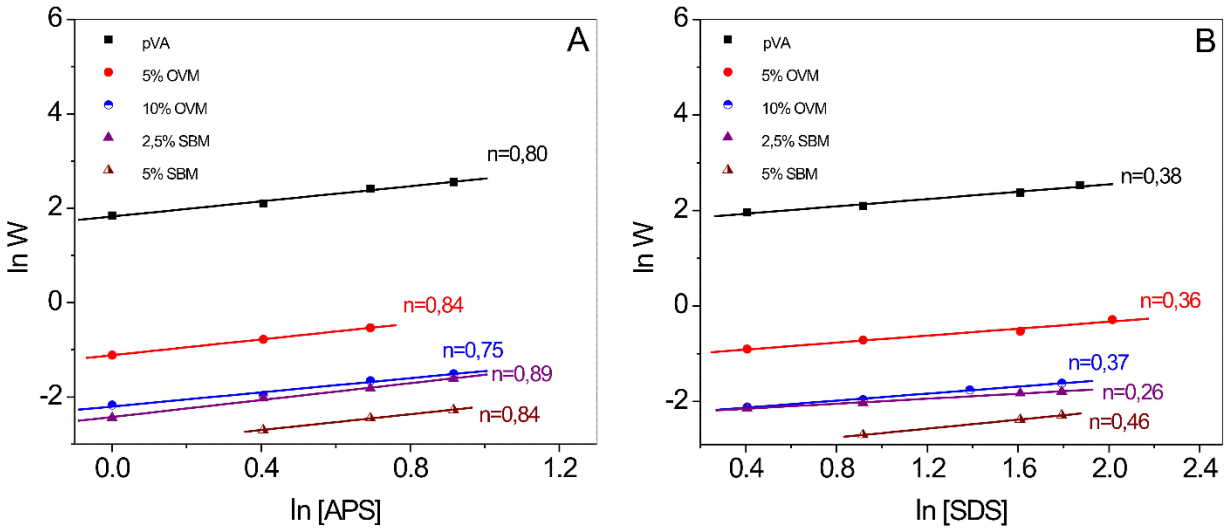

Figure 5.5. Log–log plots of the rate of emulsion (co)polymerization of VA and POBMs vs. [APS] at 2.5% of SDS (**A**) and vs. [SDS] at 1.5% APS (**B**)

In this study, methyl acrylate (MA) was the most hydrophilic comonomer (aqueous solubility of 4.9 wt.%) chosen for copolymerization with POBMs. The obtained results for the emulsion homopolymerization of PMA show that the orders of reaction with respect to the emulsifier and initiator (0.32 and 0.52, respectively) are close to those for PMMA, typical of monomers with relatively high aqueous solubility (**Fig. 5.6**). However, the effect of POBM content in the monomer feed on kinetics parameters is found to be much more pronounced for POBM reaction mixtures with MA, in comparison to MMA. For instance, while the initiator reaction order only slightly changes in MA copolymerization with OVM, it increases (from 0.52 to 0.86) for reaction with SBM at POBM concentration of 5 wt.% (**Fig. 5.6 A**). The latter could be explained by the higher amount of unsaturation for SBM and, thus, a greater contribution of the termination by chain transfer to monomer. The impact of the POBM content on the order of reaction with respect to the emulsifier is even more drastic (**Fig. 5.6 B**). In the presence of POBM in the monomer feed, polymerization rate decreases by the increasing emulsifier concentration that is reflected by a negative emulsifier reaction order.

In several works[39-42], adsorption layers on growing polymer-monomer particles were considered to act as "quasireactors" in which the polymerization process occurs. In addition, some anomalous variation of emulsion polymerization rate with surfactant concentration, particularly for surfactants possessing unsaturation (*e.g.*, certain fatty acid soaps) have been reported by Odian[33]. With this in mind, in our case, the reason for such an impact of the emulsifier concentration on the copolymerization behavior in MA/POBM mixtures can be the formation of mixed micelles from SDS and POBM (Chapter 4)[30]. When the SDS concentration rises, both the number of mixed micelles and the POBM concentration in the adsorbed layers (apparent polymerization loci) increase, thus triggering the experimentally observed retardation effect.

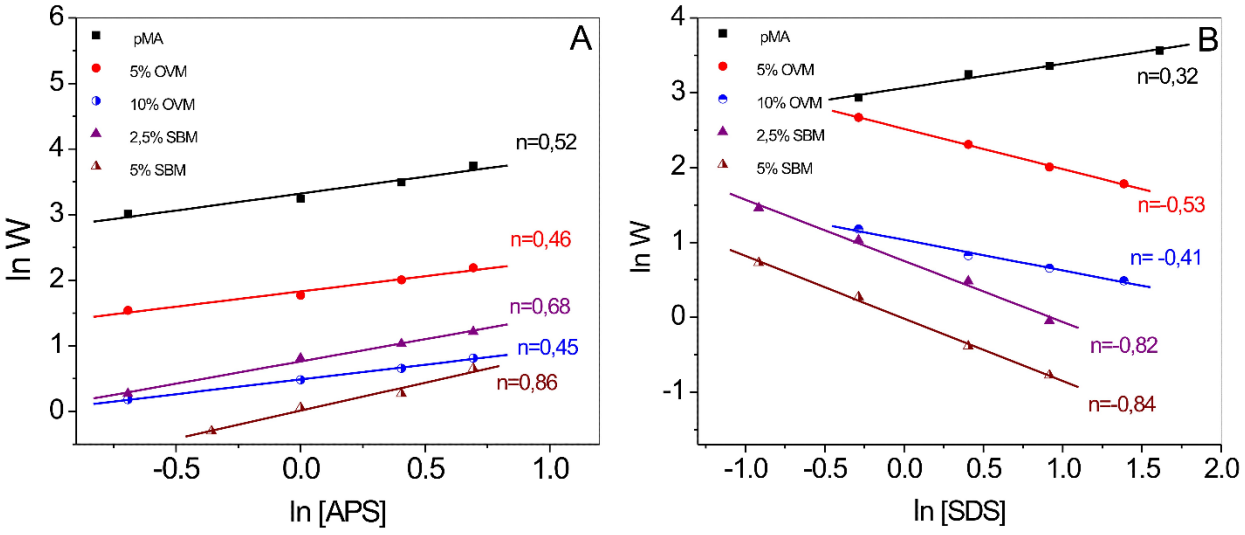

Figure 5.6. Log–log plots of the rate of emulsion (co)polymerization of MA and POBMs vs. [APS] ([SDS]=2.5% for MA homopolymerization and copolymerization with OVM and 0.75% for copolymerization with SBM (**A**) and vs. [SDS] ([APS]=1.5%) (**B**)

Actually, this assumption is evidenced in our study by the decrease in the molecular weights of the resulted copolymers with the rising concentration of emulsifier (**Fig. 5.7 A**). As it is seen, the molecular weight of the copolymers dropped, although it is generally recognized that in emulsion polymerization, molecular weight either increases with an increasing concentration of

a surfactant or does not depend on surfactant concentration according to the nature of both the monomer and surfactant[41].

Conversion – time plots recorded for emulsion copolymerization of POBM with MMA, VA and MA at different concentrations of SDS reveal that the increase of the POBM content in monomer feed results in decreasing polymerization rate for all chosen comonomers (**Figs. 5.4-5.6**). Similar retardation in the presence of POBMs was reported for their copolymerization with styrene in our recent work (Chapter 3)[26] and explained by the effect of the degradative chain transfer due to the presence of allylic protons in unsaturated acyl fragments of POBM[22-23]. Similar to the results in Chapter 3, the retardation of copolymerization with MMA, VA and MA is more pronounced for the more unsaturated SBM compared to OVM, due to the fact that SBM molecules undergo chain transfer reactions more readily (C_M (SBM) = 0.026, C_M (OVM) = 0.015)[22].

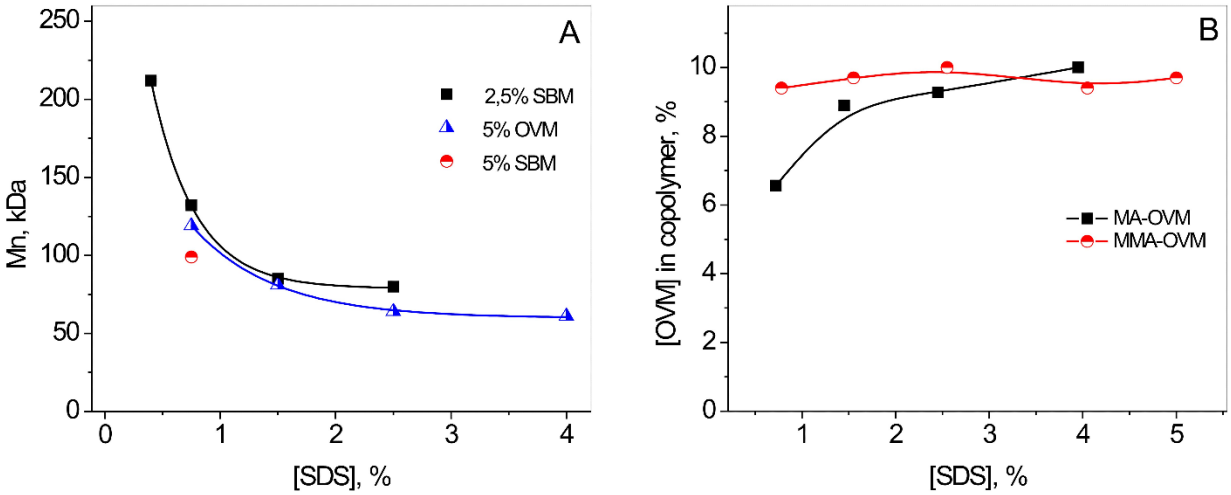

Figure 5.7. Dependence of MA/POBM copolymer molecular weight (**A**) and OVM content in resulted copolymers (**B**) on [SDS] for monomer feed ratio [MA/MMA]:[OVM]=90:10

Furthermore, analysis of the ^{1}H NMR spectra of the resulting copolymers shows that at the constant monomer ratio in the initial feed ([MA]:[OVM] = 90:10, wt.%), the OVM content in the copolymer increases from 6.5 to 10% when the SDS concentration increases (**Fig. 5.7 B**). At the same time, the copolymer composition is generally not affected by the emulsifier concentration in

the case of POBM copolymerization with MMA. Our explanation for this observation is the following; At lower concentrations of SDS, diffusion of the POBM molecules to the polymerization loci is hindered by the extremely low solubility of POBM in water. When the emulsifier concentration increases, the portion of the particles formed through micellar nucleation increases as well, accompanied by rising number of POBM molecules present in the mixed micelles. As a result, POBM molecules become more available for the polymerization process. In other words, the POBM concentration in the polymerization loci increases with the rising concentration of SDS, due to POBM/SDS interactions and resultant incorporation of POBM into the mixed micelles. The latter causes an increased impact from chain transfer, thus leading to the retardation of the polymerization and lower molecular weights of the resulting copolymers.

5.5. Conclusions

Highly hydrophobic vinyl monomers from plant oils [soybean (SBM) and olive (OVM)] that have different amounts of unsaturation were copolymerized in emulsion with comonomers having significantly higher water solubility, methyl methacrylate (MMA), vinyl acetate (VA), and methyl acrylate (MA). Our intention was to demonstrate that the higher aqueous solubility of the comonomer impacts the mechanism of emulsion process by balancing latex particle nucleation from homogeneous and heterogeneous (micellar) modes.

Using an experimental method based on water insoluble dye Blue 70, it is shown that particle nucleation indeed depends, to a great extent, on aqueous solubility of the comonomer along with the plant oil-based monomer content in the feed. Upon adding POBM into the monomer mixture with MMA (aqueous solubility 1.5 wt.%), the latex polymer particles originating from micellar nucleation essentially increases (up to 87% at 20 wt.% of POBM). In copolymerization of POBM with MA (aqueous solubility 4.9 wt.%), this effect is even more pronounced (threefold

increase for the same POBM content). Those findings clearly indicate that copolymerization loci change essentially when monomer feed hydrophobicity increases, as well as the magnitude of this effect being reliant on the comonomer aqueous solubility.

It was hypothesized that experimentally observed changes in nucleation loci for copolymerizations with POBM can also impact kinetics, particularly reaction orders with respect to emulsifier and initiator. Upon adding POBM into the reaction mixture with MMA, the emulsifier reaction order indeed increases considerably (up to 0.7 at 20 wt.% of POBM), thus indicating that latex particle formation occurs mainly through micellar nucleation. This impact on copolymerization of POBM with MA is even more pronounced.

The portion of latex particles originating through micellar nucleation is overall higher in the copolymerization of more unsaturated SBM (with both MMA and MA) in comparison to OVM. This can be explained by the more expressed chain transfer reactions in copolymerization of SBM, leading to the overall lower number of particles growing in the continuous aqueous phase.

No impact of POBM content on the reaction kinetics was observed in copolymerization with VA (aqueous solubility 2.5 wt.%). Unlike PMMA and PMA radicals, growing PVA radicals are highly reactive in chain transfer reactions. This has a substantial influence on polymerization kinetics, and apparently makes the presence of POBM in monomer feed kinetically irrelevant.

5.6. References

1. Chern, C., Emulsion polymerization mechanisms and kinetics. *Progress in polymer science* **2006,** *31* (5), 443-486.
2. Gilbert, R. G., *Emulsion polymerization: a mechanistic approach*. Academic Pr: 1995.
3. Thickett, S. C.; Gilbert, R. G., Emulsion polymerization: State of the art in kinetics and mechanisms. *Polymer* **2007,** *48* (24), 6965-6991.

4. van Herk, A. M., *Chemistry and technology of emulsion polymerisation*. John Wiley & Sons: 2013.

5. Harkins, W. D., A general theory of the reaction loci in emulsion polymerization. *The Journal of Chemical Physics* **1945,** *13* (9), 381-382.

6. Harkins, W. D., A general theory of the reaction loci in emulsion polymerization. II. *The Journal of Chemical Physics* **1946,** *14* (1), 47-48.

7. Harkins, W. D., A general theory of the mechanism of emulsion polymerization1. *Journal of the American Chemical Society* **1947,** *69* (6), 1428-1444.

8. Smith, W. V.; Ewart, R. H., Kinetics of emulsion polymerization. *The journal of chemical physics* **1948,** *16* (6), 592-599.

9. Smith, W. V., Chain initiation in styrene emulsion polymerization. *Journal of the American Chemical Society* **1949,** *71* (12), 4077-4082.

10. Gardon, J., Emulsion polymerization. II. Review of experimental data in the context of the revised Smith-Ewart theory. *Journal of Polymer Science Part A-1: Polymer Chemistry* **1968,** *6* (3), 643-664.

11. Gardon, J. L., Emulsion polymerization. I. Recalculation and extension of the Smith-Ewart theory. *Journal of Polymer Science Part A-1: Polymer Chemistry* **1968,** *6* (3), 623-641.

12. Maxwell, I. A.; Morrison, B. R.; Napper, D. H.; Gilbert, R. G., Entry of free radicals into latex particles in emulsion polymerization. *Macromolecules* **1991,** *24* (7), 1629-1640.

13. Priest, W., Partice growth in the aqueous polymerization of vinyl acetate. *The Journal of Physical Chemistry* **1952,** *56* (9), 1077-1082.

14. Joseph Schork, F.; Back, A., Inhibition effects in emulsion and miniemulsion polymerization of monomers with extremely low water solubility. *Journal of applied polymer science* **2004,** *94* (6), 2555-2557.

15. Schork, F. J.; Luo, Y.; Smulders, W.; Russum, J. P.; Butté, A.; Fontenot, K., Miniemulsion polymerization. In *Polymer Particles*, Springer: **2005,** 129-255.

16. Tauer, K.; Ali, A. I.; Yildiz, U.; Sedlak, M., On the role of hydrophilicity and hydrophobicity in aqueous heterophase polymerization. *Polymer* **2005,** *46* (4), 1003-1015.

17. Asua, J., Prog Polym Sci 27: 1283. doi: 10.1016. *S0079-6700 (02)* **2002**, 00010-2.

18. Saygı-Arslan, Ö.; Sudol, E. D.; Daniels, E. S.; El-Aasser, M. S.; Klein, A., In situ surfactant generation as a means of miniemulsification? *Journal of applied polymer science* **2009,** *111* (2), 735-745.

19. Leyrer, R. J.; Mächtle, W., Emulsion polymerization of hydrophobic monomers like stearyl acrylate with cyclodextrin as a phase transfer agent. *Macromolecular Chemistry and Physics* **2000,** *201* (12), 1235-1243.

20. You, X.; Dimonie, V. L.; Klein, A., Kinetic study of emulsion copolymerization of ethyl methacrylate/lauryl methacrylate in propylene glycol, stabilized with poly (ethylene oxide)–block–polystyrene–block–poly (ethylene oxide) triblock copolymer. *Journal of applied polymer science* **2001,** *82* (7), 1691-1704.

21. Tarnavchyk, I.; Popadyuk, A.; Popadyuk, N.; Voronov, A., Synthesis and free radical copolymerization of a vinyl monomer from soybean oil. *ACS Sustainable Chemistry & Engineering* **2015,** *3* (7), 1618-1622.

22. Demchuk, Z.; Shevchuk, O.; Tarnavchyk, I.; Kirianchuk, V.; Kohut, A.; Voronov, S.; Voronov, A., Free Radical Polymerization Behavior of the Vinyl Monomers from Plant Oil Triglycerides. *ACS Sustainable Chemistry & Engineering* **2016**.

23. Demchuk, Z.; Shevchuk, O.; Tarnavchyk, I.; Kirianchuk, V.; Lorenson, M.; Kohut, A.; Voronov, S.; Voronov, A., Free-Radical Copolymerization Behavior of Plant-Oil-Based Vinyl Monomers and Their Feasibility in Latex Synthesis. *ACS Omega* **2016,** *1* (6), 1374-1382.

24. Quintero, C.; Delatte, D.; Diamond, K.; Mendon, S.; Rawlins, J.; Thames, S., Reaction calorimetry as a tool to determine diffusion of vegetable oil macromonomers in emulsion polymerization. *Progress in organic coatings* **2006,** *57* (3), 202-209.

25. Booth, G.; Delatte, D. E.; Thames, S. F., Incorporation of drying oils into emulsion polymers for use in low-VOC architectural coatings. *Industrial Crops and Products* **2007,** *25* (3), 257-265.

26. Kingsley, K.; Shevchuk, O.; Demchuk, Z.; Voronov, S.; Voronov, A., The features of emulsion copolymerization for plant oil-based vinyl monomers and styrene. *Industrial Crops and Products* **2017,** *109* (Supplement C), 274-280.

27. Chern, C.-S.; Lin, C.-H., Particle nucleation loci in emulsion polymerization of methyl methacrylate. *Polymer* **2000,** *41* (12), 4473-4481.

28. Chern, C.-S.; Lin, C.-H., Using a water-insoluble dye to probe the particle nucleation loci in styrene emulsion polymerization. *Polymer* **1999,** *40* (1), 139-147.

29. de Bruyn, H. The Emulsion Polymerization of Vinyl Acetate. 1999.

30. Kingsley, K.; Shevchuk, O.; Voronov, S.; Voronov, A., Effect of highly hydrophobic plant oil-based monomers on micellization of sodium dodecyl sulfate. *Colloids and Surfaces A: Physicochemical and Engineering Aspects* **2019,** *568*, 157-163.

31. Lee, P.; Longbottom, H., The dependence of the rate of emulsion polymerization of methyl methacrylate on the soap concentration. *Journal of Applied Polymer Science* **1970,** *14* (5), 1377-1379.

32. Dunn, A. S., Absorption of Emulsifiers and Its Effects on Kinetics of Polymerization. In *Science and Technology of Polymer Colloids*, Springer: 1983; pp 314-334.

33. Odian, G., *Principles of polymerization*. **2004,** 198-349.

34. Dunn, A.; Taylor, P., The polymerization of vinyl acetate in aqueous solution initiated by potassium persulphate at 60° C. *Die Makromolekulare Chemie: Macromolecular Chemistry and Physics* **1965,** *83* (1), 207-219.

35. Dunn, A.; Chong, L. H., Application of the theory of colloid stability to the problem of particle formation in aqueous solutions of vinyl acetate. *British Polymer Journal* **1970,** *2* (1), 49-59.

36. Nomura, M.; Harada, M.; Nakagawara, K.; Eguchi, W.; Nagata, S., The role of polymer particles in the emulsion polymerization of vinyl acetate. *Journal of Chemical Engineering of Japan* **1971,** *4* (2), 160-166.

37. Okamura, S.; Motoyama, T., Emulsion polymerization of vinyl acetate. *Journal of Polymer Science* **1962,** *58* (166), 221-228.

38. Yamak, H. B., Emulsion polymerization: effects of polymerization variables on the properties of vinyl acetate based emulsion polymers. In *Polymer Science*, InTech: 2013.

39. Brodnyan, J. G.; Cala, J. A.; Konen, T.; Kelley, E. L., The mechanism of emulsion polymerization. I. Studies of the polymerization of methyl methacrylate and n-butyl methacrylate. *Journal of Colloid Science* **1963,** *18* (1), 73-90.

40. Volkov, V. P.; Roginskaya, G.; Chalykh, A. E.; Rozenberg, B. A., Phase Structure of Epoxide–Rubber Systems. *Russian Chemical Reviews* **1982,** *51* (10), 994.

41. Eliseeva, V. I.; Ivanchev, S.; Kuchanov, S.; Lebedev, A., *Emulsion polymerization and its applications in industry*. Springer Science & Business Media: 2012.

42. Khaddazh, M.; Gritskova, I.; Litvinenko, G., An Advanced Approach on the Study of Emulsion Polymerization: Effect of the Initial Dispersion State of the System on the Reaction Mechanism, Polymerization Rate, and Size Distribution of Polymer-Monomer Particles. In *Polymerization*, IntechOpen: 2012.

CHAPTER 6. DUAL ROLE OF METHYL-β-CYCLODEXTRIN IN THE EMULSION POLYMERIZATION OF HIGHLY HYDROPHOBIC PLANT OIL-BASED MONOMERS WITH VARIOUS UNSATURATIONS[1]

6.1. Abstract

Although a series of latexes from plant oil-based acrylic monomers (POBMs) were recently synthesized in emulsion, two factors—allylic termination (the chain transfer reaction to the fatty acid double bonds) and the poor aqueous solubility of POBMs—lead to lower total monomer conversion and molecular weight of the resulting latex polymers.

In this study, an amphiphilic oligosaccharide, methyl-β-cyclodextrin (M-β-CD), was used to improve the polymerizability of monomers from high oleic soybean (HO-SBM) and linseed (LSM) oil in copolymerization with styrene. Using X-ray diffractometry and differential scanning calorimetry, interactions between the monomers and M-β-CD were confirmed, while the formation of 1:1 complex from oligosaccharide and each monomer molecules was demonstrated by mass spectrometry.

In the presence of "host-guest" complexes, polymer yield increases as the coagulum amount drops during the emulsion polymerization of both plant oil-based monomers with styrene indicating their enhanced aqueous solubility. Remarkably, latex polymers with a consistently higher molecular weight were obtained in the presence of M-β-CD. The complex formation and

[1] The material in this chapter was co-authored by Kyle Kingsley, Ananiy Kohut, Zoriana Demchuk, Stanislav Voronov, and Andriy Voronov. Kyle Kingsley had the primary responsibilities of analyzing the results from ESI-MS. Kyle Kingsley also synthesized and characterized polymer latexes. Kyle Kingsley was involved in drafting and revising all versions of this chapter. Ananiy Kohut helped Kyle Kingsley perform and analyze results of PXRD and DSC experiments. Oleh Shevchuk and Andriy Voronov helped describe the role of inclusion complexes in the emulsion process and checked calculations performed by Kyle Kingsley. Published article can be found at https://doi.org/10.1016/j.eurpolymj.2018.09.010.

incorporation of monomer molecules into the oligosaccharide cavities protect the fatty acid moieties and diminish chain transfer. The latter assumption was quantitatively confirmed in ^{1}H NMR spectroscopy by determining the number of protons of the alkyl carbon−carbon double bonds (–C**H**=C**H**–) and the bisallylic hydrogen atoms (–CH=CH–C**H**$_2$–CH=CH–) in the unsaturated fatty acid moieties of the latex copolymers. The observed effect is more pronounced for the more unsaturated monomer from linseed oil. Based on the obtained results, M-β-CD plays a dual role in both enhancing POBM polymerizability as well as protecting against allylic termination chain transfer.

6.2. Introduction

Industrially viable materials with a positive environmental impact can be provided by designing new polymers from renewable resources (bio-based polymers)[1-5]. Being relatively inexpensive and abundant, vegetable oils are currently considered the most important sustainable feedstock in the production of bio-based polymers[6-10].

In the manufacturing of industrial waterborne polymeric materials (in particular, latexes), the emulsion polymerization process has been conventionally employed to synthesize commercial polymers by a free radical polymerization mechanism. However, in the plant oil-based polymer synthesis for making industrial coatings, the emulsion process is not currently employed due to challenges related to the highly hydrophobic nature of plant oils, as well as the absence of monomers with proper functionality[11-16]. Only very recently has converting triglyceride oils into vinyl monomers for synthesizing waterborne polymeric materials (coatings, paints, binders, adhesives, etc.) *via* classic chain radical copolymerization been described in the literature.

Tang et al. synthesized fatty monomers from high oleic soybean oil (HO-SBM) and demonstrated their ability to yield thermoplastic polymers in free radical polymerization[17].

Macromolecules with a broad range of glass transition temperatures were synthesized from a library of HO-SBM-based (meth)acrylate monomers[18]. The resulting bio-based polymers show the physical properties of materials with viscoelastic and thermoplastics behavior were obtained. Maiti et al. converted oleic acid into methacrylate derivatives which were polymerized via RAFT mechanism with a feasibility for post-polymerization modifications[19-20]. Recently, Lomege et al. reported on the synthesis of various fatty acid-based methacrylates and their further polymerization for application as mineral oil viscosity modifiers[21].

We have developed a one-step method to synthesize vinyl monomers from plant oils (exemplified by sunflower, linseed, soybean, hydrogenated soybean and olive oil), and employed new plant oil-based monomers (POBMs) in free radical (co)polymerization[22-24]. The POBMs' rate of polymerization depends noticeably on the unsaturation of triglycerides' fatty acids in the molecules of monomer. During polymerization, chain propagation co-exists with effective chain transfer. Due to the allylic termination, the molecular weight of the resulting polymers decreases with increasing the unsaturation amount in monomers and the POBM content in the reaction feed[22-25]. The synthesis of latexes with a high bio-based content was attempted in our group using emulsion and miniemulsion copolymerization of POBMs with conventional vinyl monomers[24-25]. The miniemulsion polymerization process was also reported by Moreno et al. as a feasible method to synthesize eco-paints from bio-based fatty acid derivative latexes[26]. Although a series of latexes with up to 70 wt.% of plant oil-based content was successfully developed using the miniemulsion process, the synthesis of POBM-containing latexes in emulsion still remains challenging. The copolymerization of styrene with up to 20 wt.% of each soybean oil- and olive oil-based monomers follows a typical phenomenology for the emulsion process for hydrophobic monomers. However, experimental proof of mixed modes of nucleation (micellar and homogeneous) were observed by

determining latex particle size and number (Chapter 3)[25]. Both the hydrophobicity of plant oil-derived monomers and taking part in the chain transfer of allylic protons influence the overall polymerization kinetics and latex particle formation in emulsion.

Several authors have found that the aqueous solubility and, thus, polymerizability of highly hydrophobic monomers in emulsion can be enhanced through monomer complexes with cyclodextrin, a cyclic oligosaccharide, resembling a truncated cone geometry of molecules with a hydrophobic cavity and hydrophilic exterior[27-30]. Hydrophobic monomers, lauryl methacrylate, stearyl methacrylate, stearyl acrylate, etc. have been (co)polymerized in conventional emulsion polymerization conditions using a relatively small amount of cyclodextrin (less than 2 wt.%)[31-35]. Due to the hydrophobic cavity of cyclodextrin, host-guest complexes with monomers are formed that enhance monomers' aqueous solubility and availability in the emulsion polymerization process. Researchers have shown that both hydrophobic interaction and hydrogen bonds are responsible for "host-guest" complex formation[36].

Motivated by previous findings and results, here we report on the emulsion polymerization of POBMs from high oleic soybean (HO-SBM) and linseed (LSM) oils widely used in plastics and rubber industry styrene (St) in the presence of methyl-β-cyclodextrin (M-β-CD). HO-SBM and LSM possess different compositions of fatty acids in the triglycerides of the plant oils with HO-SBM being significantly less unsaturated (**Table 6.1**). Both HO-SBM and LSM form complexes with methyl-β-cyclodextrin. The degree of unsaturation in the triglycerides' fatty acids was utilized as a criterion in studying the effect of host-guest interactions on latex polymer preparation (total monomer conversion) and properties (molecular weight).

Table 6.1. The chemical structure of triglyceride and compositions of plant oils used in this study in percentages. R (x:y) is the structure of the fatty acids (x is the number of carbon atoms in the fatty acid chain and y is the number of double bonds in the fatty acid).

R (x:y)	16:0	18:0	18:1	18:2	18:3
High oleic soybean oil	4–5	3–4	74-76	12–14	3-5
Linseed oil	4–7	2–5	12–34	17–24	35–60

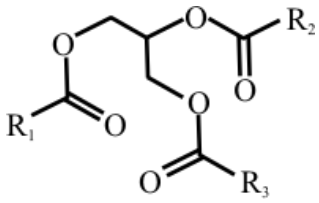

In the presence of M-β-CD, latex polymers with a consistently higher molecular weight were obtained from both HO-SBM and LSM (the observed effect is more pronounced for more unsaturated LSM). We hypothesized that the incorporation of POBM molecules into the methyl-β-cyclodextrin cavity diminishes chain transfer contribution by protecting the allylic moiety of the POBM fatty acid fragments and simultaneously enhances aqueous solubility and availability of POBMs in emulsion polymerization process. Consequently, higher molecular weight of latex polymers from highly hydrophobic plant oil-based monomers can be obtained with higher monomer conversion and lower coagulum formation.

6.3. Materials and methods

6.3.1. Materials

High oleic soybean oil (Perdue AgriBusiness LLC, Salisbury, MD), N-(hydroxyethyl)acrylamide (TCI America, Portland, OR), methyl-β-cyclodextrin (mixture of several methylated; M-β-CD; TCI America, Portland, OR), ammonium persulfate (APS, VWR; Solon, OH), and sodium dodecyl sulfate (SDS, VWR; Solon, OH) were used as received. Styrene (Sigma-Aldrich, St. Louis, MO) was distilled under a vacuum to remove the inhibitor and stored in a refrigerator. Hydrogenated soybean oil-based monomer (H-SBM) and linseed monomer were synthesized from N-(hydroxyethyl)acrylamide and, respectively, hydrogenated soybean oil or linseed oil using previously reported methods[22, 37]. All solvents used were reagent grade or better

and were used as received. Deionized water was used for all reactions and swelling measurements (Milli-Q, 18 MΩ).

6.3.2. Syntheses

6.3.2.1. Synthesis of high oleic soybean oil-based monomer

High oleic soybean oil-based monomer (HO-SBM) was prepared in our laboratory using a reaction pathway previously reported by the current research group for other POBMs[22]. In brief, about 115 g of N-(hydroxyethyl) acrylamide was added to 150 g of high oleic soybean oil (with an acrylamide alcohol to triglyceride molar ratio of 5.9 to 1), 150 mL of tetrahydrofuran, and 0.1 g of 2,6-di-*tert*-butyl-p-cresol in a 500 mL, two-necked round-bottomed flask equipped with a mechanical stirrer. The reaction mixture was heated to 40 °C in the presence of a catalytic amount of ground sodium hydroxide (1.5 g), which was slowly added to the reaction mixture with continuous stirring. The reaction mixture was stirred at 40 °C until complete homogenization (approximately 3 h) and was allowed to remain overnight at room temperature. The reaction mixture was diluted with CH_2Cl_2, purified by washing with brine, treated with magnesium sulfate, and dried under a vacuum, yielding about 170 g of acrylic monomer (94−96% of the theoretical yield). The resulting monomer contains one acrylic double bond linked to one fatty chain, which is mainly mono-unsaturated oleate (**Figure 6.1**).

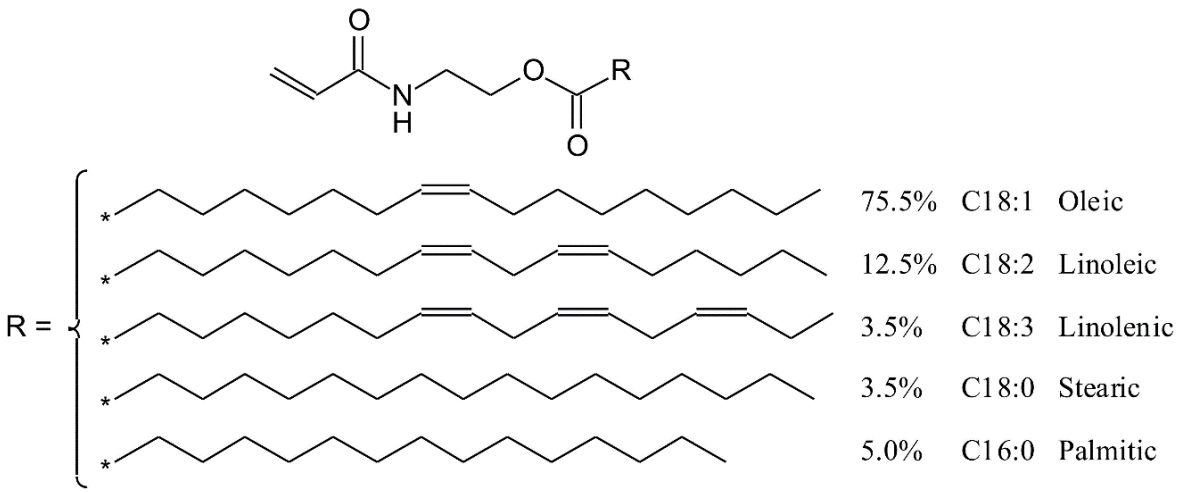

Figure 6.1. Chemical structure of HO-SBM and its typical fatty acid composition

6.3.2.2. Synthesis of the inclusion complexes and preparation of the physical mixtures

The inclusion complex of HO-SBM with m-β-CD was prepared by freeze-drying method using an equimolar ratio of the components. HO-SBM (0.113 g, 0.3 mmol) was dissolved in absolute methanol (10 mL) and added drop-wise to a solution of M-β-CD (0.399 g, 0.3 mmol) in water (10 mL) at 38 °C over 15 min. The resulting mixture was stirred at 38 °C during 4 h. Thereafter, methanol was removed under a vacuum in a rotary evaporator maintaining a bath temperature at 40 °C. Once the methanol was completely removed, the solution was cooled at room temperature, centrifuged at 1000 rpm for 5 min, and a supernatant was recovered by freeze drying to obtain a white powder.

The inclusion complex of H-SBM with M-β-CD was prepared using the same technique except that isopropyl alcohol was used instead of methanol since H-SBM is not soluble in methanol. The physical mixture of HO-SBM (or H-SBM) with M-β-CD was performed by mixing the components in a 1:1 molar ratio in a glass mortar for 15 min.

6.3.2.3. Synthesis of latex from POBMs and styrene

The series of latexes from high oleic soybean oil- and linseed oil-based monomers were formed using emulsion polymerization with styrene (St). The oil phase was prepared by mixing POBMs with styrene at various ratios. The aqueous phase was formed by dissolving sodium dodecyl sulfate (4 wt.%) in deionized water. The oil phase was added dropwise to the aqueous phase and mixed for 40 min. The formed pre-emulsion was purged with argon gas for 10 min and polymerized at 60 °C for 4 h. The aqueous solution of ammonium persulfate (1.5 wt.%) was added to the preheated emulsion at the start of polymerization. The latex solid content was kept at 30 wt.%. To investigate the effect of methyl-β-cyclodextrin on the polymerization of POBMs in emulsion, the certain amount of methyl-β-cyclodextrin was added to the aqueous phase (POBM:M-β-CD = 1:1 w/w).

6.3.3. Characterization

6.3.3.1. ^{1}H NMR spectroscopy

^{1}H NMR spectra of HO-SBM and latex copolymers were recorded on an AVANCE III HDTM 400 high-performance digital NMR spectrometer (Bruker, Billerica, MA) using $CDCl_3$ as a solvent.

6.3.3.2. Powder X-ray diffractometry (PXRD)

The X-ray powder diffraction patterns of HO-SBM, H-SBM, M-β-CD, physical mixtures of each monomer with M-β-CD (molar ratio 1:1) as well as HO-SBM/M-β-CD and H-SBM/M-β-CD inclusion complexes were measured for comparative purposes. PXRD patterns were collected using a Rigaku Ultima IV Powder X-ray Diffractometer with Ni-filtered Cu-Kα radiation powered at 40 kV and 44 mA. The samples were packed into a 25 × 25 × 2.5 mm^3 channel in a glass slide

and analyzed over an angular range from 2° to 40° in continuous scan mode using a step size of 0.02° and a scan rate of 1 °/min.

6.3.3.3. Differential scanning calorimetry (DSC)

The DSC thermograms of HO-SBM, H-SBM, M-β-CD, physical mixtures of each monomer with M-β-CD (molar ratio 1:1) as well as HO-SBM/M-β-CD and H-SBM/M-β-CD inclusion complexes were measured with a TA Instruments Q1000 calorimeter. Dry nitrogen with a flow rate of 50 mL/min was purged through the sample. The samples in a hermetic aluminum pan were subjected to a heating rate of 10 °C/min. An empty hermetic pan was used as the reference.

6.3.3.4. Electrospray ionization mass spectrometry (ESI-MS)

The electrospray ionization high-resolution mass spectra of HO-SBM, H-SBM, M-β-CD, HO-SBM/M-β-CD, and H-SBM/M-β-CD inclusion complexes were obtained using a Waters Synapt G2-Si high resolution Mass Spectrometer. The methanol solutions were introduced into the electrospray ion source (ESI) *via* a syringe pump at a flow rate of 10 µL/min. After the optimization of the Q/TOF MS parameters, they were set as follows: electrospray ionization (positive ion mode), capillary voltage 2.9 kV, cone voltage 35.0 V, cone gas flow 6.0 L/h, desolvation temperature 100 °C, desolvation gas flow 198 L/h, nebulizer pressure 6.5 Bar. The full-scan mass spectra of the investigated compounds were acquired in the range *m/z* 100–3000. The mass scale was calibrated using the standard calibration procedure and compounds provided by the manufacturer.

6.4. Results and discussion

The primary focus of the present study was to investigate if the presence of methyl-β-cyclodextrin enhances the efficacy of using the POBMs in emulsion polymerization, particularly,

increase the polymer yield and molecular weight as well as make the process more feasible (including reducing the amount of coagulum).

For this purpose, interactions between POBMs and methyl-β-cyclodextrin were investigated first. For the experiments, HO-SBM and fully saturated monomer from hydrogenated soybean oil (H-SBM) were chosen. To generate the inclusion complex, samples from POBMs and M-β-CD were prepared through a freeze-drying method at the mole ratio of reactants as 1:1 (monomer:M-β-CD). Powder X-ray diffractometry (PXRD) is a powerful technique to detect the cyclodextrin complexation of small molecules in a powder or crystalline state[38]. PXRD differentiates the formation of complexes due to clear alterations between the diffraction pattern superposition of the components and the diffraction pattern of the inclusion complex. The PXRD spectra of H-SBM, M-β-CD, H-SBM/M-β-CD inclusion complex, and the physical mixture are shown in **Fig. 6.2 A**. The diffractogram of H-SBM displays numerous characteristic peaks due to its self-lattice arrangement, which indicates the crystallinity of the monomer. In contrast, M-β-CD is an amorphous substance, thus its diffractogram shows two wide peaks related to the non-crystalline form. The diffraction pattern of the physical mixture of H-SBM and M-β-CD was just the superposition of the monomer and M-β-CD. This may indicate that there is no interaction between H-SBM and M-β-CD in the simple physical mixture[39]. Compared with the diffractogram of pure H-SBM and M-β-CD, the diffraction pattern of the inclusion complex is similar to that of the M-β-CD with increased intensity of the peak at 17.9° at 2θ scale and showed no characteristic peaks that pure HS-BM had. These results indicate that the self-lattice arrangement of H-SBM was changed from a crystalline to amorphous state, which can be attributed to the H-SBM inclusion into the M-β-CD cavity.

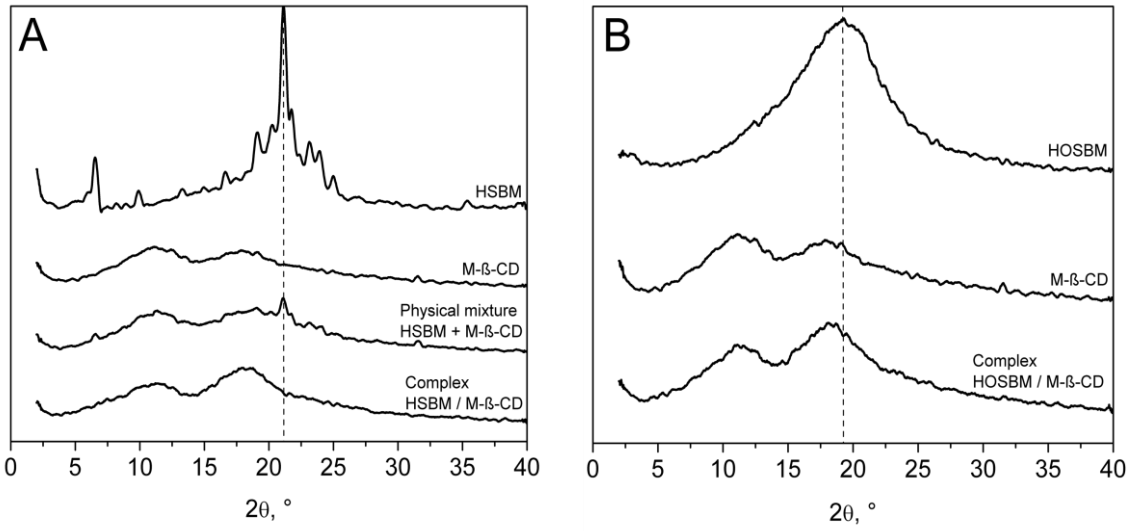

Figure 6.2. PXRD spectra of POBMs, methyl-β-cyclodextrin, their physical mixture and inclusion complexes (**A** – H-SBM, **B** – HO-SBM)

The PXRD pattern of HO-SBM, M-β-CD, and HO-SBM/M-β-CD inclusion complex are presented in **Fig. 6.2 B**. HO-SBM is an oily viscous substance, and its diffractogram displays two wide peaks attributed to the non-crystalline form. Since both M-β-CD and HO-SBM are non-crystalline substances, the formation of HO-SBM/M-β-CD inclusion complex cannot be confirmed unambiguously by PXRD.

The inclusion of a guest molecule into cyclodextrin can also be studied using differential scanning calorimetry, as the cavity alters the boiling and melting points of the initial substances by shifting or suppressing them[40]. The DSC thermograms of H-SBM, M-β-CD, H-SBM/M-β-CD inclusion complex, and the physical mixture are shown in **Fig. 6.3**. The DSC curve of H-SBM shows two sharp endothermic peaks corresponding to the melting of the monomer. The DSC thermogram of M-β-CD shows a broad endothermic band at 110 °C due to the dehydration process. The endothermic peaks of H-SBM were observed in the thermogram of the physical mixture of H-SBM and M-β-CD. These results indicate that the complexation has not occurred, and the initial substances are simply mixed together. However, no peak in the melting range of H-SBM was

detected in the DSC curve of H-SBM/M-β-CD samples prepared using the thin films method. This indicates that that the monomer molecules are completely included into the M-β-CD cavities, monomer appears in an amorphous state, and H-SBM/M-β-CD inclusion complex forms.

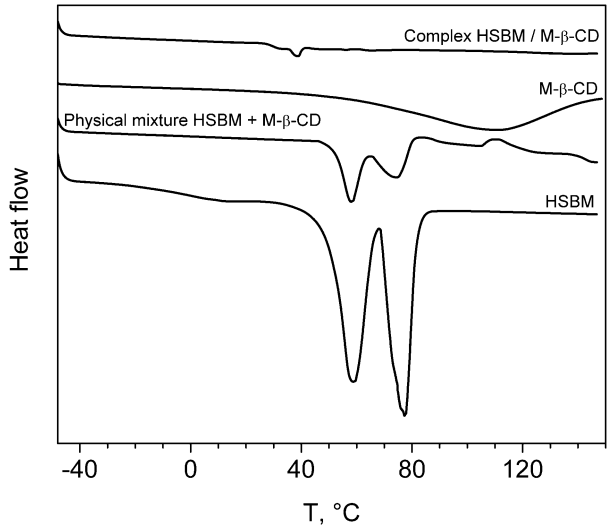

Figure 6.3. DSC thermograms of hydrogenated soybean (H-SBM) monomer, methyl-β-cyclodextrin, their physical mixture and inclusion complex

The DSC thermogram of HO-SBM exhibited an endothermic peak at around 17 °C corresponding to the melting point of the monomer. However, no peak in the melting range of HO-SBM was detected in the DSC curves of HO-SBM/M-β-CD inclusion complex and their physical mixture. This may imply that there was some interaction between the pure components. A plausible explanation is that unlike H-SBM, HO-SBM is an oily liquid and, thus, monomer molecules might be able to penetrate into the M-β-CD cavities when the two substances are mixed together. In principle, this procedure is similar to the kneading method, which is used for the synthesis of cyclodextrin-guest complexes when a liquid guest component is added to a slurry of cyclodextrin and kneaded thoroughly in a mortar[41-43].

Although PXRD and DSC analyses indicate changes from a crystalline to amorphous state of H-SBM upon its interaction with M-β-CD, these techniques can neither unambiguously confirm

whether inclusion complexation (especially for HO-SBM) occurs, nor determine the complex stoichiometry. To this end, electrospray ionization–mass spectrometry (ESI–MS), which is an extremely sensitive and specific analytical technique, capable of providing the molecular masses within a sample and determination of molecular association of non-covalent bonding[42], was used in this work to monitor the formation of POBM/M-β-CD inclusion complexes. The feasibility of ESI to maintain the non-covalent structure upon the transition of inclusion complexes from the liquid to gas phase has been widely applied to investigate the complexation of cyclodextrins with various organic substances[44-45].

Before the POBM/M-β-CD inclusion complexes were studied by ESI–MS, the initial substances—methyl-β-cyclodextrin, H-SBM, and HO-SBM—were analyzed individually to determine their composition to distinguish between initial M-β-CD and its inclusion complexes. Methyl-β-cyclodextrin used in this study is not an individual compound but consists of a mixture of several methylated β-cyclodextrins, as indicated by the manufacturer; however, neither the methylation degree of the β-cyclodextrin nor the average molecular weight is available. The ESI mass spectrum for the M-β-CD in methanol is shown in **Fig. B1** (in **Appendix B**), where the most abundant peaks at *m/z* 1312 and 1326 correspond to sodium adducts of M-β-CD having 11 and 12 methyl groups, respectively (M_{11}-β-CD and M_{12}-β-CD). It should be noted that a β-cyclodextrin molecule is composed of seven α-D-glucopyranoside units and contains 21 hydroxyl groups. So, the methylation degree of the studied M-β-CD is about 55%.

H-SBM and HO-SBM are synthesized from hydrogenated and high oleic soybean oils, respectively, and neither is an individual chemical substance. **Fig. B2** (in **Appendix B**) depicts the ESI mass spectra of the POBMs. In the ESI mass spectrum of H-SBM (**Fig. B2 A**), the most abundant peaks observed at *m/z* 404.3 and 376.3 correspond to sodium adducts of [stearate-H-

SBM + Na]$^+$ and [palmitate-H-SBM + Na]$^+$, respectively. This indicates that fatty acid chains incorporated in the H-SBM molecules are mainly saturated ones. Although a small amount of monounsaturated oleate is also present in H-SBM, as evidenced by the peak at *m/z* 402. The molecular weight of the stearate-H-SBM (381.3) was calculated by subtracting the mass of the sodium ion from the mass of the [stearate-H-SBM + Na]$^+$ adduct.

The highest peak in the HO-SBM spectrum is at *m/z* 402.3 (**Fig. B2 B**), corresponding to [oleate-HOSBM + Na]$^+$, which demonstrates that the main component of HO-SBM is an oleic acid derivative (**Fig. 6.1**). After subtracting the mass of the sodium ion, the molecular weight of the oleate-HOSBM was determined as 379.3. Besides the oleate, HO-SBM molecules also contain small amounts of other fatty acid chains (saturated palmitate and stearate as well as di-unsaturated linoleate), as indicated by mass peaks at *m/z* 376.3, 404.3, and 400.3, respectively. Thus, electrospray ionization–mass spectrometry confirmed that the main component of HO-SBM is monounsaturated oleate, whereas H-SBM is predominantly saturated stearate in terms of its fatty acid chain structure. Once H-SBM, HO-SBM, and M-β-CD were successfully analyzed by ESI–MS, the inclusion complexes were explored to prove the molecular association of POBM molecules and methyl-β-cyclodextrin, as well as determine the stoichiometry of the complexes.

Figure 6.4 shows the ESI mass spectra of inclusion complexes of the POBMs with methyl-β-cyclodextrin. In the spectrum of H-SBM/M-β-CD (**Fig. 6.4 A**), ions detected at *m/z* 1665, 1679, 1693, 1707, and 1721 correspond to sodium adducts of complexes of stearate-H-SBM with M-β-CD having 9, 10, 11, 12, and 13 methyl groups, respectively.

The ESI mass spectrum of the HO-SBM/M-β-CD inclusion complex is depicted in **Figure 6.4 B**. Ions that correspond to the inclusion of oleate-HO-SBM by $M_{10\text{-}13}$-β-CD (sodium adducts) are detected at *m/z* 1677, 1691, 1705, and 1719. It is worth noting that stearate-H-SBM and oleate-

HO-SBM are the main components of H-SBM and HO-SBM, respectively; M-β-CD is a mixture of β-cyclodextrins in which 9–13 hydroxyl groups are substituted with methyl groups. For that reason, these above-mentioned inclusion complexes are the most pronounced in the ESI spectra. Hence, the ESI–MS data directly confirmed the methyl-β-cyclodextrin complexation of POBM molecules (both H-SBM and HO-SBM) resulting in the 1:1 complex formation (**Figure 6.5**).

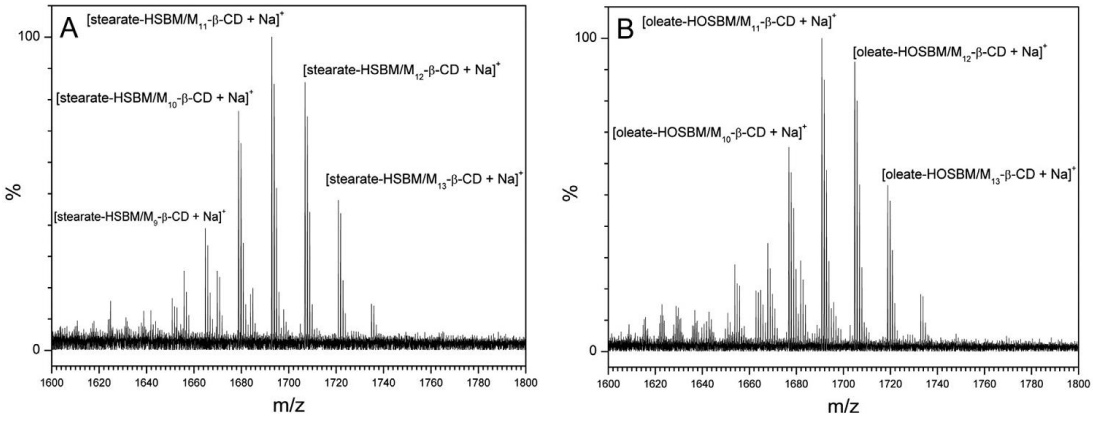

Figure 6.4. ESI mass spectra of H-SBM/M-β-CD (**A**) and HO-SBM/M-β-CD (**B**) inclusion complexes

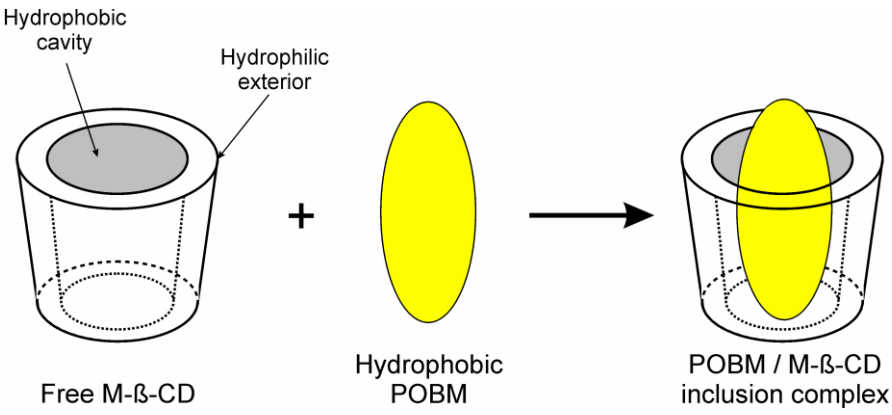

Figure 6.5. Schematic illustration of the association of free methyl-β-cyclodextrin and POBM to form a 1:1 inclusion complex

Since the complexation of cyclodextrins with highly hydrophobic monomers is known to allow for the enhancement of the aqueous solubility and availability of the latter in emulsion polymerization process, a series of latexes from POBMs (HO-SBM and LSM, very different in terms of unsaturation amounts), were synthesized using emulsion copolymerization with styrene

in the presence of methyl-β-cyclodextrin. To define the impact of M-β-CD onto the polymerization features and polymer latex properties, another series of latexes without adding M-β-CD was prepared as well.

Latexes from an initial monomer mixture containing HO-SBM or LSM (5−15 wt.%) and styrene (85−95 wt.%), both in combination with M-β-CD (5−15 wt.%) and without M-β-CD, were synthesized using emulsion polymerization at 60 °C under stirring. Synthesized latexes exhibit high stability at room temperature over several months.

The characteristics of the resulting POBM-based latex polymers are shown in **Tables 6.2** and **6.3**. As expected, the molecular weight of the latex copolymers synthesized from LSM is systematically lower than that of the HO-SBM-based latexes with the same composition of the monomer feed. The lower M_n for LSM-based latex can be explained by the effect of degradative chain transfer on the POBM provided by differing numbers of allylic hydrogen atoms in monomer molecules (**Figure 6.1**). The values of chain transfer constant on monomers determined earlier[24] clearly depend on the monomer structure (number of C−H groups in the α-position of the fatty acid double bonds) and increases with an increasing monomer unsaturation. The extent of the chain transfer reaction is more pronounced for the most unsaturated LSM. A similar effect was observed during miniemulsion copolymerization by changing the unsaturation of POBMs in the initial mixture, as our group reported earlier[36].

Table 6.2. Properties of latex polymers from HO-SBM and St.

Monomer feed, wt.%			Bio-based content (polymer), wt.%	Latex solid content, %	Yield, %	Coagulum, %	M_n, g/mol	Alkyl carbon−carbon double bond protons[#] (–C<u>H</u>=C<u>H</u>–)
HO-SBM	St	M-β-CD*						
5	95	0	4.2	30.0	97.5	2.4	192,200	1.03 H
5	95	5	4.9	30.8	99.4	0.4	234,400	1.34 H
10	90	0	6.0	29.7	93.6	3.6	95,900	0.92 H
10	90	10	7.5	31.7	97.2	0.5	165,900	1.12 H
15	85	0	13.3	29.4	88.8	1.0	116,400	1.19 H
15	85	15	11.3	31.2	93.9	0.7	127,500	1.78 H

*The amount of M-β-CD was based on the monomer feed

[#]The number of the alkyl carbon−carbon double bond protons (chemical shift 5.38−5.40 ppm) in the high oleic soybean monomer is 1.96 H

Table 6.3. Properties of latex polymers from LSM and St.

Monomer feed, wt.%			Bio-based content (polymer), wt.%	Latex solid content, %	Yield, %	Coagulum, %	M_n, g/mol	Alkyl carbon−carbon double bond protons[#] (–C<u>H</u>=C<u>H</u>–)	Bisallylic protons[##] (–CH=CH–C<u>H</u>$_2$–CH=CH–)
LSM	St	M-β-CD*							
5	95	0	3.7	29.1	84.4	3.3	86,000	1.89 H	1.35 H
5	95	5	3.9	28.9	91.3	3.0	125,200	2.51 H	1.74 H
10	90	0	7.2	27.6	89.6	1.1	79,700	1.76 H	1.25 H
10	90	10	7.8	27.2	96.5	1.2	96,700	2.56 H	1.68 H
15	85	0	10.8	27.7	83.7	3.1	82,000	2.11 H	1.28 H
15	85	15	10.7	30.3	91.5	0.5	97,400	3.24 H	2.19 H

*The amount of M-β-CD was based on the monomer feed

[#]The number of the alkyl carbon−carbon double bond protons (chemical shift 5.38−5.40 ppm) in the linseed monomer is 3.67H.

[##]The number of the bisallylic protons (chemical shift 2.85 ppm) in the linseed monomer is 2.44 H.

As shown in **Tables 6.2** and **6.3**, in the presence of "host-quest" complexes, the polymer yield increases as the coagulum amount drops during the emulsion polymerization of both POBMs with styrene, indicating the POBMs enhanced aqueous solubility and availability for polymerization. Remarkably, the presence of M-β-CD in the formulations also considerably

increases the molecular weight of latex polymers. We hypothesized that the incorporation of POBM molecules into the methyl-β-cyclodextrin cavity not only increases the POBM aqueous solubility, but also diminishes the allylic termination by protecting the allylic moiety of the POBM fatty acid fragments against chain transfer reactions. Consequently, latex polymers with higher molecular weights from highly hydrophobic POBMs can be synthesized at a higher polymer yield. Furthermore, the obtained data show that this effect is more pronounced for latexes from more unsaturated LSM.

To quantify the impact of methyl-β-cyclodextrin on chain transfer reactions during the emulsion copolymerization of POBMs, ^{1}H NMR spectroscopy was used to determine the number of protons of the alkyl carbon−carbon double bonds (–C**H**=C**H**–) and the bisallylic hydrogen atoms (–CH=CH–C$\mathbf{H_2}$–CH=CH–) in the unsaturated fatty acid moieties of the latex copolymers. By comparing those numbers obtained for different amounts of M-β-CD in the reactive mixture, one can conclude that the presence of oligosaccharide indeed facilitates chain propagation over the chain transfer.

To this end, the peak of the methyl group protons of the fatty acid chain (–C$\mathbf{H_3}$) was used as a reference. The results of the ^{1}H NMR study of the synthesized latex polymers are summarized in **Tables 6.2** and **6.3**. (characteristic peaks are presented in **Fig. B3** in **Appendix B**). It should be noted that a peak of the bisallylic protons (chemical shift about 2.85 ppm) was not found in the ^{1}H NMR spectra of the HO-SBM-based latex copolymers because the major component of HO-SBM is monounsaturated oleate and the number of the bisallylic protons in the monomer itself is 0.16 H only.

The data in **Tables 6.2** and **6.3** clearly show that the emulsion copolymerization of POBMs with styrene in the presence of M-β-CD allows for the protection and preservation of both fatty

acid double bonds of the monomers and the bisallylic hydrogen atoms in the case of latex polymers from LSM and St and fatty acid double bonds when HO-SBM is copolymerized with St. These results are consistent with previously reported literature on the cyclodextrin complexation of unsaturated fatty acids, reflecting protection of the latter against oxidation even in pure oxygen due to burying the fatty acid double bonds into the CD cavity[46]. Thus, in the presence of M-β-CD, latex polymers with a consistently higher molecular weight can be obtained evidently because of the incorporation of POBM molecules into the M-β-CD cavities that protects the fatty acid moieties and therefore decreases the chain transfer and addition of the fatty acid double bonds to growing radicals.

Furthermore, in the presence of M-β-CD during the emulsion polymerization, the polymer yield increases, and the coagulum amount decreases (**Tables 6.2** and **6.3**). The obtained data imply the dual role of M-β-CD in the emulsion polymerization of POBMs, that is the enhanced aqueous solubility of highly hydrophobic monomers and their availability for the emulsion process as well as diminishing monomer chain transfer reactions due to "host-guest" complex formation. To the best of our knowledge, this feature of amphiphilic oligosaccharide molecules has not been reported before in literature discussing free radical polymerization reactions.

6.5. Conclusions

In this study, the feasibility of methyl-β-cyclodextrin and POBM interactions *via* inclusion complexation using a freeze-drying technique was demonstrated, and POBM/M-β-CD inclusion complexes were successfully prepared. The PXRD, DSC, and ESI-MS studies show the actual complexes are formed, while ESI-MS data determined the presence of only 1:1 stoichiometry for both the HO-SBM/M-β-CD and H-SBM/M-β-CD complexes.

A series of latexes from high oleic soybean- and linseed oil-based monomers was synthesized using emulsion copolymerization with styrene. In the presence of methyl-β-cyclodextrin, latex polymers with a consistently higher molecular weight were obtained from both HO-SBM and LSM (this effect is more pronounced for more unsaturated LSM). Moreover, the emulsion copolymerization adding M-β-CD resulted in an increased polymer yield and latex solid content accompanied by reduced coagulum formation. We hypothesized that the incorporation of POBM molecules into the methyl-β-cyclodextrin cavity diminishes the chain transfer contribution by protecting the allylic moiety of the POBM fatty acid fragments and simultaneously enhances the aqueous solubility and availability of POBMs in the emulsion polymerization process. Consequently, a higher molecular weight of latex polymers from highly hydrophobic POBMs can be obtained with higher monomer conversion and lower coagulum formation.

6.6. References

1. Gandini, A.; Belgacem, M. N., *Monomers, polymers and composites from renewable resources*. Elsevier Amsterdam: 2008.
2. Lu, Y.; Larock, R. C., Novel polymeric materials from vegetable oils and vinyl monomers: preparation, properties, and applications. *ChemSusChem: Chemistry & Sustainability Energy & Materials* **2009,** *2* (2), 136-147.
3. Williams, C. K.; Hillmyer, M. A., Polymers from renewable resources: a perspective for a special issue of polymer reviews. *Polymer reviews* **2008,** *48* (1), 1-10.
4. Gallezot, P., Conversion of biomass to selected chemical products. *Chemical Society Reviews* **2012,** *41* (4), 1538-1558.
5. Lligadas, G.; Ronda, J. C.; Galia, M.; Cadiz, V., Renewable polymeric materials from vegetable oils: a perspective. *Materials today* **2013,** *16* (9), 337-343.

6. Verhe, R.; De Caro, P.; Mouloungui, Z.; Stevens, C. V., Industrial products from lipids and proteins. *Renewable bioresources: scope and modification for non-food applications* **2004**, 208-250.

7. Güner, F. S.; Yağcı, Y.; Erciyes, A. T., Polymers from triglyceride oils. *Progress in Polymer Science* **2006,** *31* (7), 633-670.

8. Sharma, V.; Kundu, P., Addition polymers from natural oils—a review. *Progress in Polymer Science* **2006,** *31* (11), 983-1008.

9. Wool, R.; Sun, X. S., *Bio-based polymers and composites*. Elsevier: 2011.

10. Gunstone, F. D., *Fatty acid and lipid chemistry*. Springer: 2012.

11. Bailey, A. E., *Industrial oil and fat products*. Interscience Publishers, Inc.; New York: 1945.

12. Reimers, J.; Schork, F., Predominant droplet nucleation in emulsion polymerization. *Journal of Applied Polymer Science* **1996,** *60* (2), 251-262.

13. Lligadas, G.; Ronda, J. C.; Galia, M.; Cádiz, V., Plant oils as platform chemicals for polyurethane synthesis: current state-of-the-art. *Biomacromolecules* **2010,** *11* (11), 2825-2835.

14. Pan, X.; Sengupta, P.; Webster, D. C., High biobased content epoxy–anhydride thermosets from epoxidized sucrose esters of fatty acids. *Biomacromolecules* **2011,** *12* (6), 2416-2428.

15. Wang, Z.; Zhang, X.; Wang, R.; Kang, H.; Qiao, B.; Ma, J.; Zhang, L.; Wang, H., Synthesis and characterization of novel soybean-oil-based elastomers with favorable processability and tunable properties. *Macromolecules* **2012,** *45* (22), 9010-9019.

16. Türünç, O.; Meier, M. A., The thiol-ene (click) reaction for the synthesis of plant oil derived polymers. *European journal of lipid science and technology* **2013,** *115* (1), 41-54.

17. Yuan, L.; Wang, Z.; Trenor, N. M.; Tang, C., Robust Amidation Transformation of Plant Oils into Fatty Derivatives for Sustainable Monomers and Polymers. *Macromolecules* **2015,** *48* (5), 1320-1328.

18. Yuan, L.; Wang, Z.; Trenor, N. M.; Tang, C., Amidation of triglycerides by amino alcohols and their impact on plant oil-derived polymers. *Polymer Chemistry* **2016,** *7* (16), 2790-2798.

19. Maiti, B.; De, P., RAFT polymerization of fatty acid containing monomers: controlled synthesis of polymers from renewable resources. *RSC Advances* **2013,** *3* (47), 24983-24990.

20. Maiti, B.; Kumar, S.; De, P., Controlled RAFT synthesis of side-chain oleic acid containing polymers and their post-polymerization functionalization. *RSC Advances* **2014,** *4* (99), 56415-56423.

21. Lomège, J.; Negrell, C.; Robin, J.-J.; Lapinte, V.; Caillol, S., Fatty acid-based methacrylate polymers as viscosity modifiers for mineral oils. *Green Materials* **2018,** *6* (3), 97-107.

22. Tarnavchyk, I.; Popadyuk, A.; Popadyuk, N.; Voronov, A., Synthesis and free radical copolymerization of a vinyl monomer from soybean oil. *ACS Sustainable Chemistry & Engineering* **2015,** *3* (7), 1618-1622.

23. Demchuk, Z.; Shevchuk, O.; Tarnavchyk, I.; Kirianchuk, V.; Kohut, A.; Voronov, S.; Voronov, A., Free Radical Polymerization Behavior of the Vinyl Monomers from Plant Oil Triglycerides. *ACS Sustainable Chemistry & Engineering* **2016**.

24. Demchuk, Z.; Shevchuk, O.; Tarnavchyk, I.; Kirianchuk, V.; Lorenson, M.; Kohut, A.; Voronov, S.; Voronov, A., Free-Radical Copolymerization Behavior of Plant-Oil-Based

Vinyl Monomers and Their Feasibility in Latex Synthesis. *ACS Omega* **2016,** *1* (6), 1374-1382.

25. Kingsley, K.; Shevchuk, O.; Demchuk, Z.; Voronov, S.; Voronov, A., The features of emulsion copolymerization for plant oil-based vinyl monomers and styrene. *Industrial Crops and Products* **2017,** *109* (Supplement C), 274-280.

26. Moreno, M.; Miranda, J. I.; Goikoetxea, M.; Barandiaran, M. J., Sustainable polymer latexes based on linoleic acid for coatings applications. *Progress in Organic Coatings* **2014,** *77* (11), 1709-1714.

27. Lau, W., Method for forming polymers. Google Patents: 1996.

28. Rimmer, S.; Tattersall, P., Emulsion polymerizations in the presence of β-cyclodextrin. *Polymer* **1999,** *40* (24), 6673-6677.

29. Rimmer, S.; Tattersall, P., The inclusion of β cyclodextrin provides a supramolecular solution to the problem of polymerization of dodecyl and octadecyl methacrylates in aqueous emulsion. *Polymer* **1999,** *40* (20), 5729-5731.

30. Lau, W. In *Emulsion polymerization of hydrophobia monomers*, Macromolecular Symposia, Wiley Online Library: **2002;** pp 283-289.

31. Leyrer, R. J.; Mächtle, W., Emulsion polymerization of hydrophobic monomers like stearyl acrylate with cyclodextrin as a phase transfer agent. *Macromolecular Chemistry and Physics* **2000,** *201* (12), 1235-1243.

32. You, X.; Dimonie, V. L.; Klein, A., Kinetic study of emulsion copolymerization of ethyl methacrylate/lauryl methacrylate in propylene glycol, stabilized with poly (ethylene oxide)–block–polystyrene–block–poly (ethylene oxide) triblock copolymer. *Journal of applied polymer science* **2001,** *82* (7), 1691-1704.

33. Vähä-Nissi, M.; Kervinen, K.; Savolainen, A.; Egolf, S.; Lau, W., Hydrophobic polymers as barrier dispersion coatings. *Journal of applied polymer science* **2006,** *101* (3), 1958-1962.

34. Ding, L.; He, Q.; Deng, J., Using hydroxypropyl-β-cyclodextrin for the preparation of hydrophobic poly (ketoethyl methacrylate) in aqueous medium. *Journal of applied polymer science* **2010,** *115* (5), 2933-2939.

35. Assem, Y.; Yehia, A., Studying the Effect of β-Cyclodextrin in Aqueous Polymerization of Some Acrylate Monomers Bearing Hydrophobic Moiety. *EGYPTIAN JOURNAL OF CHEMISTRY* **2015,** *58* (3), 387-401.

36. Hu, J.; Tao, Z.; Li, S.; Liu, B., The effect of cyclodextrins on polymer preparation. *Journal of materials science* **2005,** *40* (23), 6057-6061.

37. Demchuk, Z.; Kohut, A.; Voronov, S.; Voronov, A., Versatile Platform for Controlling Properties of Plant Oil-Based Latex Polymer Networks. *ACS Sustainable Chemistry & Engineering* **2018,** *6* (2), 2780-2786.

38. Michalska, P.; Wojnicz, A.; Ruiz-Nuño, A.; Abril, S.; Buendia, I.; León, R., Inclusion complex of ITH12674 with 2-hydroxypropyl-β-cyclodextrin: Preparation, physical characterization and pharmacological effect. *Carbohydrate polymers* **2017,** *157*, 94-104.

39. Liao, Y.; Zhang, X.; Li, C.; Huang, Y.; Lei, M.; Yan, M.; Zhou, Y.; Zhao, C., Inclusion complexes of HP-β-cyclodextrin with agomelatine: preparation, characterization, mechanism study and in vivo evaluation. *Carbohydrate polymers* **2016,** *147*, 415-425.

40. Marques, H. C.; Hadgraft, J.; Kellaway, I., Studies of cyclodextrin inclusion complexes. I. The salbutamol-cyclodextrin complex as studied by phase solubility and DSC. *International Journal of Pharmaceutics* **1990,** *63* (3), 259-266.

41. Saenger, W., Cyclodextrin inclusion compounds in research and industry. *Angewandte Chemie International Edition in English* **1980,** *19* (5), 344-362.

42. Guo, M.; Song, F.; Liu, Z.; Liu, S., Characterization of non-covalent complexes of rutin with cyclodextrins by electrospray ionization tandem mass spectrometry. *Journal of mass spectrometry* **2004,** *39* (6), 594-599.

43. Tao, F.; Hill, L. E.; Peng, Y.; Gomes, C. L., Synthesis and characterization of β-cyclodextrin inclusion complexes of thymol and thyme oil for antimicrobial delivery applications. *LWT-Food Science and Technology* **2014,** *59* (1), 247-255.

44. Marangoci, N.; Mares, M.; Silion, M.; Fifere, A.; Varganici, C.; Nicolescu, A.; Deleanu, C.; Coroaba, A.; Pinteala, M.; Simionescu, B. C., Inclusion complex of a new propiconazole derivative with β-cyclodextrin: NMR, ESI–MS and preliminary pharmacological studies. *Results in pharma sciences* **2011,** *1* (1), 27-37.

45. Szejtli, J.; Bánky-Elöd, E., Inclusion complexes of unsaturated fatty acids with amylose and cyclodextrin. *Starch-Stärke* **1975,** *27* (11), 368-376.

46. Jyothirmayi, N.; Ramadoss, C. S.; Divakar, S., Nuclear magnetic resonance studies of cyclodextrin complexes of linoleic acid and arachidonic acid. *Journal of agricultural and food chemistry* **1991,** *39* (12), 2123-2127.

CHAPTER 7. CONCLUSIONS AND FUTURE WORK

7.1. General conclusions

The goal of this research was to synthesize novel vinyl monomers derived from highly hydrophobic plant oils and polymerize them *via* cationic and free radical polymerization processes to obtain polymer coatings and films. As described in Chapter 2, the first method involved the synthesis of a vinyl ether monomer derived from soybean oil (2-VOES) which can be polymerized *via* cationic polymerization mechanism. The ability to tailor thermomechanical properties of these alkyd-type coatings was investigated by preparing poly(vinyl ether) copolymers *via* cationic copolymerization of 2-VOES and vinyl ether monomers synthesized from poly(ethylene glycol) (PEG). To study the impact of copolymer composition and molecular weight on coatings properties, different chain lengths (n = 3, 5, or 24) of PEG vinyl ether monomer were utilized. Furthermore, for each PEG series (i.e. PEG3, PEG5, and PEG24), three different copolymers were prepared with increasing amounts of PEG vinyl ether, 15, 25, and 50 wt.%. In total, nine different 2-VOES-based copolymers were prepared by cationic copolymerization and compared to the homopolymer, poly(2-VOES).

From GPC results, it was determined that the ten samples could be classified into two distinct categories; "lower" molecular weight copolymers (~10 kDa) and "higher" molecular weight copolymers (~25 kDa). Additionally, the PDI of resultant copolymers was broader than can be expected for polymers synthesized *via* cationic polymerization mechanism, ranging from 1.7-2.1. These features in molecular weight and PDI could be explained by synthetic variations of the ratio between the concentrations of monomer and coinitiator ($Et_3Al_2Cl_3$) or from side reactions triggered by the presence of unsaturation in 2-VOES throughout the polymerization, which was confirmed by ^{1}H NMR spectroscopy.

(Co)polymer coatings and free films were formed at room temperature by autoxidation and further crosslinking *via* unsaturated pendent fatty acid chains of the 2-VOES fragments. Tack-free times were extended as the amount of the PEG*n* vinyl ether monomers increased. Thermomechanical properties of the 2-VOES-based coatings were dependent on molecular weight and PDI. As the molecular weight increased, a larger presence of unsaturation provided by 2-VOES fragments per macromolecule was available to participate in polymer network formation *via* autoxidation. For thermoset networks having T_g values below ambient conditions, as was the case for the polymer coatings in this study, the physical properties were directly related to XLD, and ultimately final copolymer molecular weight and molecular weight distribution.

From AFM, it was shown that the PEG vinyl ether fragments undergo phase separation from the hydrophobic 2-VOES moieties and diffused to the surface of the coatings to form certain morphological domains. The greater presence of PEG at the surface increased the wettability of the 2-VOES-based coatings, shown by changes in water contact angle as a function of time, and reduced the protein adsorption. However, the 2-VOES-based coatings exhibited unacceptable levels of hemolytic activity, possibly due to their extensive hydrophobicity or presence of drier package ingredients, suggesting they are not suitable for applications in blood contact devices.

Chapters 3-6 investigated the feasibility of incorporating highly hydrophobic acryl amide-functional POBMs derived from soybean (SBM), high oleic soybean (HO-SBM), hydrogenated soybean (H-SBM), and olive (OVM) oils in emulsion copolymerization with commercially available, styrene (St.), methyl (meth)acrylate (MMA/MA), and vinyl acetate (VA). In Chapter 3, SBM and OVM were copolymerized in emulsion with styrene as a proof-of-concept for investigating the features of the emulsion mechanism (i.e. reaction kinetics, mode(s) of particle nucleation, and molecular weight), as well as feasibility of POBM-based latexes formation and

further making latex films with tailorable thermomechanical properties. Copolymerization of St. with up to 20 wt.% POBM follows the Smith-Ewart theory, which predicts that latex particles are formed primarily by micellar nucleation and the number of nucleated particles is proportional to the surfactant and initiator concentration to the powers 0.6 and 0.4, respectively. The effects of POBM content and amount of unsaturation are essentially irrelevant in the copolymerization reaction when determining reaction orders with respect to initiator and emulsifier. Nevertheless, evaluation of latex particle size and number revealed that, although copolymerization of St. with POBM follows conventional phenomenology of emulsion polymerization for hydrophobic monomers, a mixed mode of particle nucleation (micellar and homogeneous) is occurring, both of which contribute to particle formation.

From GPC, it was shown that the molecular weight of the latex copolymers (M_n=120,000-380,000) decreased with increasing POBM content and unsaturation amount in the reaction mixture due to degradative chain transfer on the monomer, established in our previous work. The thermomechanical properties of resulting latex films were dependent on the amount of incorporated POBM. Unlike polystyrene, which yields brittle and rigid polymers, the incorporation of POBM, acting as an internal plasticizer, reduced the T_g by up to more than 40 °C and provided some flexibility and toughness to the latex films.

Due to the findings of apparently mixed mode of particle nucleation in copolymerization of POBMs and styrene, along with the fact that the chemical structures of POBM and surfactant (sodium dodecyl sulfate, SDS) are similar, POBM/SDS interactions were assumed. The aim of Chapter 4 was to investigate the effect of highly hydrophobic POBMs on the micellization of SDS at different surfactant and monomer concentrations. From static fluorescence spectroscopy, micellar aggregation number decreased while the number of micelle-bound monomer molecules

increased with an increasing presence of POBM in the mixture with SDS. This result indicated that intermolecular interactions occurred between POBM and SDS molecules and facilitated the formation of mixed SDS/POBM micelles. Similar conclusions were found after observing an increase in surface activity of SDS/POBM mixtures compared to pure SDS.

Micellar association was observed by DLS and TEM, which produced mixed micellar structures in the range of 25-30 nm. This was explained by the interaction between the polar "heads" of the POBM found in the micellar exterior. Not only did they interact with other polar "heads" (from SDS or POBM) within the same micelle, but also with neighboring micelles. The results from this work demonstrated that solubilization of POBM by SDS molecules could impact reaction kinetics and mechanism of emulsion polymerization, as well as latex particle formation and resulting particle morphology.

Based on previous findings, the effect of comonomer aqueous solubility on emulsion polymerization mechanism and particle nucleation was studied. It was hypothesized that POBM-SDS interactions, along with comonomer aqueous solubility, might impact this mechanism by balancing micellar and homogeneous nucleation modes. In Chapter 5, OVM and SBM were copolymerized in emulsion with significantly more water-soluble methyl methacrylate (MMA), vinyl acetate (VA), and methyl acrylate (MA) in order to demonstrate the impact of increased comonomer aqueous solubility on the emulsion mechanism. The balance between micellar and homogeneous modes of particle nucleation was experimentally quantified using water insoluble dye Blue 70. In POBM copolymerization with MMA (aqueous solubility 1.5 wt.%) and MA (aqueous solubility 4.9 wt.%), it was determined that micellar nucleation became the predominate mode of particle nucleation as the hydrophobicity of the monomer mixture increased (upon the addition of up to 20 wt.% POBM), while homogeneous nucleation dominated in

homopolymerization of PMMA and PMA. The magnitude of the shift from homogeneous (more hydrophilic monomer mixture) to micellar (more hydrophobic monomer mixture) nucleation modes was more pronounced with greater comonomer aqueous solubility. Modes of particle nucleation are also dependent on the nature (unsaturation amount) of the POBM. Latex particles originating by micellar nucleation were more common in copolymerizations of more unsaturated SBM (with both MMA and MA) compared to OVM. This was explained by the more expressed chain transfer reactions in the copolymerization of SBM, which yielded fewer number of particles growing in the continuous aqueous phase.

Changes in nucleation loci were correlated to impacts on reaction kinetics after determining reaction orders with respect to emulsifier and initiator. Upon adding POBM into the reaction mixture with MMA, the reaction order with respect to emulsifier increased from 0.34 (at 0 wt.% POBM) to 0.7 (at 20 wt.% POBM), which indicated there was in fact a transition to predominately micellar nucleation of latex particles. As in the Blue 70 dye study, the impact on copolymerization of POBM with MA was even more pronounced. No impact of POBM content on reaction orders was observed in copolymerization with VA (aqueous solubility 2.5 wt.%). This was explained by the high reactivity of growing PVA radicals in chain transfer reactions, which has a substantial influence on polymerization kinetics, and makes the presence of POBM in the monomer feed kinetically irrelevant.

Based on previous observation of diminishing total monomer conversion and molecular weight of resulting macromolecules in emulsion polymerization of POBMs, due to extensive chain transfer reactions, an attempt to overcome those technical drawbacks has been made. Chapter 6 demonstrated the feasibility of using methyl-β-cyclodextrin (M-β-CD) and POBM/M-β-CD interactions *via* inclusion complexation in order to enhance both monomer conversion in emulsion

process and final polymer molecular weight. Successful formation of POBM/M-β-CD inclusion complexes by a freeze-drying technique was confirmed by the results of the PXRD, DSC, and ESI-MS studies. Inclusion complex stoichiometry was determined to only be 1:1 for both the HO-SBM/M-β-CD and H-SBM/M-β-CD complexes, as determined by ESI-MS.

Latex copolymers from HO-SBM and linseed (LSM) oil-based monomers were synthesized using emulsion copolymerization with St. The addition of M-β-CD into the emulsion reaction increased total polymer yield, solid content, and molecular weight. This was achieved by the incorporation of POBM into the M-β-CD cavity, enhancing the aqueous solubility of the hydrophobic POBM while simultaneously diminishing the contribution of degradative chain transfer reactions to the unsaturation of the fatty acid chains.

7.2. Future work

In Chapter 2, the morphology of 2-VOES-based poly(vinyl ether) coatings was analyzed by AFM and showed phase separation of the hydrophilic PEG vinyl ether fractions, which were located on the surface. It would be of interest to investigate changes in morphology after the coatings have been wetted water and/or methylene iodide to determine if phase separation between the hydrophobic and hydrophilic fractions still exists. Additionally, the surface energy of the polymer coatings can be calculated after measuring changes in contact angle with respect to time with a number of different liquids. As a candidate, non-polar methylene iodide can be used. Finally, it has been suggested that the high hemolytic activity of the 2-VOES-based coatings could have been caused by the presence of the drier package in the reactive mixtures. To determine if this is the cause for increased hemolytic activity, a repeat of the biocompatibility assay should be conducted for 2-VOES-based copolymers without the presence of the drier package.

A rather complete fundamental study was conducted on the feasibility of emulsion copolymerization of highly hydrophobic acrylic monomers derived from plant oils with different amounts of unsaturation in the fatty acid chains. However, in order to be considered for industrial applications, the total monomer conversion must be drastically improved. For the majority of this work, batch emulsion polymerization was utilized, and monomer conversion was shown to decrease as the content of POBM increased in the monomer mixture. There are a number of different processes to explore as possibilities for increasing total monomer conversion. The most obvious alteration to try first lies within the polymerization process itself. Switching from batch process to a semi-batch, starved-feed, or seeded emulsion polymerization process may reduce the difficulty of highly hydrophobic POBM to diffuse through the aqueous medium. These results can be compared to yields achieved by the preparation of POBM-based latexes *via* miniemulsion polymerization, where POBM is not required to diffuse through the aqueous medium because polymerization occurs within the monomer droplets.

Once the optimum process has been identified, it would be of interest to investigate initiators and surfactants with different hydrophobicity. If the monomer mixture is significantly more hydrophobic than the initiator and emulsifier, it will be difficult for these components to "find each other" in the dynamic emulsion process. For example, if a relatively hydrophilic water-soluble initiator is used in the emulsion copolymerization of POBM, the initiator will remain mostly in the water phase, whereas POBM will be primarily located in monomer droplets or the monomer swollen micelles. A less soluble-in-water initiator would have a greater affinity of entering the micelles and continue propagation. Different initiator systems, thermal or redox, can also be investigated and used during the main polymerization period and/or at the end of the polymerization (chase period) to convert any remaining monomer within the polymer micelles.

Lastly, preparation of fully bio-based copolymer latexes has been proposed by emulsion polymerization of POBM with bio-based styrene. Collaboration with the Department of Chemistry and Biochemistry at North Dakota State University would be required to achieve the preparation of a fully bio-based copolymer latex. To begin, investigations into the emulsion mechanism should be conducted by replacing portions of styrene with the bio-styrene in copolymerization with POBM, essentially making a type of terpolymer.

APPENDIX A. SUPPLEMENTARY MATERIAL FOR CHAPTER 4

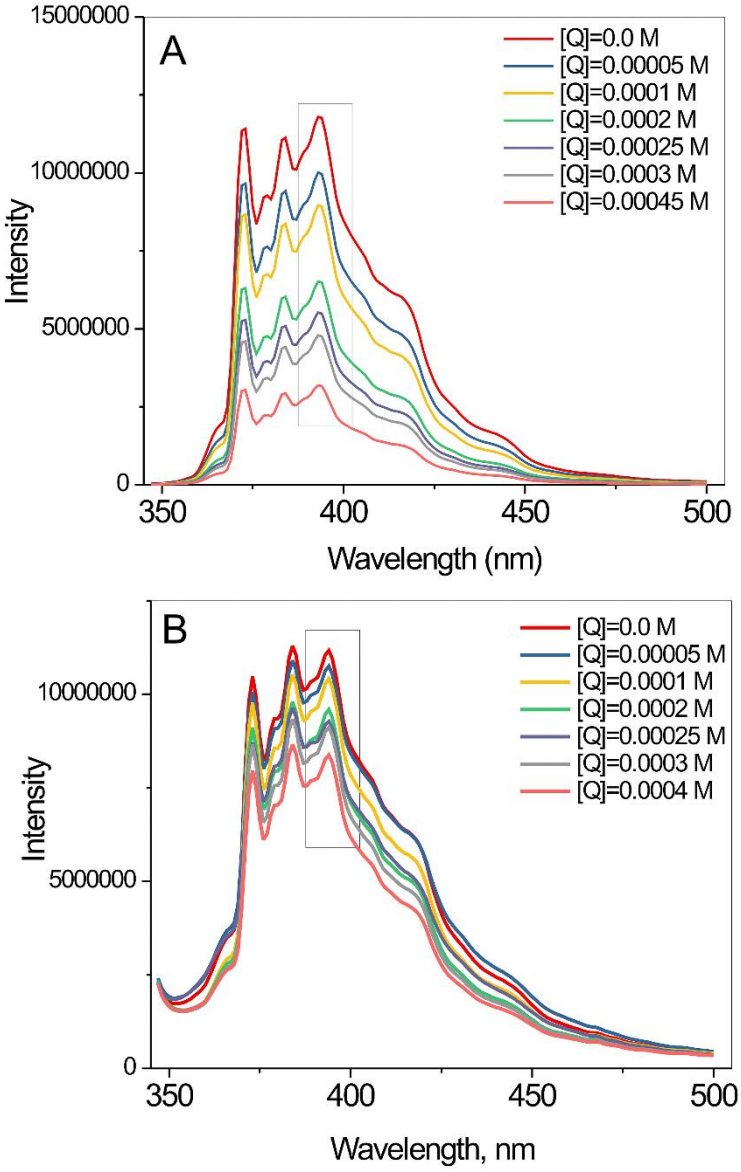

Figure A1. Fluorescence spectra of 0.02 M SDS aqueous solution (**A**) and in the presence of POBM (**B**) with an increasing concentration of quencher ([pyrene]=3.8×10^{-6} M)

APPENDIX B. SUPPLEMENTARY MATERIAL FOR CHAPTER 6

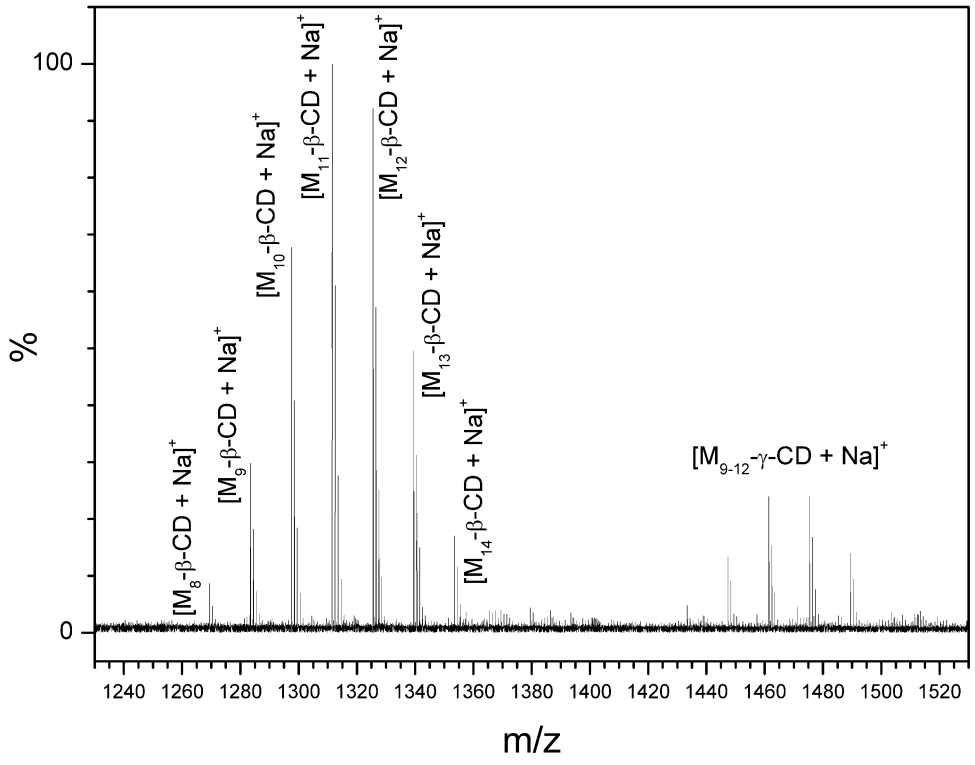

Figure B1. ESI mass spectrum of methyl-β-cyclodextrin

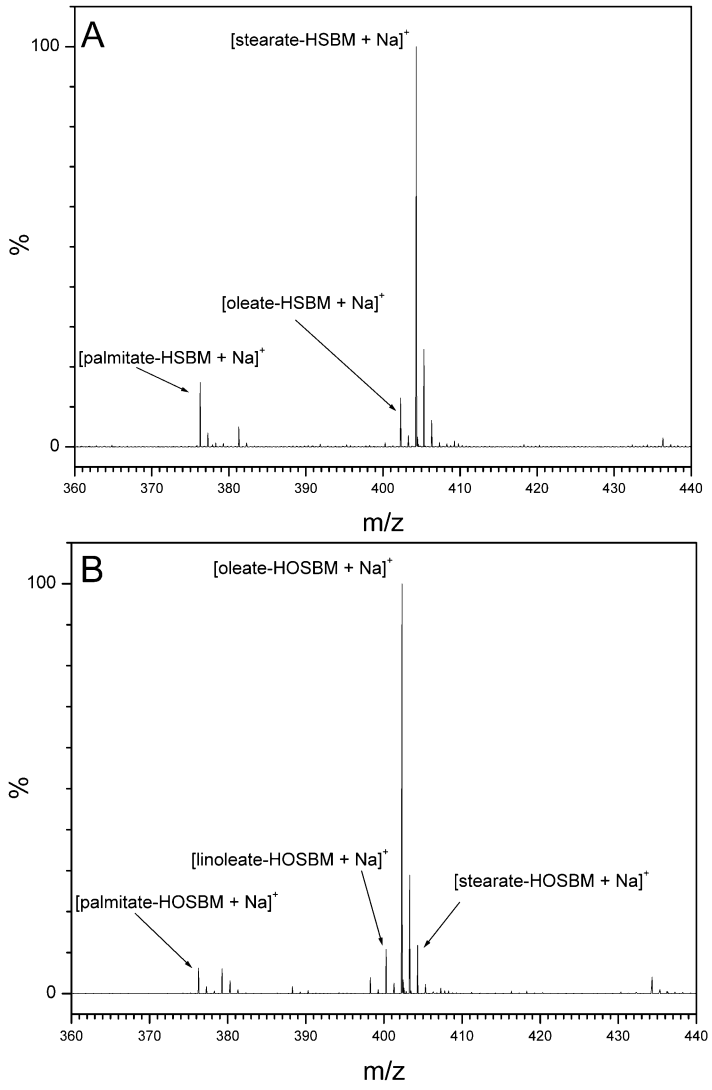

Figure B2. ESI mass spectra of H-SBM (**A**) and HO-SBM (**B**)

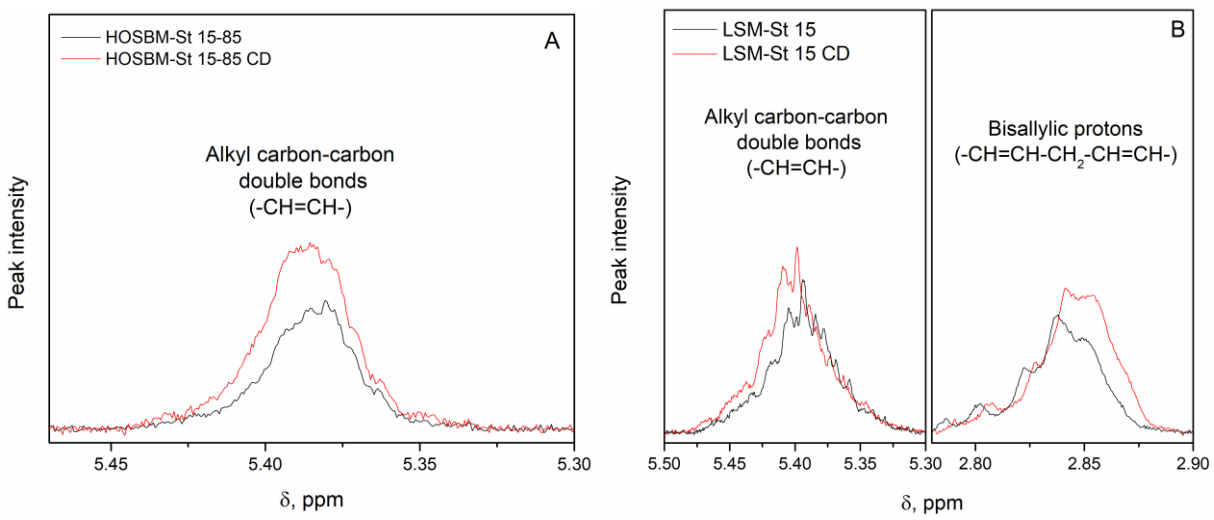

Figure B3. Characteristic peaks on the ^{1}H NMR spectrum of latex polymers from HO-SBM and St. (**A**), and LSM and St. (**B**)